23-26 MAY 2011, GRANADA

THE INTERRELATIONSHIP BETWEEN DEFORMATION AND METAMORPHISM

(DEFMET)

AN INTERNATIONAL CONFERENCE IN HONOUR OF PROFESSOR T.H. BELL

23-26 MAY 2011, GRANADA

THE INTERRELATIONSHIP BETWEEN DEFORMATION AND METAMORPHISM

AN INTERNATIONAL CONFERENCE IN HONOUR OF PROFESSOR T.H. BELL

ABSTRACTS VOLUME

THE CONFERENCE IS FINANCIALLY SUPPORTED BY:

MICINN, Ministerio de Ciencia e Innovación, Spain (grant CGL2010-11920-E)

MINISTERIO
DE CIENCIA
E INNOVACIÓN

UGR, Universidad de Granada, Spain

ugr | Universidad de Granada

JCU, School of Earth and Environmental Sciences, James Cook University, Australia

JAMES COOK UNIVERSITY
AUSTRALIA

QMC, Queensland Mining Corporation

QMC
Queensland Mining Corporation

We express our gratitude to several conference participants who anonymously contributed with major donations

COMPILED AND EDITED BY

Domingo G.A.M. Aerden

RECOMMENDED CITATION FOR ABSTRACTS

Bell, T.H. (2011). Deformation partitioning and its effects during multiple generations of folding, metamorphism, granite emplacement and modelling experiments. In: Aerden D.G.A.M. & Johnson, S.E. (eds) "The Interrelationship Between Deformation and Metamorphism. Abstracts Volume. University of Granada.

COPIES

Copies of this volume are available at the price of 15 Euros from Domingo Aerden

FOREWORD

The rapid growth of scientific research since the early 20th century has resulted in a significant degree of specialization that more than ever requires interdisciplinary collaboration. In the Earth Sciences, the plate tectonics paradigm provides the framework in which a multitude of geological processes that were formerly studied in isolation by different disciplines could be interrelated. The interrelationships between deformation processes and metamorphic mineral transformations is the primary focus of this conference, and the primary research focus of Professor Tim H. Bell.

This conference celebrates the major achievements of Tim Bell, and in particular his work on the convergence of structural geology, metamorphic petrology, and economic geology. Tim attracted worldwide attention with his model of deformation partitioning in metamorphic rocks, and has published prolifically on its implications for foliation development, lack of porphyroblast rotation, folding mechanisms, and the formation of ore deposits. Over the past two decades, Tim and approximately 70 former Ph.D. students have worked toward integrating 3D microstructural analysis in porphyroblastic rocks with techniques from thermobarometry and geochronology to date the successive fabrics trapped in porphyroblasts and to determine the metamorphic conditions under which they formed. This approach has revealed new, high-resolution information about orogenic histories, though many researchers remain skeptical both of the methodologies and the conclusions. Tim has never been deterred by this skepticism, and in fact part of the joy he gains from scientific pursuits is stirring the community with new, often controversial ideas.

With more than 70 abstracts from 184 contributing authors representing all continents, this conference aims to celebrate Tim's career by bringing together a large, diverse group of researchers, and to promote a better mutual understanding of equally diverse methodologies and concepts. These contributions span the disciplines that Tim is best known for, with a strong focus on microstructural processes and unraveling the evolution of mountain belts. Amongst the participants are many old friends who have known Tim as a student, as a thesis supervisor, or through research collaborations. We welcome these individuals and all other participants to four days of technical sessions and field trips.

Domingo Aerden, Scott Johnson

CONVENORS

D.G.A.M. Aerden, Departamento de Geodinámica, Universidad de Granada, Spain
S.E. Johnson, Department of Earth Sciences, University of Maine, USA

ORGANIZING COMMITTEE

D.G.A.M. Aerden, Universidad de Granada, Spain
S.E. Johnson, Department of Earth Sciences, University of Maine, USA
J.A. Lozano Rodriguez, Instituto Andaluz de Ciencias de la Tierra (CSIC), Universidad de Granada, Spain
E. Puga Rodriguez, Instituto Andaluz de Ciencias de la Tierra (CSIC), Universidad de Granada, Spain

SCIENTIFIC COMMITTEE

D.G.A.M. Aerden, Universidad de Granada, Spain
A. Azor Pérez, Universidad de Granada, Spain
E. Baxter, Boston University, USA.
J. Carreras, Universitat Autònoma de Barcelona, Spain
J. Galindo Zaldivar, Universidad de Granada, Spain
N. Hayward, Teck Resources Limited, Perth, Australia.
B. Hobbs, CSIRO, Canberra, Australia
S.E. Johnson, Uiversity of Maine, USA
M. Jessell, Institut de Recherche pour le Développement, Toulouse, France
R. Law, Virginia Tech, USA
D. Robinson, University of Bristol, UK
E. Puga Rodriguez, Universidad de Granada, Spain
F. Simanca Cabrera, Universidad de Granada, Spain
R. Vernon, Macquarie University, Australia
M. Williams, University of Massachusetts, USA
R. P. Wintsch, Indiana University at Bloomington, USA

TECHNICAL SECRETARIAT

N. Bethencort, Fase20 Congresos, Granada
C. Redondo Navacues, Fase20 Congresos, Granada
B. Montes Serrano, Fase20 Congresos, Granada

Acknowledgements

E. González García provided assistance with designing the conference Web page
V. Pérez Peña provided ArcGIS generated maps for the field guide

CONTENTS

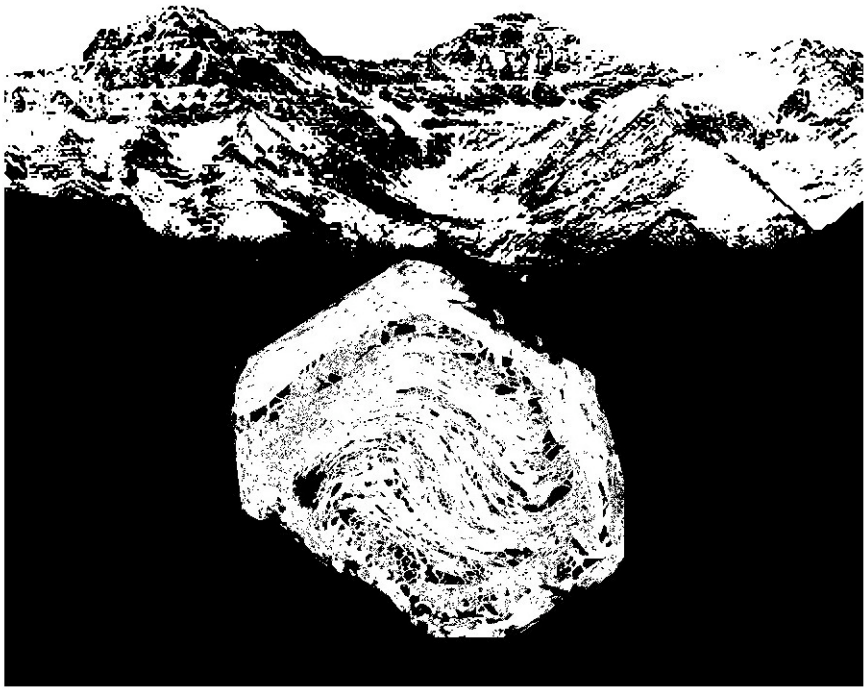

THE INTERRELATIONSHIP BETWEEN DEFORMATION AND METAMORPHISM

Granada, 23-26 May, 2011

PROGRAM

MONDAY, 23 MAY 2011

8:30 Reception and Registration
AULA MAGNA, FACULTAD DE CIENCIAS, AVDA. DE FUENTENUEVA, GRANADA

9:20 Opening Session
With collaboration of the chorale of the Faculty of Sciences (University of Granada)

9:45 Mark Jessell
Strain partitioning in heterogeneous geological systems *24*

10:15 Robert P. Wintsch, Meng-Wan Yeh
Lower Greenschist Facies Oscillations Across the 'Brittle-Ductile' Transition Induced by Alternating Reaction Softening and Hardening..... *32*

10:45 Isabel Abad, J. B. Murphy, F. Nieto, G. Gutiérrez-Alonso, E. Walsh
Distinction Between Deformation and Contact Metamorphism by Very Low-Grade Metamorphism Indicators in the Georgeville Group (Nova Scotia, Canada)..... *38*

11:05 POSTER SESSION with coffee and tea

11:40 Ricardo Arenas, Sonia Sánchez Martínez, Jacobo Abati, Javier Fernández Suárez, Rubén Díez Fernández, Pilar Andonaegui, José Manuel Fuenlabrada, Francisco J.Rubio Pascual
Terranes Involved in the Variscan Suture from NW Iberia: A Review of Their Origin and Tectonothermal Evolution *18*

12:10 F.J. Rubio Pascual, R. Arenas, J.R. Martínez Catalán, L.R. Rodríguez-Fernández, J. Wijbrans
Thickening and Exhumation of the Variscan Roots in the Spanish Central System: Tectonothermal Processes and 40Ar/39Ar Ages..... *64*

12: 30 Sonia Sánchez Martínez, Axel Gerdes, Ricardo Arenas, Jacobo Abati
The Origin of a Fragment of the Iapetus-Torquist Ocean and its Accretion in the Variscan suture of NW Iberia: The Bazar Ophiolite. *57*

12:50 M. Rebecca Stokes, R. P. Wintsch, D. L. Bish, J. Schieber
Deformation Induced Solution-Creep in the Ductile Lishan Fault Zone, Taiwan..... *37*

13:10 Gisella Rebay, Maria Iole Spalla
Interaction Between Deformation and Metamorpism During the Exhumation of Subducted Hydrated Oceanic Mantle: Insights From the Western Alps..... *62*

13:30 M. Iole Spalla, Gisella Rebay, Davide Zanoni, Guido Gosso, Luca Baletti
Structural vs Metamorphic Hetherogeneities in the HP Metagabbros From the Western Alps Austroalpine Continental Crust *67*

13:50 LUNCH BREAK (Hotel Granada Center)

15:40 Bruce Hobbs, Alison Ord, Weronika Gorczyk, Dan Lester, Klaus Gessner
A Multi-scale Approach to Giant Hydrothermal Mineral Systems..... *28*

16:10 Nick Hayward
On Structural Targeting Giant Ore Deposits *26*

16:40 Peter J. Treloar, James Lambert-Smith, David M. Lawrence, Paul Harbidge
Structural Controls on Fluid Migration and Orogenic Gold Deposition in the Birimian of West Mali and East Senegal, West Africa..... *68*

17:00 Philippe Muchez, Hamdy A. El Desouky, David Banks, Adrian Boyce, Dieter Brems, Jacques L.H. Cailteux, An De Cleyn, Lennert Lammens, Osbert Sikazwe
Metamorphism and Structural Control on the Cu-Co ore Deposits in the Central African Copperbelt..... *56*

17:20 Philippe Goncalves, Emilien Oliot, Didier Marquer
Role of metasomatism on the formation of shear zones: an example from a metagranodiorite in the Aar massif (Central Alps) *46*

17:40 Colin Wilkins
Structural Control of high grade Au-shoots at Hill End, NSW, Australia. *70*

18:00 POSTER SESSION with wine, beer and tapas

TUESDAY, 24 MAY 2011

9:00 - 19:00 Field trip to Sierra de Baza:
(Caniles-Fiñana-Dolar-Ferreira)
departure from Hotel Granada Center

(see field guide)

WEDNESDAY, 25 MAY 2011

11:10 POSTER SESSION with coffee and tea

13:40 LUNCH BREAK

18:10 POSTER SESSION with tapas and wine

THURSDAY, 26 MAY 2011

9:30-16:00 field trip to Sierra Nevada (ski resort area)

18:00-20:00 Visit to the Alhambra

20:00-24:00 Closing dinner at the Carmen de los Martires

KEYNOTE ORAL PRESENTATIONS

Terranes Involved in the Variscan Suture from NW Iberia: A Review of Their Origin and Tectonothermal Evolution

Ricardo Arenas*[1], Sonia Sánchez Martínez[1], Jacobo Abati[1], Javier Fernández Suárez[1], Rubén Díez Fernández[2], Pilar Andonaegui[1], José Manuel Fuenlabrada[3], Francisco J.Rubio Pascual[4]

[1]Departamento de Petrología y Geoquímica e Instituto de Geociencias (UCM-CSIC), Universidad Complutense, 28040 Madrid, Spain
[2]Departamento de Geología, Universidad de Salamanca, 37008 Salamanca, Spain
[3]CAI de Geocronología y Geoquímica Isotópica, Facultad de Geología, Universidad Complutense, 28040 Madrid, Spain
[4]Instituto Geológico y Minero de España, La Calera 1, 28760 Tres Cantos, Madrid, Spain
*arenas@geo.ucm.es

NW Iberia includes an excellent section of the Variscan suture, where different terranes with continental or oceanic affinities appear with clear structural relationships. The great exposures in the Cantabrian coastal section (Cabo Ortegal and Órdenes complexes, and the Malpica-Tui Unit) are a unique natural laboratory to approach the origin of the terranes involved in the suture zone and their internal structure and tectonothermal evolution. Three groups of terranes and a lower tectonic mélange constitute the huge allochthonous pile thrust over the Iberian autochthonous and parautochthonous domains, the section of the Gondwanan margin not involved in continental subduction during the Variscan deformation (Schistose Domain of Galicia-Trás-os-Montes and Central Iberian Zone). The allochthonous terranes are formed, from top to bottom, by upper units, ophiolitic units, basal units and lower mélange.

In the upper units, c. 12.000 m of terrigenous sediments intruded by large massifs of cambrian calc-alkaline granitoids (I-type) and tholeiitic gabbros with some bodies of ultramafic rocks, are considered to represent a section of a magmatic arc, built up in the periphery of Gondwana during Neoproterozoic-Cambrian times. The Nd model ages from a topmost turbiditic series (Ares-Sada greywackes) show close relationships with some Avalonian terranes, suggesting proximity in the paleomargin of Gondwana. A section of this arc rifted from the continent in Early Ordovician time, drifted towards the North and opened a wide Paleozoic oceanic domain, the Rheic Ocean. An uppermost part of this terrane affected by metamorphism ranging between the greenschist facies and the low pressure granulite facies, dated at 496-484 Ma, is a relic preserving almost intact the tectonothermal activity occurred in the peri-Gondwanan arc. Otherwise, the lower part shows a generalized high P-T event dated at c. 400 Ma developing extensive recrystallization in the eclogite and granulite facies. This subduction related event marks the accretion of this arc-derived terrane to the southern margin of Laurussia during Early Devonian times, coinciding with the widest spreading of the Rheic Ocean right before starting to contract.

True MORB ophiolites derived from the Rheic Ocean lithosphere are unknown in the suture zone of NW Iberia. On the contrary, this ocean is represented by a group of island-arc tholeiitic mafic units (supra-subduction zone type) suggesting two critical moments in its evolution: a first Late Cambrian stage (c. 500 Ma, Vila de Cruces Unit) representing the opening of peri-Gondwanan back-arc basins which are the origin of this ocean; a second stage dated at c. 395 Ma (Careón Unit) marking the activity of intra-Rheic subduction zones that removed completely the older and cold lithosphere developed in the mid-Rheic Ocean ridge, which also disappeared during the closure of this ocean. Due to their buoyant nature, the ophiolites generated during this stage scaped from early-Variscan subduction and they are the most common ophiolites preserved in the Variscan suture across Europe. Apart from the Rheic Ocean ophiolites, other mafic and ultramafic sections in NW Iberia have been related to Cambrian-Ordovician accretionary stages affecting sections of the peri-Gondwanan ocean, i.e. in previous moments to the opening of the Rheic Ocean. This is the case of the Bazar Unit, which appears accreted below the arc-deried terrane in the western part of the Órdenes Complex and it is considered to preserve a section of the Iapetus-Tornquist Ocean.

The basal units are formed by a thick sequence of Ediacaran-Early Ordovician terrigenous metasediments intruded by granitoids (calc-alkaline to peralkaline) and other mafic igneous rocks.

These units are considered to represent the most external part of the Gondwanan paleomargin, with an original position located further to the East than the arc-related section preserved in the upper units. The basal units are a continental subduction complex, where continental layers were subducted towards the W-SW (present coordinates) and imbricated below previously accreted ophiolites at c. 370 Ma, at the onset of the Variscan deformation. This subduction finished the closure of the Rheic Ocean and is the first true Variscan deformation affecting the margin of Gondwana. A variety of C-type eclogites, blueschists and lawsonite bearing metabasites developed during this second high-P event affecting the materials assembled in the allochthonus pile. In detail, the basal units can be subdivided in two main groups according to their tectonothermal evolution: an upper group with high-P and medium-high-T metamorphism (Agualada and Espasante units); and a lower group with high-P and low-medium-T metamorphism (Cean, Malpica-Tui, Santiago, Lalín and Forcarei units). The whole ensemble represents a well preserved paleosubduction zone, the Variscan subduction zone, with the upper group representing the sector in contact with the mantle wedge, and the lower part preserving a section of the cooler slices that were underthust later. The accretion of new continental slices finally blocked the subduction. However, continental convergence did not declined during the Mississippian, thus triggering the transference of the allochthonous pile and the Rheic suture onto the Gondwana mainland followed by the extensional collapse of the collisional wedge. The convergence remained during the Pennsylvanian and produced further reworking of the allochthonous nappe pile in strike-slip systems.

Finally, the Somozas mélange is the frontal mélange zone developed between the mantle wedge and the section of the Gondwanan margin under subduction. It is a piece of the subduction channel with c. 500 m of serpentinite mélange containing variably sized blocks of metasediments, volcanics, gabbros, granitoids and several high-P rocks. The subducted continental margin was exhumed later on and emplaced over the mélange zone, that appears now as a unique element located at the contact between the allochthonous terranes and the parautochthonous Schistose Domain.

Deformation partitioning and its effects during multiple generations of folding, metamorphism, granite emplacement and modelling experiments

T. H. Bell*

School of Earth and Environmental Sciences, James Cook University Townsville, Qld 4811, Australia
*tim.bell@jcu.edu.au

Regional distributions of axial plane trends retain information on the orientation in which successive generations formed because multi-scale partitioning results in most orogenic belts preserving subsequently undeformed portions of all large-scale folds, providing a deformation partitioning approach to resolving the sequence of fold events and the orientations in which they formed across multiply deformed large-scale regions. At depths greater than ~10 kms within orogens, successions of regional folds are accompanied by the sequential development of crenulation hinges in pelites, which are commonly overgrown early during their development by successive generations of porphyroblasts. Consequently, the original trends of the axial planes of these folds are preserved within the distribution of foliation inflection/intersection axes within porphyroblasts (FIAs). Peaks in the distribution of FIA trends in Western Maine predominantly coincide with peaks in the distribution of trends of the axial planes of macroscopic and regional folds. The WNW-ESE (~420 Ma), N-S (408±10 Ma), W-E (388±9 Ma), WSW-ENE (372±5 Ma), SW-NE (353±4 Ma) succession of FIA peaks defines the sequence of folds and accords with map scale overprinting relationships. This quantitative approach to interpreting fold successions in multiply deformed terrains resolves timing where overprinting criteria are rare, uncertain or obliterated by younger events in portions of the orogen. Significantly, lengthy detailed histories of structural development can be extracted from a small area containing porphyroblastic rocks and applied to very large-scale regions.

This is confirmed by the distribution of folds associated with different periods of orogeny across a large-scale region in the Mount Isa Inlier where radical changes in bulk shortening directions resulted in regionally spatially partitioned deformation during 4 distinct orogenic cycles. NE-SW shortening (O_{00}) from 1672 to ~1648 Ma, involving a succession of five phases of deformation produced NW-SE striking macroscopic folds, plus cleavages that are mainly only preserved in porphyroblasts. N-S shortening (O_1) from ~1648 Ma to 1600 Ma, involving at least three phases of deformation and rotated large portions of the NW-SE trending regional folds into W-E trends and the dominance of locally well-preserved W-E trending sub-vertical matrix foliations as well as the intensification of foliation parallel to bedding. W-E shortening (O_2) from 1600 to ~1515 Ma formed at least three near orthogonal foliations and the N-S trending regional folds that dominate the Mount Isa Inlier. Subsequent NW-SE shortening (O_3) produced locally developed SW-NE trending folds and weak crenulations until ~1500Ma. Inclusion trail asymmetries in garnet porphyroblasts that developed during O_{00} indicate thrusting to the SW and reduce the displacement required on the Meerenurker roof thrust near Mount Isa from 234 to ~ 65 kms. N to S thrusting to form the Kokkalukkernurker duplex that lies below this thrust took place during O_1. At this time garnet, staurolite and andalusite porphyroblasts developed near Cloncurry that indicate thrusting to the N confirming a 180° change in thrust direction across the N-S striking Wonga Duchess belt that lies between these locations. The foliations that progressively developed in the matrix during these orogenies were composite fabrics resulting from the effects of multiple discrete orthogonal increments in each case, but are preserved locally in the matrix where the folds retain NW-SE or W-E orientations. Numerous phases of sub-vertical foliation development due to horizontal bulk shortening were followed by phases of gently dipping foliation formation due to gravitational collapse that accompanied thrusting during O_{00} and O_1.

FIAs combined with pseudosections and garnet core isopleths in NW Maine, reveal only small changes in *P-T* conditions during orogenesis lasting 70 Myr. Garnet grew throughout this period at overstepped conditions where staurolite growth was also possible. Different porphyroblast growth

patterns in the same bulk composition/outcrop samples reveal that their reaction start/stop behaviour was controlled by the manner in which deformation partitioned through the outcrop. Regional isograds, established during the first period of bulk shortening near orthogonal to the orogen trend, did not migrate across lower grade rocks during each of the subsequent periods of metamorphism in spite of dramatic changes in the direction of bulk shortening. The isograds were folded about axial planes parallel to the fold belt during the youngest periods of orogenesis directed at a high angle to the current orogen trend. Their regional distribution directly reflects the oldest period of pluton emplacement with both controlled by orogen-scale partitioning of bulk shortening at a high angle to the current orogen trend relative to intervening zones of transform-like shear. Most significantly, multiple changes in the direction of horizontal bulk shortening provided pathways for the emplacement of plutons during the following periods of collisional orogenesis.

Such consistent sequences of FIAs derived from core to rim changes in orientation and recorded in orogens all over the world, cannot develop if porphyroblasts rotate during ductile deformation. Confirmation of these FIA successions by monazite dating provides independent evidence that the porphyroblasts from which they were obtained did not rotate in spite of the numerous periods of ductile deformation that accompanied orogenesis. Numerical modelling that does not reproduce the deformation-partitioning environment in which porphyroblasts grow and nucleate around them in subsequent events, results in their rotation and cannot reproduce the FIA data; modelling that does reproduce this environment results in no porphyroblast rotation during non-coaxial deformation for all matrix rheologies tested.

Advances in Sm-Nd Geochronology of Zoned Garnet Crystals

Ethan F. Baxter*

Department of Earth Sciences, Boston University
*efb@bu.edu

The potential for direct dating of discrete portions of growth zoned garnets was demonstrated over twenty years ago in a series of pioneering contributions. Recent advances in: (a) analysis of very small Nd aliquots, (b) partial dissolution cleansing of inclusions, (c) chemically contoured microsampling of garnet growth zones, have been integrated to permit a more full exploitation of the Sm-Nd geochronologic record of zoned garnets [1]. Here, I describe these three areas of advance and show several examples of the success – and current limitations – of these integrated methods.

Because Nd concentrations in pure garnet are exceedingly low (<< 1ppm), a major limitation to high resolution and high precision geochronology is the ability to precisely measure small aliquots of Nd. Using a method to ionize Nd as the oxide (NdO+) with a Ta2O5 activator slurry [2], we are able to achieve 10ppm (2s) external precision on 4ng loads of Nd. This permits precise analysis of up to ~10 concentric zones of garnet in a single 2cm diameter crystal.

Every garnet has mineral inclusions. They cannot be avoided by handpicking and physical separations. If they are not removed, inclusions can dominate the Sm-Nd signal and lead to less precise and often inaccurate ages. Using a combined HF-HNO3-HClO4 partial dissolution method on crushed garnet, we are able to cleanse garnets of their inclusions yielding pure garnet with high 147Sm/144Nd. Because each garnet sample is different, several parameters of the partial dissolution including temperature, duration, acids used, and grain size must be experimented with to find the optimal procedure.

Roughly concentric growth patterns in garnet crystals can be illuminated by electron microprobe major element mapping. Using this contour map as a guide, discrete growth zones can be extracted with a precision microdrilling apparatus. Because fine powders cannot be properly cleansed of inclusions, we use the drill as a knife, discarding the drilled powder and extracting the solid annulus between drill trenches for analysis. There is thus significant loss of sample due to drilling which represents one of the major current limitations of the method.

To demonstrate the precision, accuracy, and spatial-temporal resolution that is possible, I review zoned garnet data from three locations: (a) garnet-biotite-chlorite schist from a shear zone in the Tauern Window, Austria [3], (b) garnet-bearing pelitic schist from Townshend Dam, Vermont [4], (c) garnet-bearing blueschist from Sifnos, Greece [5].

References

[1] Pollington & Baxter 2011 Chem Geol **281**, 270-282.
[2] Harvey & Baxter 2009 Chem Geol **258**, 251-257.
[3] Pollington & Baxter 2010 EPSL 293, p. 63-71.
[4] Baxter et al. 2010 GSA Annual Meeting Denver, CO USA
[5] Dragovic et al. 2010 Goldschmidt Meeting Knoxville, TN USA

Strain partitioning in heterogeneous geological systems

Mark Jessell*

IRD ; Université de Toulouse III; UPS (SVT-OMP); LMTG; 14 Av. Edouard Belin, F-31400 Toulouse, France
*mark.jessell@ird.fr

Recent 2D and new 3D mechanical modelling of two-phase aggregates has shown that we can analyse the geometry of these systems both in terms of their finite deformation and their mechanical contrast. As has already been postulated in the past, hese experiments also show that strain partitioning can at the local scale totally swamp the character of the regional deformation.

These results are applied to the Palaeoproterozoic Sefwi-Comoé region that straddles Ghana and the Ivory Coast in West Africa, which has been characterised as resulting from a combination of compression and simple shear during late synkinematic leucogranite intrusion. The analysis of regional geophysical datasets allows us to better define the geometry of the major lithostratigraphic packages and their structural contacts in this region. This geophysical analysis reveals a series of well defined leucogranites intrusions enveloped by high strain zones.

We interpret the geometries we see in the Sefwi-Comoé region as reflecting the activity of a major crustal deformation zone which was dominated by simple shear. The comparison with the modelling suggests a finite shear strain of approximately 5 gamma, which in turn implies a lateral displacement of 400 km across the belt. Our analysis suggests that the leucogranites were already acting as more rigid bodies during the (dextral?) shearing, suggesting that their emplacement was predominantly pre-kinematic, and which has implications for their potential subsequent remobilization by gravitational forces.

Without detailed dating of the different structural domains found in this region, the experiments suggests that care needs to be taken in assigning multiple episodes of deformation in these mechanically heterogeneous terrains.

Inferring a Geotectonic Regime From Structural and Kinematic Analysis in a Tectonometamorphic Belt: the Variscan Cap de Creus Case Study

Jordi Carreras*[1], Elena Druguet [1]

[1,] MIET - Departament de Geologia, Universitat Autònoma de Barcelona
*Jordi.Carreras@uab.cat

Many recent interpretations on the tectonometamorphic evolution of orogenic belts are based on emphasizing the P-T-t determinations and fitting these with widely accepted models of orogenic collapse and/or crustal extension. These has lead to some controversial interpretations like those proposed by Wickham and Oxburg (1986), interpreting the Variscan segment of the Pyrenees as the result of a rift system. Other less radical authors have incorporated an extensional regime at a given stage (early or late) of the Variscan evolution (see Carreras and Capellà, 1994 for review). This contribution emphasizes the relevance of structural and kinematic data to interpreting the tectonic evolution and deducing the associated geotectonic regime of orogenic belts.

This case study refers to the Northern Cap de Creus tectonometamorphic belt. In this belt a Neoproterozoic and Lower Cambrian Series, including some intercalated pre-Variscan igneous rocks, suffered during the Variscan times a polyphase tectonics, a prograde LP/HT metamorphism associated with igneous activity and a late retrograde metamorphism. Despite the evidence for a prevailing progressive deformation, for the sake of simplicity the deformational history can be simplified into three main phases. The first phase (D_1) occurs at prograde metamorphic conditions and is responsible for a S_1 foliation, generally sub-parallel to layering. The second event (D_2) is highly inhomogeneous, forming high strain domains of a prevalent S_2 foliation which is axial planar to isoclinal folds, while in lower strain domains S_2 is represented by a weak crenulation cleavage. D_2 broadly coincides with the peak of the LP/HT metamorphism and associated magmatism, mainly represented by granitoids and pegmatites and local anatectic leucosomes. The late D_3 event occurs under greenschist facies conditions and is responsible for both folds and shear zones, depending of the rheological properties of the rocks involved. During this event, the sporadic replacement of andalusite by kyanite (Autran and Guitard, 1970) reveals a relative pressure increment during cooling.

This contribution focuses on the D_2 tectonometamorphic event. The D_2 high deformation zone forms an E-W trending belt on the northern part of the Cap de Creus peninsula that broadly coincides with medium to high grade metamorphic and magmatic domains (Fig. 1a).

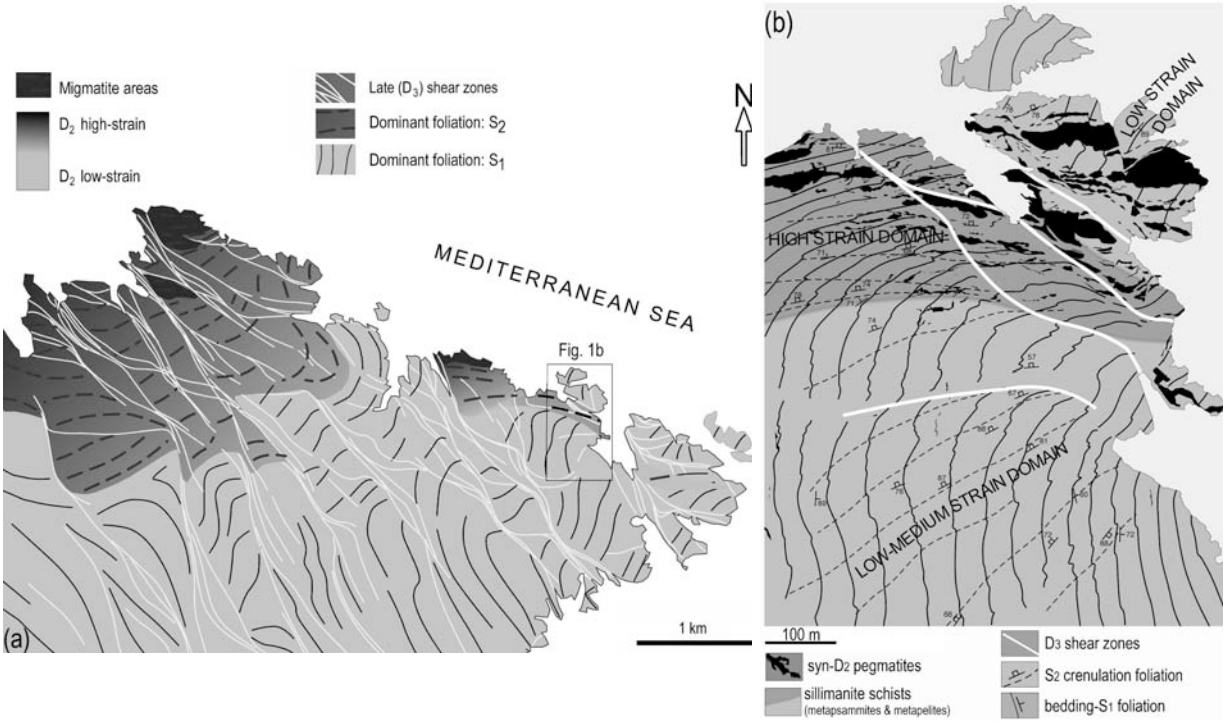

Fig. 1 (a) Setting of the Cap de Creus tectonometamorphic belt. (b) The Culip area case study.

In this area the E-W trending S_2 schistosity has a steep attitude and the associated stretching lineation is sub-vertical or moderately plunging towards the WNW. The boundaries between D_2 high and low strain domains can vary from gradual to sharp. The analysis of structures in a zone displaying a gradual passage

between low and high D_2 strain domains offers a good opportunity to characterize strain and kinematics. This is the Culip area (Carreras and Druguet,1994; Druguet et al., 1997; Fig.1b). In the low strain domains, a layer-parallel S_1 foliation strikes N-S, and gradually rotates clockwise towards E-W orientations with increasing strain, recovering a N-S orientation in the northern-most seated low strain domains. The high strain domain coincides with a syntectonic pegmatite dyke-swarm, evidencing a space and time relation between tectonics, LP/HT metamorphic peak and associated magmatism.

On a map scale, the D_2 high deformation belt delineates a complex steep shear zone with a dextral geometry (Fig.1b). Structural analysis in the area shows apparently contradictory sinistral rotations, about sub-vertical axes, of porphyroblasts (mainly andalusite) and quartz rods (Fig. 2). Folds are systematically "S"-shaped. Towards high strain domains, both structural surfaces, bedding/S_1 and S_2 foliations rotate clockwise (Fig. 3). The rotation of S_2 is about 15º greater than expected in a simple shear model (Fig. 2d). In addition, strain determinations using differently oriented quartz-veins (Druguet and Griera, 1998), indicate that, on the outcrop section at a high angle to the stretching lineation and fold hinges, a marked area reduction is present.

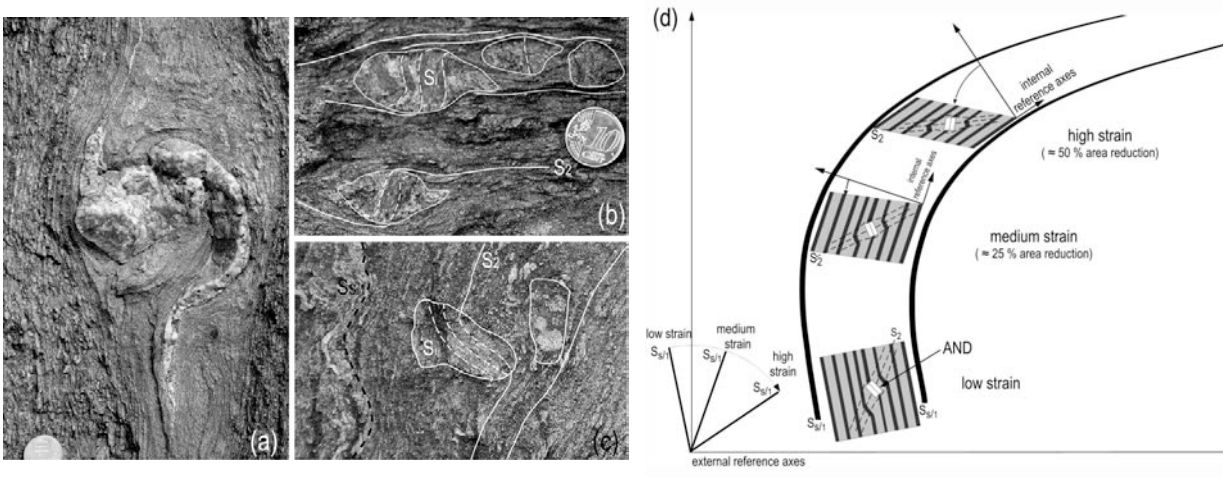

Fig. 2 Anticlockwise rotation of a quartz-rod (a) and of andalusite porphyroblasts in high strain domain (b) and in low strain domain (c). (d) 2D-interpretation of the transition from low strain domains to high strain domains.

All these data can be explained taking into account the following circumstances: (I) The structures developed are strongly controlled by the orientation of the previous layering/anisotropy. (II) In a deformation involving the bedding/S_1 shortening associated to sub-vertical extension, the rotation axis is predetermined by the angular relationship between the bedding/S_1 plane and the "flow plane", in analogy to what happens in shear zones across foliated rocks (Carreras, 1997). This causes the nearly parallelism between the vorticity axis and the extension direction. (III) Rocks accommodate the dextral deflection by layer/foliation-parallel flow, causing the anti-clockwise rotation of rigid body elements. All these features explain the coexistence of anti-clockwise (when using the layer/foliation as reference frame) and clockwise (when using a external reference frame) rotations. Thus, porphyroblasts rotate simultaneously anti-clockwise by rock strain and clockwise by bulk rotation (Fig. 2d). Due to the counterbalancing of both rotations, the finite result is a relatively small clockwise rotation of rigid bodies.

The final analysis requires a three-dimensional approach as the analyzed section lies closely parallel to the YZ plane of the finite strain ellipsoid, with about a 50% area reduction on this plane. The sub-vertical attitude of the extension direction indicates that the analyzed mid-crustal rocks were submitted to a D_2 transpression involving crustal shortening and complex shearing. The time and space coincidence of transpression with LP/HT metamorphic peak and igneous activity evidence that the common interpretation of LP/HT metamorphism as related to extensional regimes is debatable (Druguet, 2001). In addition, the subsequent evolution after peak metamorphism is characterized by folding and shearing associated to a wrench-dominated transpression (Carreras, 2001), being in this segment of the Variscides no evidence for late orogenic extension.

Autran, A. and Guitard, G. 1970. Formation hystérogène de disthène dans les micaschistes mésozonaux a andalousite et sil.limanite de la série paleozoique du Cap de Creus, Pyrénées Orientales. C.R. Acad. Sc. Paris, 270, 2616 - 2619

Carreras, J. 1997. Shear zones in foliated rocks: geometry and kinematics. In: Sengupta, S. (Ed.), Evolution of geologic Structutres in Micro- to Macro-scales. Chapman and Hall. London, pp. 185-201.

Carreras, J. 2001. Zooming on Northern Cap de Creus shear zones. Journal of Structural Geology 23: 1457-1486.

Carreras, J. and Druguet, E. 1994. Structural zonation as a result of inhomogeneous non-coaxial deformation and its control on syntectonic intrusions: an example from the Cap de Creus area (eastern-Pyrenees). Journal of Structural Geology 16: 1525-1534.

Carreras, J., Capellà, I. 1994. Tectonic levels in the Palaeozoic basement of the Pyrenees: a review and a new interpretation. Journal of Structural Geology 16, 1509-1524.

Druguet, E. 2001. Development of high thermal gradients by coeval transpression and magmatism during the Variscan orogeny: insights from the Cap de Creus (Eastern Pyrenees). Tectonophysics, 332: 275-293.

Druguet, E., Passchier, C.W., Carreras, J., Victor, P. and den Brok, S. 1997. Analysis of a complex high-strain zone at Cap de Creus, Spain. Tectonophysics, 280: 31-45.

Wickham, S.M. and Oxburgh E.R. 1986. A rifted tectonic setting for Hercynian high-thermal gradient metamorphism in the Pyrenees. Tectonophysics, 129 (1-4): 53-59.

On Structural Targeting Giant Ore Deposits

Nick Hayward*

Teck Australia Ltd
*Nicholas.Hayward@teck.com

With the current Commodity Supercycle, demand for new resource discoveries is higher than ever. World consumption of copper over the next 25 years will exceed all copper metal ever mined, yet production rates are flat, grades are declining, and discoveries are fewer. Giant ore deposits are very rare, yet they account for the majority share of the world's resource wealth. The top 10% largest Au deposits, for example, account for two thirds of the total value of Au resources. Consequently, one of the biggest challenges for industry and academic geoscientists is to develop innovative new concepts and technologies that significantly improve our capacity to predict and detect the location of buried giant ore deposits. Effective structural targeting of ore giants is one of several critical success factors required to enable this.

Formation of giant ore deposits requires extreme concentration of metals from large source volumes via focused transport into small, highly effective trap sites. The geodynamic setting is critical. Extreme concentration processes are governed by at least two expressions. The first is the Second Law of Thermodynamics**: E = F + TS,** where E = total energy of the system, F = free energy, T = temperature (diffuse heat) and S = entropy. Creating order (i.e. discrete metal concentrations) requires work; that is, a reduction in free energy of the system to maximize total system entropy (TS) and removal of energy gradients. Large metal concentrations require both high total energy input (E) and highly efficient free energy sinks. Energy flux can include stress transfer and the advective energy of magma and aqueous fluid flux along structures. Energy sinks are provided by physicochemical barriers that impede energy transfer.

Trap dynamics can be further characterized by Phillips' law for the rate of mineralization: $\mathbf{Qm} \propto \mu(\nabla T, \nabla P, \nabla C), t$ where fluid flux is determined by the Darcy fluid velocity (μ) integrated over time (t), and mineral precipitation is proportional to gradients in temperature (∇T), pressure (∇P), and solute concentrations (∇C). Extremely high rates of mineralization require both high fluid fluxes and free energy reduction via the work required to overcome large temperature, pressure and/or chemical gradients. These expressions contribute to a quantitative framework for computational modeling of ore systems, as undertaken, for example, by CSIRO researchers in Australia (e.g. Hobbs et al., 2000). They can also be applied qualitatively to 3D mapping and structural targeting in the prediction of giant ore deposit locations, as demonstrated by examples in this presentation.

High mass flux and energy flow requires large-scale permeable structures, typically comprising the weakest crustal to lithospheric-scale fault zones. Explorers recognize that big deposits typically require big structures, but they face challenges in identifying which large-scale structures are best mineralized: many are barren or poorly endowed, and the best structures are frequently the least well defined. Targeting prospective large-scale structures requires shifting from a conventional "top-down" (near surface mapping) approach to a "bottom-up" approach, with emphasis on the deep crustal to lithospheric mantle attributes (e.g. gravity, seismic, magnetotellurics). Important unifying characteristics of the large-scale structural habitat of giant ore deposits include:

- Temporal link to a low bulk strain event, compressional or extensional, following a thermal peak, where maximum permeability achieved.
- Crustal high-strain zones formed parallel to, and linked with, the edge of rigid domain in the lower crust / lithospheric mantle, typically comprising a paleosuture zone or terrain boundary, which may be concealed beneath upper crustal magmatic arcs or sedimentary basins.
- Moderate- to steeply-dipping fault zones with high internal complexity and broad damage zones, linked to deep crustal shears (above).

- Steeply-dipping, second- to third-order, subsidiary structures in hangingwall envelopes of the first-order crustal shear zones, particularly at intersections with steeply-plunging, more tensional oblique fault zones. Buoyant, low-viscosity fluids typically ascend hangingwall structural shortcuts.

Conversely, efficient trap sites commonly form not where it is easiest, but where it hardest, necessitating large reduction in free energy in breaching barriers to energy and fluid flow. These breaches are frequently manifest by rapid release of overpressured fluids that confront the steepest physical and chemical gradients. Energy sinks common to the formation of giant ore deposits include:

- Local extensional jogs/releasing bends within steeply-dipping compressional faults that resist simple shear
- Closed antiformal culminations in aquicludes or sealed intrusion cupolas that dam ascending fluid flow (e.g. syn-orogenic deposits). Also closed synformal culminations that dam descending fluid flow (e.g. syn-sedimentary and supergene deposits).
- Soft-linkages or terminations along fault conduits that traverse rheologically weak rock units or aquifers.
- Magmatic conduit and strata aquifer chokes.

Stochastic energy transfer through the earth's crust typically leads to Self Organized Critical Systems characterized by fractal patterns. Fractal dimensions are recognized in several aspects of ore distribution, such as their power-law size-frequency distribution and spatial clustering. There are also common, but not ubiquitous, quasi-periodic spacing patterns between giant ore deposits that remain poorly documented and poorly understood – a further manifestation of Self Organized Critical Systems. Examples include major orogenic Au deposits (frequently spaced around 30-40 km apart), major stratiform Ag-Pb-Zn deposits in the Carpentaria province of Australia, arc volcanoes along the Pacific Rim, and kimberlite pipe clusters in Africa. Possible controls on spatial periodicity include (Rayleigh-Taylor-like) gravitational instabilities in subarc melt zones, equidimensional convection cells in the seismogenic zone and above extensive sill complexes, or (quasi-)regular-spaced oblique fault set intersections. These processes are not mutually exclusive and likely interact in concert to produce dynamic self-organized systems.

The challenge for researchers and explorers alike remains to integrate all these aspects into a robust and coherent conceptual-exploration model for a step change in prediction and detection success rates for buried giant ore deposits.

A Multi-scale Approach to Giant Hydrothermal Mineral Systems

Bruce Hobbs[1, 2], Alison Ord [1], Weronika Gorczyk [1], Dan Lester [3], Klaus Gessner [1]

[1]Centre for Exploration Targeting, Earth and Environment, The University of Western Australia, WA, Australia
[2]CSIRO Earth Science and Resource Engineering, WA, Australia,
[3]CSIRO Mathematics, Informatics and Statistics, VIC, Australia
*bruce.hobbs@csiro.au

The mineral explorer seeking giant hydrothermal ore bodies faces two fundamental questions: *What kind of geodynamic settings do I look for to host giant hydrothermal systems?* And, having selected the right area on that scale*, where do I focus my attention?* This paper addresses these two questions.

It is becoming clear that some large hydrothermal systems form relatively late in a geotectonic episode in an intracratonic setting at the boundary between older cratonic blocks. A hypothesis is that such boundaries were metasomatised relatively early and a later reactivation-melting-devolatilisation event produced the hydrothermal system; such an event involves the sub-continental lithosphere and is not necessarily intimately associated with a subducting boundary. Examples include the largest hydrothermal systems on Earth: Olympic Dam, Kalgoorlie, Carlin and Witwatersrand. We explore the reactivation of such intracratonic sutures and show that Rayleigh-Taylor instabilities, driven by changes in yield strength, nucleate and evolve at old sutures with low yield stress leading to the introduction of alkaline melts and CO_2 rich fluids into the overlying crust; late deep sedimentary basins flank the instability. We consider the controls on the localisation of such melts and fluids together with the exploration implications.

Most mineralised hydrothermal systems show the development of redox fronts with mineralisation concentrated at or near the maximum gradient in redox. In many instances a pH front is also spatially related to the redox front. These fronts occur at all spatial scales: from the regional scale, where they define the position of mineral camps, to the deposit scale where they define the positions of individual ore bodies, to the outcrop scale where they define the localisation of grade and down to the micro- to nano-scale where they define the positions of metal concentration within say grains of pyrite or arsenopyrite. Such scale invariance (over perhaps 10^{14}orders of magnitude!) is reminiscent of critical systems and is characteristic of non-linear systems not at equilibrium. One common explanation of the fronts is the mixing of two or more fluids that originate in diverse chemical and physical environments. Proponents of fluid mixing need to demonstrate the intricate and intimate fluid mixing regimes that produce scale invariance over a range of 10^{14}. In this paper we explore the proposition that a single fluid is involved and that the fronts with this associated scale invariance arise from instabilities in a chemically reacting advecting environment held far from equilibrium by the influx of fluid and heat.

The keys to the development of both temporal and spatial instability in coupled chemical reactions are (i) the presence of autocatalytic behaviour somewhere in the system of reactions and/or (ii) the presence of some process such as mass diffusion, deformation or fluid advection that physically moves chemical components relative to one another and relative to some initial reference frame. The resulting instabilities can be temporal in nature so that the chemical composition of the system oscillates in time, spatial in nature so that gradients or fronts in chemical composition arise or in the form of travelling waves so that waves of chemical concentration move through the system. We write the chemical equations commonly used in economic geology to describe the deposition of metals or sulphides and the formation of alteration systems with the additional equation: $Fe^{2+}+2Fe^{3+} \rightarrow 3Fe^{3+}+$electron; this reaction is autocatalytic in Fe^{3+} and immediately produces a large spectrum of unstable behaviour both in space and time. A link between pH and Eh is introduced by the reaction: $2H^{+}+2Fe^{2+} \rightarrow 2Fe^{3+}+H_2$. Additional behaviour is introduced by including fluid advection to the standard equations.

Chemical reactions at a moving fluid front introduce a range of new instabilities arising from the heat of chemical reaction (negative for many alteration minerals and positive for sulfides, silicates and oxidation reactions) and associated changes in fluid density and viscosity. Our conclusion is that the rich variety of spatial patterns that are observed in hydrothermal mineral systems can be explained, with exploration consequences, by fluid flow/chemical instabilities arising from the influx of a single fluid. If autocatalytic behaviour is included than an even richer spectrum of behaviour arises. The observed scale invariance follows directly from this behaviour.

Telescoping of Deformation Isotherms on the Main Central Thrust and South Tibetan Detachment: Himalaya of NW India and Southern Tibet

Richard D. Law

Department of Geosciences, Virginia Tech, Blacksburg, VA 24061, USA
e-mail address: rdlaw@vt.edu

Within the central-eastern sector of the Himalayan orogen the highest grade metamorphic rocks, referred to as the Greater Himalayan Series (GHS), are exposed in the Greater Himalayan slab, a 20-30 km thick northward-dipping tectonic unit of metasedimentary and granitic rocks pervasively deformed under mid-crustal conditions. The slab is bounded along the base by the south-directed Main Central Thrust (MCT), and along the top by the South Tibetan Detachment System (STDS) of north-directed normal faults. Structural studies and geochronology indicate that thrusting and normal faulting on the margins of the GHS are broadly synchronous. Both thrust and normal faults initiated synchronously with Miocene prograde metamorphism and melting and, beginning in Early Miocene time, south-southwestward extrusion and exhumation of the GHS between the MCT and STDS has had a profound influence on the geologic and geomorphic evolution of the Himalaya.

It has long been known that while metamorphic isograds along the base of the slab are inverted, isograds at the top of the slab are right way up. The lower and upper surfaces of the slab are ductile shear zones, up to 1.5-2 km wide, in which the isograds have been telescoped (or condensed) by S- and N-directed general shear, respectively. These isograds are defined by metamorphic mineral assemblages of Himalayan age that locally either predate or are broadly coeval with the penetrative shearing and crystal plastic deformation observed at outcrop along the upper and lower surfaces of the slab. However, although numerous field- and microstructures-based studies have addressed the kinematic evolution of the MCT and STDS (e.g. microstructures- and crystal fabric-based shear sense and flow vorticity studies), the thermal evolution of the rocks located along the MCT and STDS during exhumation-related motion on these fundamental fault zones has received little attention.

In this Keynote talk new quantitative data are presented on deformation temperatures associated with flow along both the MCT and the STDS. Deformation temperatures are inferred from the opening angles of quartz c-axis fabrics (Kruhl 1998) that are demonstrably related to crystal plastic deformation associated with southward-directed extrusion and exhumation of the GHS. Caveats associated with using this fabric-based deformation thermometer will be discussed. Data for southward-directed (reverse sense) flow along the MCT at the base of the GHS are taken from the Sutlej River section and Shimla Klippe of NW India. Data for northward-directed (normal sense) flow at the top of the GHS are taken from the Rongbuk area, located on the north side of the Mount Everest Massif in southern Tibet.

MCT: Along the MCT deformation temperatures indicated by quartz fabric opening angles (and recrystallization mechanism) are correlated with both structural position above the MCT and the relative foreland-hinterland positions of the sampling transects. From foreland - hinterland three sampling transects have been completed: a) the Shimla Klippe, b) the western Sutlej River section and c) the eastern Sutlej River section.

In transects on the western part of the Sutlej River section deformation temperatures of c. 615, 600, 560 and 535 °C are indicated by quartz fabric opening angles in mylonitic orthogneisses and quartzites at structural heights of 1150, 750, 200 and 75m, respectively, above the MCT, in agreement with the previously documented inversion of metamorphic isograds above the MCT. These data define a power law relationship between deformation temperature and structural height, with apparent thermal gradients smoothly increasing down section from c. 35 °C per km at 750-1150 m above the MCT, through 80-40 °C per km at 300-750 m and 150 °C per km at 200-300 m above the MCT, to ~ 175 °C per km at 75-200 m above the MCT. The temperature estimates are in good agreement with observed quartz recrystallization microstructures, and indicate that telescoping of deformation isotherms starts at ~ 800-500 m above the MCT and rapidly increases in magnitude traced structurally downwards towards the fault surface.

At a given height above the MCT estimated deformation temperatures are lower in more foreland-positioned transects and are higher in more hinterland-positioned transects. For example, close to the base of the GHS preserved in the Shimla klippe (foreland section), quartz fabrics and recrystallization mechanisms (subgrain rotation with minor grain boundary migration) at 60-80 m above the MCT indicate slightly lower deformation temperatures (510-540 °C) than those recorded at similar structural positions in the western

Sutlej mylonites. In contrast, quartz-rich tectonites located above the mapped position of the MCT in the eastern part of the Sutlej River section (occupying a more hinterland position than the western Sutlej exposures), record the highest deformation temperatures. Deformation temperatures of 685, 640, 625 and 610 °C are indicated by fabric opening angles at 2500, 800, 200 and 20 m above the MCT. These significantly higher deformation temperatures are confirmed by microstructural evidence for widespread quartz grain boundary migration recrystallization and locally prism [c] slip. Only minor telescoping of deformation isotherms is recorded on this most hinterland-positioned section across the MCT, with apparent thermal gradients of 27 °C per km at 2200 - 200 m above the MCT, increasing to c. 85 °C per km at 200-20 m above the fault.

STDS: In the Rongbuk valley three vertical sampling transects were made across GHS schists and gneisses in the footwall to the STDS, with exposures allowing samples to be collected at up to a maximum distance of ~ 550 m beneath the detachment. From north to south these are the Northern, Rongbuk Monastery and Hermit's Gorge transects. Traced towards the north the detachment cuts downward through the thermal structure of its footwall. Maximum deformation temperatures of 650 °C (Rongbuk Monastery) - 680 °C (Hermits Gorge) are recorded at distances of 450-550 m beneath the detachment, decreasing to 490 °C (Hermit's Gorge) to 540 °C (Northern transect) at < 50 m beneath the detachment. Deformation temperatures indicated by fabric opening angles in deformed leucogranite sills are always higher than in adajacent metasedimentary rocks, although the temperature difference is minimal in the thinner (10-20 cm) sills, indicating that the leucogranites were intruded during a relatively late stage of penetrative deformation associated with exhumation of the GHS.

In contrast to the MCT sections, deformation temperatures in the metasedimentary rocks beneath the STDS decrease linearly traced structurally upwards towards the detachment surface in all three transects, defining apparent thermal gradients of 369, 385 and 420 °C per km on the Northern, Rongbuk Monastery and Hermit's Gorge transects, respectively. Isothermal surfaces projected between these three traverses dip at 11° NW, sub-parallel to the sheet dip of foliation in the GHS. The exceptionally steep, apparently linear thermal gradients indicated for the three Rongbuk transects cannot continue to any great depth in the GHS rocks below the floor of the Rongbuk Valley, but must rapidly decrease traced structurally downwards towards the core of the GHS where peak temperatures of c. 700-750 °C are indicated by metamorphic mineral assemblages.

Telescoping of isotherms in the hanging wall to the MCT and footwall to the STDS could be due to a number of tectonic processes acting either singly or in tandem with each other. For the STDS we currently favor a scenario in which the locus of active penetrative deformation migrates up structural section during exhumation progressively accreting rocks that are penetratively deformed at lower and lower temperatures on to the upper margin of the shear zone, with microstructures and fabrics in the structually lower and originally hotter parts of the shear zone being progressively 'frozen in' as they are passively carried to shallower crustal levels.

We have investigated the likely magnitudes of detachment-parallel displacements associated with exhumation of the GHS that are compatible with the observed telescoping of deformation of isotherms in the footwall to the STDS using a range of particle flow path models. The assumed particle paths are very similar to those predicted by Grujic et al. (2002) for channel flow in the GHS, with displacement magnitudes increasing inwards from the walls of the channel to the high temperature core of the GHS. Simple geometric analyses using sections drawn parallel to the local transport direction indicates that detachment-parallel transport magnitudes of 25-170 km are needed to explain the extreme telescoping of isotherms in the immediate footwall to the STDS, depending on assumed originally geothermal gradient, dip of detachment, etc. These particle transport estimates are similar to those previously calculated by Searle et al. (2006) using barometry data of GHS rocks in the Everest region (90-216 km). Although subject to a wide degree of uncertainty, these transport magnitudes are at least compatible with, and probably conservative compared to, transport magnitudes associated with channel flow models for extrusion/exhumation of the GHS (e.g. Beaumont et al. 2001, 2004). However, these displacement estimates are more difficult to reconcile with recently proposed tectonic models in which the GHS was transported southwards on underlying thrusts with the STDS acting as roof fault and playing only a minor role in extrusion/exhumation of the GHS.

Lower Greenschist Facies Oscillations Across the 'Brittle-Ductile' Transition Induced by Alternating Reaction Softening and Hardening

Robert P. Wintsch*[1], Meng-Wan Yeh[2]

[1,]Department of Geological Sciences, Indiana University, Bloomington IN 47405, USA; wintsch@indiana.edu
[2,] Center for General Education, National Taiwan Normal University, Taipei, Taiwan

Reaction textures associated with multiple fabrics in the Red River shear zone show evidence for both brittle and ductile deformation. Rocks on the eastern flank of the shear zone in the Diancang Shan block near Dali, Yunnan Province, China are dominated by granodiorites, many porphyritic, and form the protoliths of the Red River fault rocks. The earliest deformed rocks are cataclasites where fracture processes broke matrix feldspar grains. Even better preserved are grain-scale brittle fractures and crushed regions preserved in the >cm size relic K-feldspar phenocrysts (K), where multiple fractures are filled with newly precipitated quartz (Q, figure below). Progressive deformation has displaced broken K-feldspar fragments into the evolving S-C mylonitic matrix establishing a cataclastic texture with abundant feldspar porphyroclasts.

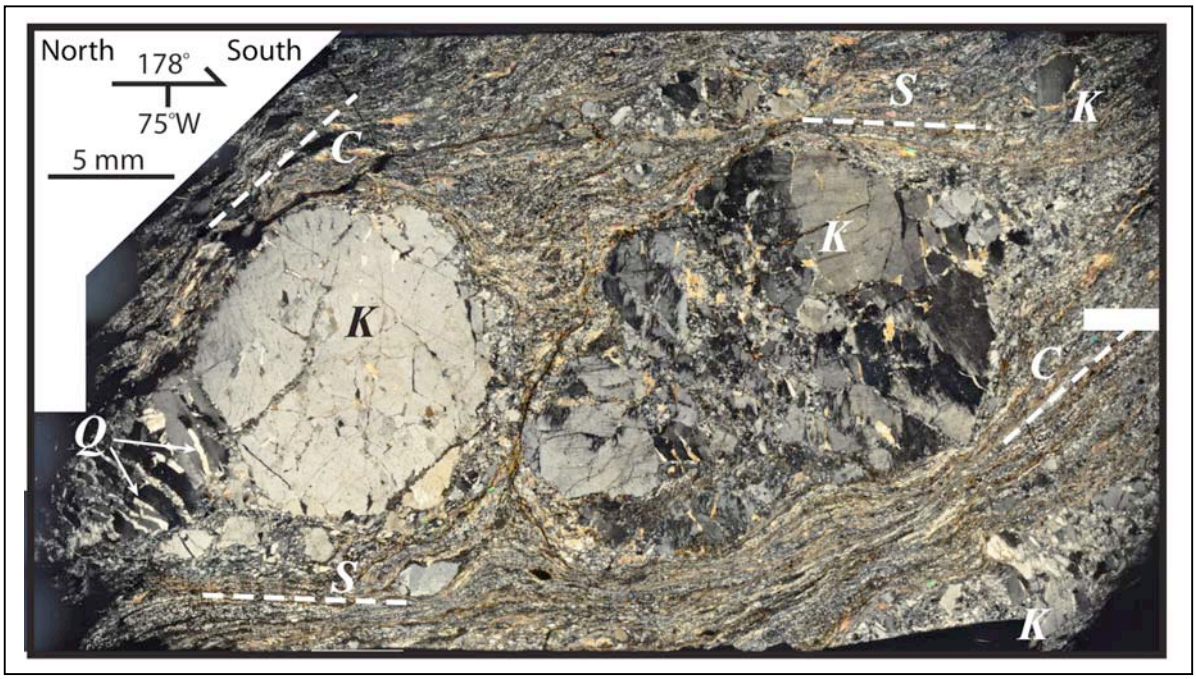

Ductile deformation is manifest in multiple generations of fabrics that wrap around these broken phenocrysts. The fabrics are defined primarily by muscovite and chlorite that may form S-C folia that may exceed the length of a thin section (several cm.). Truncations and embayments of these minerals show that earlier magmatic feldspars and biotites have been dissolved and muscovite + chlorite + quartz are the reaction products. In some samples reaction softening is manifest by the embayment of K-feldspar porphyroclasts by plagioclase, followed by quartz rinds and finally sheaths of muscovite ± chlorite ± quartz that define the mylonitic foliation. In other microstructural sites K-feldspar porphyroclasts themselves are truncated and engulfed by muscovite alone. These relationships suggest the simultaneous operation of the locally metasomatic ionic replacement reactions:

K-feldspar + Na^+ = Albite + K^+, and	ΔV = -10%
3K-feldspar + $2H^+$ = muscovite + 6 quartz + $2K^+$, and	ΔV = -16%
3Albite + K^+ + $2H^+$ = muscovite + 6 quartz + $3Na^+$.	ΔV = - 8%

The latter two reactions produce muscovite and quartz, both much weaker than the reactant K-feldspar; these constitute reaction softening. Moreover, the muscovite tends to align in contiguous

bands constituting textural softening (Shea and Kronenberg, 1993). These reactions occur without any demonstrable change in temperature, and so produce a shift from brittle to ductile behavior. The reactions also involve a volume loss, such that they will be driven by a high normal stress; thus they are deformation induced.

These ductile fabrics are in turn cut by K-feldspar veins that interrupt the mylonitic fabric produced by the above reactions. The K-feldspar veins add K-feldspar to the assemblage, and interrupt the weak fabric. These thus constitute both reaction and textural hardening. Finally these may become boudinaged by continued ductile deformation in the mylonitic matrix, thus establishing a late ductile strain event. Together these overprinting textures and microstructures demonstrate two oscillations of brittle to ductile deformation all at lower greenschist facies conditions where only frictional behavior is predicted by experiments.

Tectonic Interpretation of Metamorphic Tectonites: Integrating Deformation, Metamorphism, Plutonism, and Geochronology

Williams, Michael L.*[1], Jercinovic, M.J.[1], Dumond, Gregory[2], Mahan, Kevin E.[3]

[1] Department of Geosciences, University of Massachusetts, 611 North Pleasant St, Amherst, MA 01003-9297,
[2] Geosciences, University of Arkansas, 18A Ozark Hall, University of Arkansas, Fayetteville, AR 72701,
[3] Geological Sciences, University of Colorado, Campus Box 399, 2200 Colorado AVE, Boulder, CO 80309
*mlw@geo.umass.edu

Calculation of phase equilibria from metamorphic rocks is increasingly feasible and reliable over a broad range of P-T space. However, tectonic interpretations, as well as simple validation, of calculated P-T histories require: (1) integration of deformation on multiple scales and (2) relative and absolute timing constraints on the prograde, peak, and retrograde portions of the P-T path. Both linkages remain a significant challenge. Dynamic models can now be used to explore the thermal and rheological implications of crustal movements, both igneous and tectonic. Strain partitioning near igneous intrusions can complicate relationships, but thermal and rheological gradients (in space and time) are valuable for linking metamorphism, deformation, timing, and tectonics. On a small scale, microstructures link metamorphic and deformation events, but interpretations of Porphyroblast timing relationships can be problematical. Petrologic pseudosections are an increasingly essential tool for interpreting microtextures and for linking deformation, metamorphism, and large-scale tectonics. In-situ geochronology and petrological analysis of chronometer phases (i.e. monazite, xenotime, titanite, allanite, etc.) are a critical part of tectonic analysis of metamorphic rocks, and the electron probe plays an essential role. Compositional mapping of major and accessory phases and especially maps of larger thin section domains are particularly valuable for evaluating strain partitioning, scales of equilibrium, relationships between metamorphic textures and deformational fabrics, and in particular, for interpreting geochronologic data. Isobaric terranes in the southwestern USA (0.3 and 0.7 GPa) and northern Saskatchewan, Canada (1.0 GPa) provide excellent examples of deformation-metamorphism-plutonism interactions, and of the use of in-situ geochronology to illuminate interrelationships between extensive variables. In all areas, the principal role of strain involves providing access to fluids, sites for nucleation and growth of new phases, and especially promoting the removal of unstable (relict) phases. Feedbacks between metamorphism, igneous intrusion, and deformation exist at all scales, and can provide some of the strongest constraints on the tectonic history.

ORAL PRESENTATIONS

Deformation Induced Solution-Creep in the Ductile Lishan Fault Zone, Taiwan

M. Rebecca Stokes*[1], R. P. Wintsch[1], D. L. Bish[1], J. Schieber[1]

[1]Indiana University, Bloomington, USA
*mrstokes@indiana.edu

Textural analysis of slates and quartzites in the Lishan fault zone of central Taiwan suggest that solution-creep was the dominate deformation mechanism active during shearing at shallow crustal levels (< 10 km). The slates on either side of the Lishan fault in the study area display a single pervasive cleavage defined by chlorite and muscovite while the interbedded quartzites are commonly fractured.

Cathodoluminscence (CL) imaging of quartz grains in the slates reveal three distinct populations of quartz: (1) bright red and blue (CL) detrital quartz of mixed provenance, (2) dark blue (CL) authigenic overgrowths, and (3) dark red (CL) metamorphic quartz. CL Quartz textures show sharp truncation boundaries of the detrital quartz and authigenic overgrowths by the chlorite+muscovite folia as well as widespread crystallization of metamorphic quartz in pressure shadows and in elongated patches in the mica dominated matrix. Electron petrography of the phyllosilicates indicates 3 chemically distinct generations of muscovite: (1) detrital muscovite grains, (2) pre-tectonic chlorite-muscovite stacks, and (3) metamorphic chlorite-muscovite folia. Both the detrital grains and chlorite-muscovite stacks are truncated and dissolved by the younger, chlorite+muscovite fabric in the plane of cleavage development. Finally, detrital plagioclase grains with relict patchy zoning are truncated by the mica folia and commonly have quartz pressures shadows. These textures lead to the interpretation that deformation increases the internal energy in the older populations of minerals (by both elastic strain and strain associated with dislocations) thus increasing their solubility, and neo-crystallized, strain-free minerals precipitate in a preferred orientation orthogonal to the principal shortening direction, or plane of cleavage development.

We have assessed the degree of recrystallization of muscovite and quartz from sample to sample using Rietveld refinements of X-ray diffraction patterns and quantitative classifications of CL images. Data collected thus far show that increased proportions of new metamorphic quartz in relation to detrital and authigenic quartz coincides with increased proportions of fabric forming muscovite relative to detrital muscovite, stack muscovite, and detrital feldspars. These petrographic observations and quantitative analyses demonstrate that the deformation-induced dissolution of earlier mineral populations and precipitation of strain-free fabric forming minerals dominates the development of slaty cleavage during greenschist facies deformation.

Distinction Between Deformation and Contact Metamorphism by Very Low-Grade Metamorphism Indicators in the Georgeville Group (Nova Scotia, Canada)

Isabel Abad*[1], J. B. Murphy[2], F. Nieto[3], G. Gutiérrez-Alonso[4], E. Walsh[2]

[1] Dpto. de Geología, Universidad de Jaén. Jaén, Spain
[2] Dpt. of Earth Sciences, St. Francis Xavier University. Antigonish, Canada
[3] Dpto. de Mineralogía y Petrología e IACT, Universidad de Granada, CSIC. Granada, Spain
[4] Dpto. de Geología, Facultad de Ciencias, Universidad de Salamanca. Salamanca, Spain
*miabad@ujaen.es

The Antigonish Highlands are underlain by Neoproterozoic rocks of the Georgeville Group, which record a progressive development of a sedimentary basin within an arc regime, and is a representative of regional extensive arc-related magmatism and basin development, characteristic of the Avalon terrane (Murphy et al., 1999).

The style of deformation in the Georgeville Group is heterogeneous. These lower greenschist-subgreenschist turbidites underwent deformation in an intra-arc basin by strike-slip faulting soon after sedimentation during the Late Neoproterozoic Avalonian orogeny. Throughout the northern and central Antigonish Highlands, the main structural fabric is a weak S_1 cleavage which is typically parallel or sub-parallel to bedding, except in the hinges of rarely preserved F_1 folds where it is penetrative (Murphy et al., 1999). The deformation is much less intense in the southern highlands, where the strata are monoclinal, dip gently to the north and a cleavage is only locally developed, even in the fine-grained lithologies.

In addition, the Georgeville Group is post-tectonically intruded by the Georgeville Granite, which is a central stock, ca. 1.5 km across that is excellently exposed along a coastal section adjacent to the Hollow Fault which is inferred to have acted as a conduit for the intrusion (Murphy et al., 1998). The pluton predominantly consists of leucocratic alkali feldspar granite and pegmatite intruded by steep to moderately dipping aplite and pegmatite dykes. Intrusive contacts with the Georgeville Group are sharply defined and the host rocks show spotted hornfels and moderate to intense silicification, which overprints regional tectonic fabrics.

Geochronological data indicate that the Georgeville Group was deposited at ≈610 Ma, and was polydeformed by ca. 607 Ma. The Georgeville Granite was intruded at ca. 580 Ma during the waning stages of arc activity (Murphy et al., 2008).

The variable development of deformation as well as the post-tectonic plutonism make the Georgeville Group a favourable area to study the influence of typical shallow crustal arc processes on the mineralogy and crystal chemical parameters of these low-grade sedimentary rocks. In order to study the effects of deformation (hereafter, samples LC), the Georgeville Group shales were sampled from the polydeformed northern and central highlands as well as the less deformed southern highlands. The effects of the post-tectonic intrusion were examined by analyzing samples with visible and geochemical evidence for alteration within the contact aureole of the 580 Ma Georgeville pluton (hereafter, samples EW).

X-ray diffraction reveals that all the rocks (LC and EW samples) contain ubiquitous quartz, K-white mica, chlorite and feldspars; there are some chlorite-smectite mixed layers and illite-smectite, only in a few LC samples. The pressure and temperature of mineral growth can be determined from the crystal-chemical parameters of the white mica and are widely used to discriminate between diagenetic, anchizone, and low-grade metamorphic processes. In the LC samples, Kübler Index (KI, "illite" crystallinity) values measured in the 10 Å peak of the <2 μm fraction are lower (higher crystallinity) for the polydeformed samples (epizone - high anchizone, KI ≤0.30 Δ2θ) and higher (lower crystallinity) for the monoclinally dipping strata (diagenetic - low anchizone, KI >0.30 Δ2θ). The range of the b-cell dimension of the K-white micas is 9.023-9.049 Å in the LC samples, with an overall average value of 9.035 Å consistent with regional metamorphism at a depth of 3-5 kbar. However, in the EW samples, KI values correspond to deep diagenesis (KI= 0.42-0.76 Δ2θ) except

only for three samples (low anchizone, KI= 0.32-0.39 Δ2θ) and b parameter (8.977-9.004 Å) is typical of low-pressure conditions (1-2 kbar).

The crystal-chemical results from the regional (LC) and contact aureole (EW) samples are clearly different and comparison between the two sets of samples allows characterization of the extent of overprinting of the regional signal due to the intrusion. In the area dominated by regional metamorphism, the highest grade samples (epizone - high anchizone) occur in the polydeformed regions, which corroborates the importance of tectonic stress as a driving force for the reaction progress of the clay minerals. The EW samples, affected by the Georgeville intrusion, were from the polydeformed area and show crystal-chemical data coherent with an equilibration at a lower crustal level (1-2 kbar for the samples affected by the intrusion vs 3-5 kbar for the non-affected ones), giving an indication of the amount of uplift between 607 and 580 Ma, which coincides with the waning stages of arc development. This pluton is small but very fluid rich as indicated by the abundance of pegmatites and extensive contact aureole, and intruded adjacent to the Hollow Fault. These observations, combined with our results are indicative of the important roles that fluids and structures play in the re-equilibration of the host rock to lower pressure assemblages. More generally, our approach of comparing crystal-chemical parameters of the white mica in low-grade regional metamorphic rocks with those in the same lithologies overprinted by contact metamorphism may provide constraints on the amount of crustal uplift during the latter stages of an orogenic cycle.

References

Murphy JB, Anderson AJ, Archibald DA (1998) Can. J. Earth Sci., 35, 110-120.
Murphy JB, Nance RD, Keppie JD (1999) Tectonophysics, 305, 183-204.
Murphy JB, Dostal J, Keppie JD (2008) Tectonophysics, 461, 181–201.

Porphyroblast inclusion trails : key to unfolding the history of the Ibero-Armorican- and Central-Iberian oroclines

Domingo G.A.M. Aerden*[1]

[12] Departamento de Geodinámica, Universidad de Granada, Spain
[2]Instituto Andaluz de Ciencias de la Tierra (IACT), CSIC-UGR, Granada, Spain
*aerden@ugr.es

The term Ibero-Armorican Arc was coined by Matte and Ribeiro (1975) for a 180° curved segment of the Variscan orogen whose existence has been known at least since Baker (1936). During the Mesozoic break-up of Pangea, the arc became segmented in three pieces. The North American piece, located offshore New Foundland, is covered by shelf sediments. The European and Iberian pieces are well exposed in the Armorican and Iberian massifs. Amongst the different tectonic units that make up these massifs, there is a high-grade nappe complex, which includes remnants of the Siluro-Devonian Rheic Ocean that separated Gondwana and Laurrusia prior to their collision.

The origin of the Arc has been a long standing question with interpretations ranging from (1) an inherited pre-Variscan structure, (2) progressive indentation tectonics, and (3) late oroclinal bending of an originally straight orogen (Ries and Shackleton, 1976). Here presented new and published data (Aerden, 2004) concerning the orientation of porphyroblast inclusion-trails demonstrate oroclinal bending as a consequence of drastic change in crustal shortening direction. The same model has been concluded independently based on recent paleomagnetic work in NW Spain (Weil, 2000).

I collected over 4000 measurements of the strike of inclusion trails in a total of 70 samples from five study areas. (Fig. 1). In fifteen of these samples, additional FIA (Foliation Intersection Axes) trends could be directly determined using the technique of Hayward (1991). The combined data reveal the existence of four FIA generations in the Variscan orogen with distinctive geographic trends and showing consistent overprinting relationships. The third generation FIA trend (FIA3; solid black in Fig. 1) is conspicuously developed in most of the investigated samples and represents the Variscan orogenic trend as it was prior to the oroclinal bending. Oroclinal bending was associated with the development of FIA4 related microstructures and macroscopic folds that overprinted the FIA3-related ones.

Two early FIA sets (FIA1 and FIA2) were found to be preserved only in the alochtonous high-grade nappe complex of NW Iberia and southern Brittany, in agreement with older metamorphic ages obtained in these units by previous workers. Their respective trends (E-W and NNW-SSE) are not reflected in the geometry of map-scale scale structures, but small-scale correlative fold generations with these trends are locally preserved in low-strain zones weakly affected by subsequent deformation.

The younger two FIA generations (FIA3 and FIA4) correlate with pervasive crenulation cleavages, and associated regional-scale folds whose overprinting geometries also witness a major change in crustal shortening direction. This led to the development of a double "S"-shaped oroclinal structure of which the Ibero-Armorican Arc is only the northern part. A second, east-closing orocline in the south, largely covered by younger sediments, was discovered by Aerden (2004) as a consequence of combining conventional structural analysis with quantitative inclusion trail data. Its existence has been recently acknowledged by Martínez Catalán (2010) who has named it the "Central Iberian Arc" (Fig. 1).

Aerden, D.G.A.M., 2004. J. Struct. Geol. 26, 177-196.
Matte P, Ribeiro A 1975. C.R. Acad. Scs., Serie D, 280-25, 2825-2828.
Baker, H.B., 1936. Structural features crossing the Atlantic. Mich. Acad. Sciences, March 20.
Ries, A.C., Shackleton, R.M., 1976. Phil. Trans. Royal Soc. London A 283, 281–288.
Martínez Catalán, J.R., 2010. GSA Annual Meeting, Denver, Colorado USA (abstract)
Weil, A.B., et al. Van der Voo, R., Van der Pluijm, B. A., Parés, J.M., 2000. J. Struct. Geol. 22, 735-756.

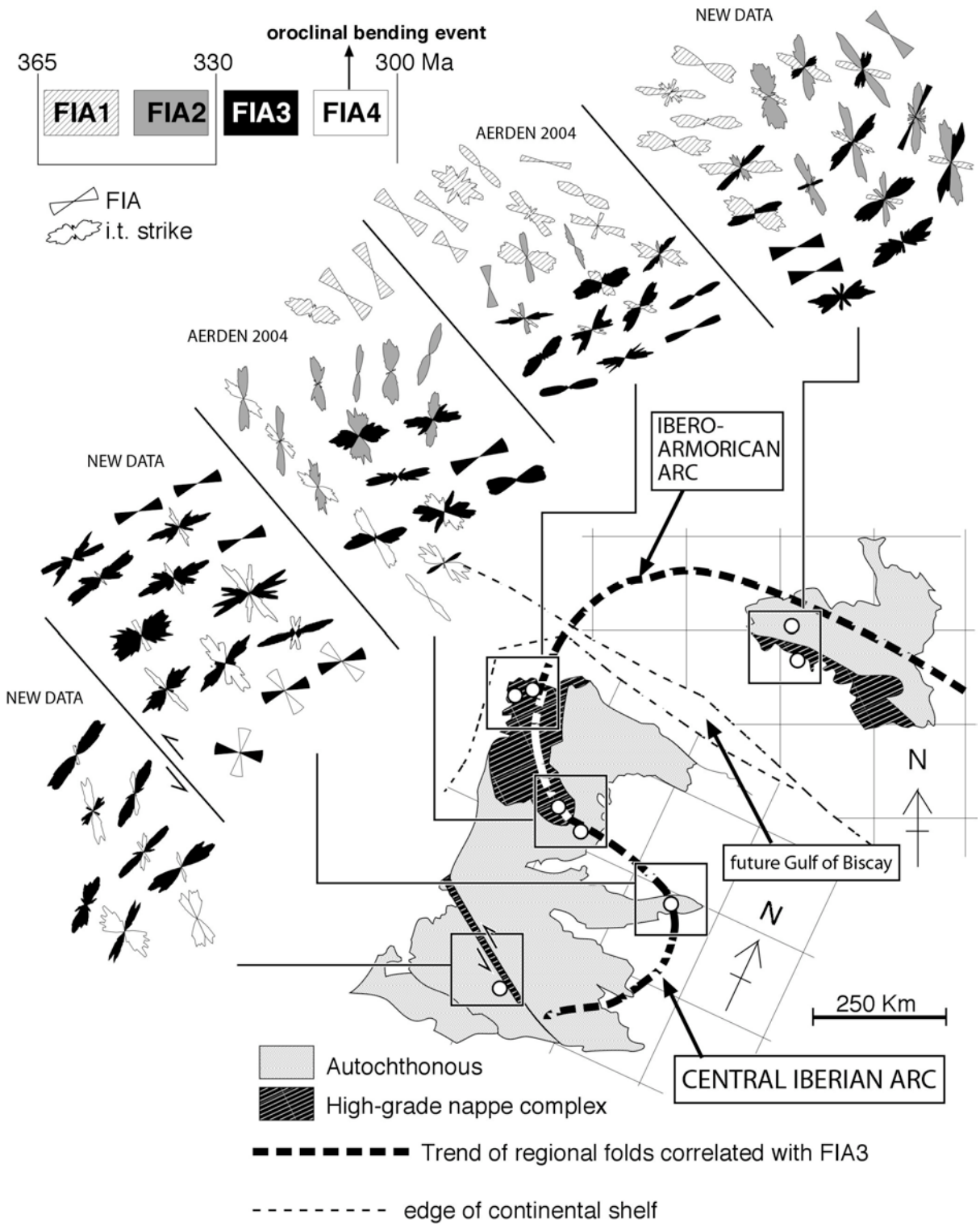

Fig. 1. Rose diagrams for 4134 strike measurements of inclusion trails in 70 porphyroblastic samples from five study areas, plus FIA trends (double pie-cake symbols) for fifteen of these samples. Four FIA generations are witnessed. Their inferred ages are based on tentative correlation with dated macroscopic fabrics. The map is a late Permian reconstruction of the Ibero-Armorican Arc, obtained by closing the Gulf of Biscay, which involves 25° back-rotation of Iberia. Inclusion trail patterns show a remarkable match in this reconstruction between Iberian and Armorica. The double, S-shaped oroclinal structure is defined by FIA3 related structures (heavy dashed line). They became curved during development of FIA4 but their original (pre-orocline) orientation is preserved as FIA3 inclusion trails.

Deformation Partitioning and Porphyroblast Growth

Asghar Ali*

Department of Geology, University of Peshawar, Pakistan
*asghar. ali@upesh.edu.pk

An identical succession of five foliation intersection/inflection axes preserved in porphyroblasts (FIAs) in a small scale mining pit area and the large scale Balcooma region shows that there were five changes in the direction of bulk shortening during tectonism between ~476±5 and 408.8±8.9 Ma. The E-W trending FIA set 1 in garnet porphyroblasts indicates N-S shortening. The NNW-SSE trending FIA set 2 in staurolite suggests rotation of the direction of shortening to ENE -WSW. The NNE-SSW trending FIA set 3 in staurolite, plagioclase and kyanite porphyroblasts suggests ~30° rotation of the bulk shortening direction to ESE-WNW between 443.2±3.8 Ma and 425.4±3.7 Ma. The E-W trending FIA set 4 in staurolite porphyroblasts indicates further rotation to N-S by 408.8±8.9 Ma. The NE-SW trending FIA set 5 in andalusite suggests subsequent rotation of the bulk shortening direction to NW-SE. Structural and metamorphic data from porphyroblasts reveal a continuous history of tectonism that is partitioned between samples in the mining pit as well as regionally. The succession of FIA sets and microstructural relationships between garnet, staurolite, plagioclase, kyanite, andalusite, cordierite and fibrolitic sillimanite reveal a regionally consistent pattern of growth during this progression of changes in the direction of bulk shortening. The local coexistence of kyanite, andalusite and sillimanite and a consistent succession in the timing of growth of the different porphyroblastic phases resulted from the effects of deformation partitioning relative to bulk composition and P-T path. Similarly distributed FIA sets 1, 2 and 3 across the pit as well as in the Balcooma region suggest that the partitioning of deformation was relatively pervasive at all scales across the Balcooma Metamorphic Group from ~476±5 to 425.4±3.7 Ma. The preferential development of FIA set 4 in the northern half of the region reveals more localized deformation partitioning effects during this period of bulk shortening.

Two-Stage Partial Melting and the Different Cooling History Within the Higher Himalayan Crystalline Sequence in the Far-Eastern Nepal Himalaya

Takeshi Imayama*[1], Toru Takeshita[2], Keewook Yi[3], Deung-Lyong Cho[4], Kouki Kitajima[5], Yukiyasu Tsutsumi[6], Masahiro Kayama[7], Hirotsugu Nishido[7], Tasuku Okumura[7], Koshi Yagi[8], Tetsumaru Itaya[7], Yuji Sano[9]

[1]Center for Chronological Research, Nagoya University, Nagoya 464-8602, Japan
[2]Department of Natural History Sciences, Hokkaido University, Sapporo 060-0810, Japan
[3]Geochronology Team, Korea Basic Science Institute, Chungbuk 363-883, Republic of Korea
[4]Korea Institute of Geoscience and Mineral Resources, Taejon 305-350, Republic of Korea
[5]Department of Geoscience, University of Wisconsin, Wisconsin 53706, USA
[6]Department of Geology and Paleontology, National Museum of Nature and Science, Tokyo 169-0073, Japan
[7]Research Institute of Natural Sciences, Okayama University of Science, Okayama 700-0005, Japan
[8]Hiruzen Institute for Geology & Chronology, Okayama 703-8248, Japan
[9]Center for advanced Marine Research, Ocean Research Institute, The University of Tokyo, Tokyo 164-8639, Japan
*imayama@nendai.nagoya-u.ac.jp

U-Pb zircon ages from the high-grade High Himalayan Crystalline Sequences (HHCS) and leucogranites revealed that two-stage partial melting occurred in far-eastern Nepal Himalaya. At the middle structural level of the HHCS, the inner and outer rim zircon ages of c. 20 and c. 17 Ma from kyanite-sillimanite migmatitic gneiss probably represent the muscovite dehydration melting at the peak *P-T* conditions of c. 10.5 kbar, 740 °C, and the subsequent crystallization by the melt-consuming reaction at retrograde stage, respectively. At the middle-upper structural level of the HHCS, the growth of inner rim zircon in sillimanite migmatitic gneiss occurred at c. 30 Ma (Early Oligocene) accompanied by biotite dehydration melting at peak *P-T* condition of c. 8 kbar, c. 760 °C. Subsequently, the outer rim zircons crystallized at c. 24 Ma, which could have been caused by the Zr-release by garnet breakdown during the hydration reaction to produce biotite on cooling. The inner rim zircon age of c. 18 Ma (Early Miocene) from biotite-muscovite leucogranite crosscutting the Early Oligocene sillimanite migmatitic gneiss could have been associated with anatectic melting, while the outer rim zircon age of c. 16 Ma represents the timing of new zircon growth by melt crystallization on cooling, based on the presence of oscillatory zoning. Based on the same FT zircon age of c. 6 Ma and the different U-Pb zircon rim ages of the two different migmatites, it is inferred that the Early Miocene and Early Oligocene migmatites had been juxtaposed by 6 Ma, and the estimated cooling rates for the two migmatites are c. 35 °C/My and c. 20 °C/My, respectively, probably indicating much higher exhumation rate in the former than in the latter migmatites. These results combined with the *P-T* paths, inferred from petrogenetic *P-T* grid and melt-consuming reactions, imply that the Early Miocene migmatite had been buried when the Early Oligocene migmatite had been exhumed. Two-stage partial melting and the different cooling history could have resulted from the return flow of the previously buried rocks and the associated tectonic loading by overthrusting, which as a whole occurred as corner flow within the orogenic wedges (i. e. multiple channel flows).

Anatomy and Thermotectonic History of a Shear Zone in the Core of the Canadian Cordillera, and its Role as the Basal Décollement of the Retrowedge at ca. 85-60 Ma

Sharon D. Carr*[1], Philip S. Simony[2]

[1]Ottawa-Carleton Geoscience Centre, Department of Earth Sciences, Carleton University, 1125 Colonel By Drive, Ottawa, ON, K1S 5B6
[2]Department of Geoscience, University of Calgary, 2500 University Drive NW, Calgary, AB, T2N 1N4
*scarr@earthsci.carleton.ca

The ~400 km wide, east-verging, retrowedge of the southeastern Canadian Cordillera was predominantly formed in a tectonic setting of oblique plate convergence during the Cretaceous to Eocene. The Late Cretaceous to Eocene metamorphic core in the Internal zone is situated ~200 km behind the coeval east-verging foreland thrust belt in the External zone. That 200 km of separation, in the central part of the retrowedge, is occupied by a relict Early Cretaceous orogen including that part of its metamorphic core that was not overprinted by Late Cretaceous metamorphism or deformation. In the External zone, no megathrust sheet or crystalline sheet with a basal shear zone overrode the foreland thrust belt as is the case is some other orogens such as the Appalachians, Caledonides and Himalaya. Thus, in the southern Canadian Cordillera, the geometric and kinematic linkages between the Internal zone and External thrust belt can be reconstructed. Thin-skinned, piggyback thrust and fold systems in the External zone accommodated ~180 km of Late Cretaceous to Eocene shortening and root westward into the Rocky Mountain basal décollement that extended westward, at the base of the retrowedge into the Internal metamorphic core zone. In the Internal zone, rocks that were deformed and metamorphosed in the mid-crust during the Late Cretaceous to Eocene were exhumed in the Eocene and are exposed as tracts of metamorphic rocks and metamorphic core complexes (e.g. Kettle, Okanagan, Priest River and Valhalla), some of which are basement-cored domes (e.g. Frenchman Cap, Thor-Odin, and Spokane). The Late Cretaceous to Paleocene top-to-the-east, ductile, thrust-sense Gwillim Creek shear zone is exposed in the Valhalla and Spokane domes and on the flanks of the Monashee complex, and can be directly linked eastward to the 200 km wide central portion of the Rocky Mountain basal décollement and to the coeval Lewis-Bourgeau thrust system in the External zone.

The Gwillim Creek shear zone is estimated to be 5 to 7 km thick on the basis of the exposed thickness of strained rocks and interpretation of seismic reflection data in the Valhalla complex. It was activated in the Late Cretaceous at ~85 Ma and was reactivated ~65-60 Ma based on relationships between dated plutons and pegmatites, and sheared rocks. The timing of the youngest stage of displacement across the Gwillim Creek shear zone is constrained to the interval between ~65 Ma and ~60 Ma based on the ages of syn-tectonic leucosome, deformed pegmatite, deformed yet cross-cutting ~63 Ma plutonic rocks and syn-tectonic monazite. At the deepest exposed levels of the shear zone, linked microstructural and thermobarometry studies show that flow took place at ~800°C and 800 MPa and was accompanied by anatexis. In the Paleocene, the Gwillim Creek shear zone was refrigerated from below prior to cooling of the overlying rocks in its hanging wall, as a result of overthrusting of hot rocks over cold footwall rocks. This interpretation is based on petrological evidence that the deepest exposed structural levels in the Gwillim Creek shear zone were quenched prior to quenching of overlying rocks in the hanging wall of the shear zone. The hot rock mass above the Gwillim Creek shear zone was translated up and over a low-angle, 10-12 km high frontal ramp. The quenching at its base is explained by cooling from below on the cool upper "flat" east of the ramp. The ramp geometry of the Gwillim Creek shear zone is supported by geologic relationships showing that it cut upward in the eastward direction of transport, as well as southward, relative to layers in the plutonic and structural edifice in its hanging wall. It is also consistent with evaluation of thermal models.

To the east of the Internal zone lies the aforementioned Early Cretaceous relict orogen, nested within the central part of the retrowedge. The Late Cretaceous to Paleocene Gwillim Creek shear zone cannot emerge there because structures and metamorphism are all older than the shear zone; they are pre-mid-Cretaceous as established by the ca. 110-90 Ma dates of cross-cutting plutons and metamorphic cooling. Thus the Gwillim Creek shear zone is interpreted to extend beneath the retrowedge as the Late Cretaceous Rocky Mountain basal décollement. The most westerly thrusts that could be connected to the Late Cretaceous Gwillim Creek shear zone are those of the Hosmer-Wigwam-McDonald-Bourgeau thrust system that daylight west of and were directly linked with the Lewis thrust system. The early ~85-75 Ma motion on the Gwillim Creek shear zone may have been largely taken up by this composite thrust system. Subsequent motion on the Gwillim Creek shear zone, between ~75 and ~60 Ma, would have been largely taken up by the Lewis thrust. Similarly, two stages of progressively younger deeper shear zones in the Internal zone are interpreted to have progressively reactivated the Rocky Mountain basal décollement and connected with coeval thrust systems in the External zone. These are the Paleocene to Eocene Monashee décollement linked to the McConnell thrust system and an inferred Eocene subsurface basal shear zone linked to thrusts of the Foothills and triangle zone.

During orogenesis, the craton was progressively underthrusting the developing retrowedge. The developing retrowedge and the rocks above the Late Cretaceous Gwillim Creek shear zone would have served to insulate the underlying rocks of the incipient Internal zone of the orogen, thus resulting in a mechanism of progressive heating, weakening and localization of the basal shear zone. At the base of the wedge, cooler stiffer rocks lay to the east of the Internal zone, at each stage, acting as an indentor. Thus, the development of a basal shear zone was coupled with flow of the hot mass of the internal zone up and over an indentor, strain softening of it, and incorporation of it into the wedge in successive stages. The base of the exposed Gwillim Creek shear zone serves as an example of the basal shear zone and décollement that was active in the Late Cretaceous to Paleocene; it was refrigerated from below, prior to that of overlying rocks in its hanging wall, as a result of overthrusting of hot rocks over cold footwall rocks. Our general model is consistent with those of Beaumont et al. demonstrating the lateral transition from stiff cool crust to hotter weaker crust where the stiff cool crust acted as an indentor, with development of a ramp at the edge of the indentor, and flow up and over the ramp.

Role of metasomatism on the formation of shear zones: an example from a metagranodiorite in the Aar massif (Central Alps)

Philippe Goncalves*[1], Emilien Oliot [1], Didier Marquer[1]

[1]Laboratoire Chrono-Environnement, CNRS / Université de Franche-Comté, Besançon, France
*philippe.goncalves@univ-fcomte.fr

The formation of a shear zone, in a homogeneous host-rock, requires firstly its nucleation on a pre-existing structural discontinuity, like a discrete brittle fracture (e.g. Mancktelow and Pennacchioni, 2005) and secondly the maintenance of a weak rheology (low stress) in a narrow domain in order to allow the propagation (broadening) of the shear zone (Holyoke and Tullis, 2006). Maintenance of the weakness is likely due to textural changes (grain-size reduction, formation of fined-grained polyphased aggregates, development of a preferred orientation, interconnection of an initially dispersed weak). The maintenance can also be promoted by dramatic mineral transformations due to syn-kinematic metamorphic reactions governed by changes in P-T conditions and metasomatism. Indeed, if deformation occurs under water saturated conditions, material transport in the fluid phase can be expected across and along the shear zone if gradients of chemical potential, composition, temperature or pressure are present (Dipple & Ferry, 1992). With material transport, metasomatic reactions can produce new assemblages favorable for the maintenance of weakness in th shear zone.

The formation of a shear zone (from its nucleation to its broadening) is therefore characterized by numerous mineralogical and geochemical changes produced by fluid-rock interactions during deformation (e.g. Oliver et al., 1990, Wibberley, 1999). The ability of predicting the mineralogical and geochemical evolution during syn-deformation fluid-rock interactions is critical to either estimate PT conditions of deformation or better understand the processes of shear zone formation. The main goal of this contribution is to test a model of shear zone formation where mass transfer and associated mineral reactions are expected to play a major role on the shear zone broadening.

We have performed a forward thermodynamic modeling on a well-characterized decameter-sized Alpine shear zones developed in the Variscan Grimsel granodiorite (Central Alps, Switzerland) (Choukroune & Gapais 1983; Marquer et al. 1985; Gapais et al. 1987). The main chemical and mineralogical features observed in the shear zone of the Grimsel granodiorite are :

(1) Loss of CaO and Na2O coupled with a gain in MgO and H2O.
(2) Crystallization of large amounts of phengite and albite with epidote at the expense of K-feldspar and plagioclase in the orthogneiss, mylonite and ultramylonite.
(3) In the highest strained sample (ultramylonite and shear bands in the orthogneiss and mylonite), the system becomes Ca-free and chlorite crystallizes in equilibrium with phengite, biotite and albite. Epidote is no more present.
(4) Phengite produced by the breakdown of K-feldspar has a limited range in Si-content from 3.25 to 3.3 p.f.u. In contrast, in the chlorite-bearing ultramylonite, the amount of Tschermak substitution in phengite decreases continuously from 3.25 to a minimum value of 3.15 Si p.f.u.

In order to determine the reactions involved during shear zone broadening and quantify the amount mass transfer associated with the reactions, we have performed a thermodynamic modeling using petrogenetic grids and pseudosections that consider variations in chemical potential (μ) of the mobile components (MgO, CaO, and Na2O) at fixed P and T. The choice of the determinative variables in this modeling is dictated by our conceptual model of the shear zone and what we assume to be the driving force of mass-transfer and metasomatic/metamorphic reactions.

In our conceptual model, the shear zone is a disequilibrium system that can be divided in two end-member sub-systems where local equilibrium is applicable. The first sub-system (A) corresponds to the unaltered and undeformed granodiorite re-equilibrated under the PT conditions of the deformation. The sub-system (B) is the metasomatised chlorite-bearing ultramylonite in equilibrium with a buffered externally-derived fluid. The interface A/B is

characterized by chemical potential gradients. To reach equilibrium, the chemical potential gradient is equalized by metamorphic/metasomatic reactions and diffusion of component down chemical potential gradient in a static fluid between the chlorite-bearing ultramylonite (B) and the wall-rock (A). Therefore, we assume that the propagation of the shear zone is due to a process of equilibration, by diffusion, of the unaltered host-rock with the highest strain rock.

On a pseudosection µMgO-µCaO calculated at 450°C and 6 kbar with the "partial" unaltered granodiorite composition, we are able to superimposed the calculated chemical potential of MgO and CaO conditions of the five studied samples (see stars in figure 1). Consequently it is possible to define the µ-µ path followed during the equilibration of the wall rocks (sub-system A) towards the chlorite-bearing ultramylonite (sub-system B) and predict the mineralogical and geochemical changes induced. It appears that the process of equilibration of the wall rocks (µ-µ path) is responsible for the formation of phyllosilicates via two mains univariant reactions: Kf + ep + ab = mu + q and ep + ab + bio = chl + mu + q. When the rock is fully equilibrated with the chlorite-bearing ultramylonite, pseudosections predicts that the system is CaO-free and has gained up to 150% of MgO in good agreement with observed mass transfer. The production of up to 35 vol% of phyllosilicates during the process of equilibration is responsible for the broadening of the shear zone.

The µMgO-µCaO pseudosection contoured for the Si content of white mica (figure 1b) shows that the process of equilibration of the host rock with the chlorite-bearing ultramylonite during the shear zone broadening induces a decrease of Si-content of phengite from 3.26, when in equilibrium with K-feldspar + epidote + albite down to 3.12 p.f.u when white mica is in equilibrium with the chlorite-bearing assemblage at the same P-T conditions. In this case, the observation of slightly substituted phengite in equilibrium with chlorite in the ultramylonite may be incorrectly interpreted in terms of decompression, while it is due to syn-deformation metasomatism at peak metamorphic conditions. This is a good example showing that application of thermobarometry on metasomatized rocks is not without pitfalls.

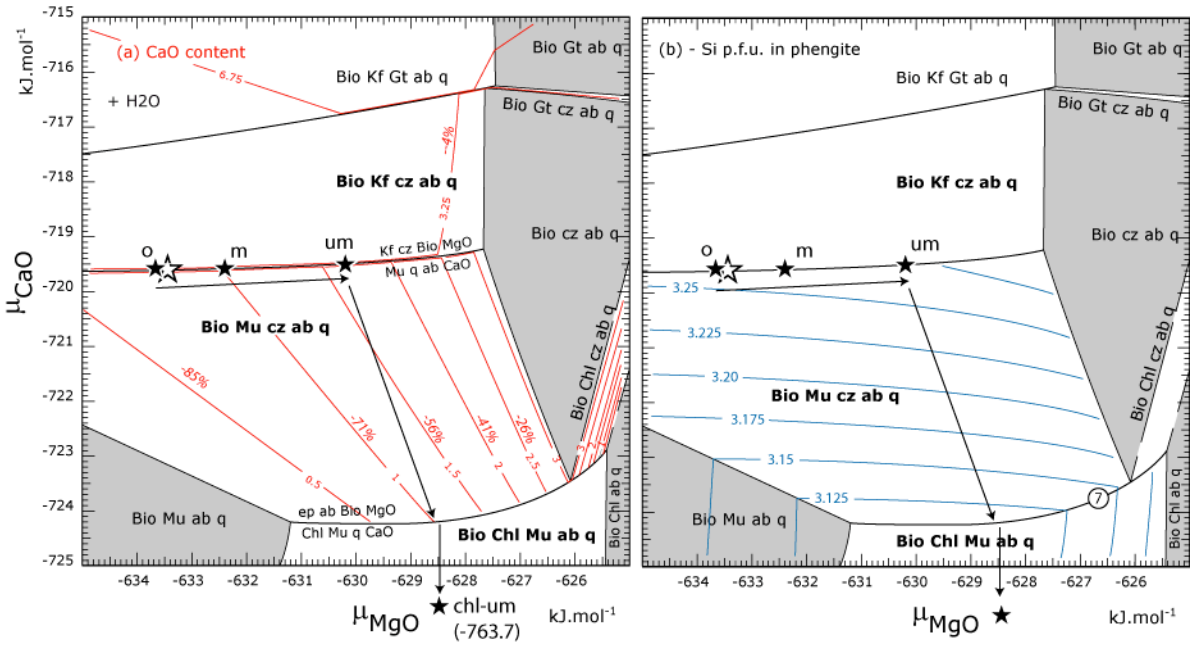

Figure 2. Quantitative µCaO-µMgO pseudosection calculated at 450°C and 6 kbar for the unaltered granodiorite "partial" composition at water-saturated conditions contoured for (a) MgO content in wt% of the system and (b) for Si-content p.f.u in white mica.

More generally, we conclude that metasomatism during shear zone broadening is controlled by (1) the sequence of mineral reaction involved during the process of equilibration, (2) the bulk compositions of two end-member rocks in contact (i.e. the unaltered host rock and the most metasomatised high strain zone) and (3) in a lesser extent P-T conditions.

Tectonometamorphic Evolution During the Permo-Triassic Orogeny in the Korean Peninsula: Evidence From Porphyroblasts in the Late Paleozoic Metasedimentary Rocks

Hyeong Soo Kim*

Department of Earth Sciences Education, Kyungpook National University, South Korea
*hskim@knu.ac.kr

The Permo-Triassic orogeny (Songrim or Indosinian orogeny) in South Korea is one of the major tectonic events to form the Korean peninsula associated with continental collisions in the eastern Eurasia margin. Structural and metamorphic characteristics of the Songrim orogeny are intensively studied in each the Paleozoic terranes (Taebaeksan basin, Okcheon basin, and Imjingang belts), but correlation of the orogeny between the different tectonic terranes is still uncertain and poorly understood.

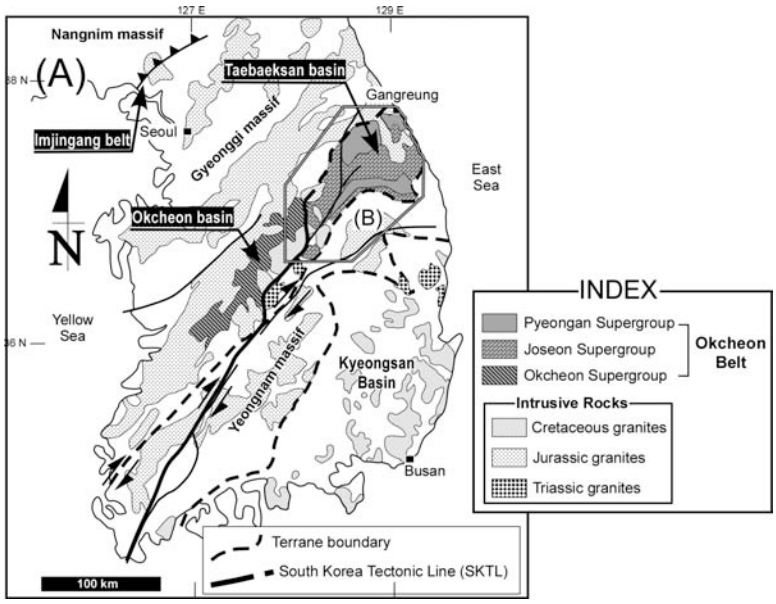

Fig. 1. Schematic tectonic map showing major sedimentary basins, orogenic belts, cratonic blocks (massif), and other geologic features in South Korea.

Foliation intersection/ inflexion axes (FIA) and the Barrovian-type medium pressure regional metamorphism, developed in the Pyeongan Supergroup in the northeastern flank of the Taebaeksan basin, are used to reveal the Permo-Triassic tectono-metamorphic evolution in South Korea. FIA trends of the porphyroblasts are grouped into two sets, NNW–NNE (set 1) and ENE–WNW (set 2), those are produced by the two contractional deformations (D_1 and D_3) and extensional deformation (D_2 and D_4) with the medium pressure regional metamorphism. The syn-D_1 chloritoid and, syn-D_1 and post-D_2 andalusite porphyroblasts preserved FIA set 1, whereas syn-D3 garnet and staurolite, and syn-D4 and/or post-D4 andalusite porphyroblasts contained FIA set 2. These observations indicate not only that these porphyroblasts have grown under E-W and N-S crustal bulk shortening, but also that directions the crustal bulk shortening changed from the E-W to N-S during the late Permian to Triassic Songrim orogeny.

The similar bulk shortening events with the Barrovian-type regional metamorphism have occurred in the Imjingang belt (N-S bulk shortening) and the Okcheon basin (NE-SW and E-W bulk shortening; Lee, 2000) during the Permian to Triassic. The characteristics and relative timing of the tectonometamorphic evolution of the Paleozoic metasedimentary rocks in three different tectonic regimes suggest that the ENE-WSW and E-W crustal bulk shortening operated on the Taebaeksan and Okcheon basins during the early stage of the Songrim orogeny, and then the N-S crustal bulk shortening dominantly activated in the Taebaeksan and the Imjingang belt during the Triassic.

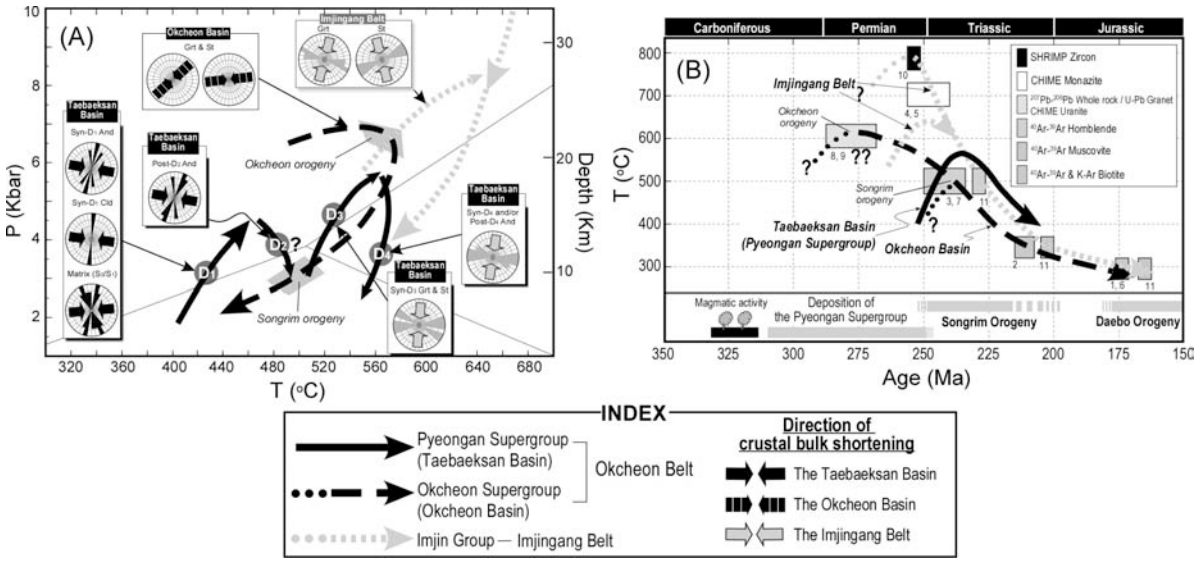

Fig. 2. (A) Pressure-Temperature-deformation (P-T-d) paths combined with FIA trends of the late Paleozoic terranes in South Korea: Taebaeksan basin (Kim and Ree, 2010), the Okcheon basin (Min and Cho, 1995; Cho and Kim, 2005; Lee, 2000), and the Imjingang belt (Kim, 2002; Cho et al., 2007; Kim and Jung, 2010). The black and gray colored thick arrows in the rose diagrams represent the direction of the crustal bulk shortening in each terrane. **(B)** The late Paleozoic Temperature-time (T-t) paths of the Taebaeksan basin, the Okcheon basin, and the Imjingang belt. Although timing of the peak temperature is a little bit different from each terrane, the trend of cooling history is almost identical. Numbers in the bottom of the boxes refer to the chronologic source data: 1 = Cliff et al. (1985), 2 = Min et al. (1995), 3 = Oh et al. (1995), 4 = Cho et al. (1996), 5 = Ree et al. (1996), 6 = Park and Cheong (1998), 7 = Cho et al. (1999), 8 = Cheong et al. (2003), 9 = Cho et al. (2005), 10 = Cho et al. (2007).

Microscale Stress and Strain Distributions, Fabric Evolution, and Crustal Seismic Anisotropy

Scott E. Johnson*[1], Senthil S. Vel[2], Christopher C. Gerbi[1], Alden Cook[2], Won Joon Song[1], Félice M. J. Naus-Thijssen[1], Andrew J. Goupee[2]

[1,3]Department of Earth Sciences, University of Maine, USA
[2]Department of Mechanical Engineering, University of Maine, USA
*johnsons@maine.edu

The grain-scale distributions of stresses and strains in rocks are generally thought to control, or strongly influence, diffusion processes and sites of metamorphic reaction, sites of dissolution-precipitation, nucleation of new metamorphic minerals, plastic strain energy in the form of dislocations, local fluid pressure gradients, and seismic wave speeds to name a few. In this presentation we focus on the use of numerical modeling to evaluate grain-scale elastic stress and strain distributions, and discuss implications for local fluid pressure gradients, transient permeability arising from anisotropic thermal expansion, and the contribution of grain-scale stress and strain fluctuations to seismic wave speeds.

Numerical modeling of microstructures is the most direct, and possibly the only, way to investigate the detailed grain-scale distributions of stress and strain in rocks subjected to thermal or mechanical loading. Although applications are abundant in fields of engineering and materials sciences (e.g., Prakash and Lebensohn, 2009; Vel and Goupee, 2010), examples of such modeling applied to rocks are relatively few (Bons et al., 2008, Wilson et al., 2009). As an example, Figure 1 shows the results of a numerical study of crenulation cleavage development. The microstructure is composed of quartz grains with randomly-oriented crystallographic axes, and muscovite grains with the c-axes in the plane of the page and perpendicular to their long dimension. The muscovite grains outline a micro-scale fold, or crenulation. The sample was subjected to small horizontal shortening, and the resulting mean elastic stress and volumetric elastic strain are shown. These results can be used to investigate fluid pressure gradients among other parameters in an attempt to understand the mass transfer associated with this fabric (Naus-Thijssen et al., 2010).

The heterogeneous, grain-scale distributions of stress and strains in anisotropic polycrystalline rocks also contribute significantly to their bulk mechanical properties. For example, owing to the abundance of highly anisotropic minerals in the crust, the Voigt and Reuss bounds on the seismic velocities can be separated by more than 1 km/s. These bounds are determined by modal mineralogy and crystallographic orientations of the constituent minerals, but where the true velocities lie between these bounds is determined by other fabric parameters such as the shapes and spatial arrangements of grains (e.g., Bunge et al., 2000; Naus-Thijssen et al, 2011). These dependencies are caused by the cumulative effects of grain-scale mechanical interactions throughout the heterogeneous sample, which vary as a function of the fabric parameters. Bunge et al. (2000) estimated that these parameters may contribute as much as 25% of the bulk elasticity for highly anisotropic materials. Thus, the contribution of these grain-scale mechanical interactions on bulk elastic properties must be determined in order to calculating accurate seismic wave-speeds in anisotropic rocks. We achieve these calculations by using asymptotic expansion homogenization combined with finite element methods (e.g., Naus-Thijssen et al., 2011). Synthetic microstructures generated by computational methods allow sensitivity analyses around fabric parameters such as modal mineralogy, grain

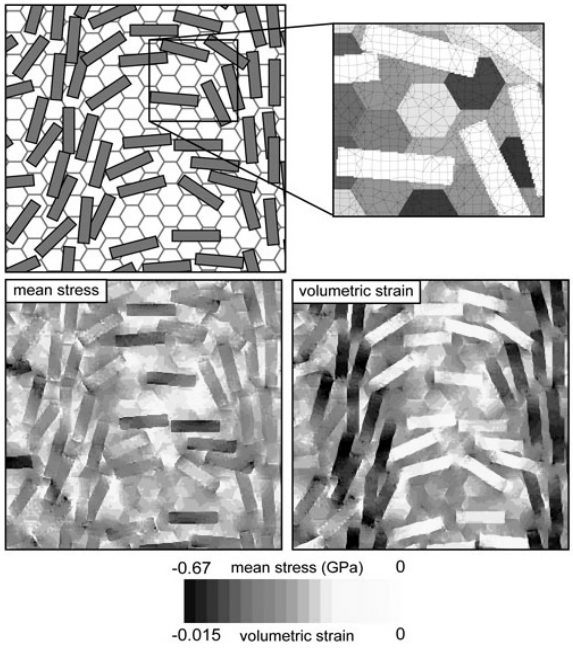

Figure 1. Numerical model of mean elastic stress and volumetric elastic strain distribution around a crenulation fold. From Naus-Thijssen et al. (2010).

orientations and distributions so that the effects of fabrics like crenulation cleavage can be interrogated. An example is shown in Figure 2.

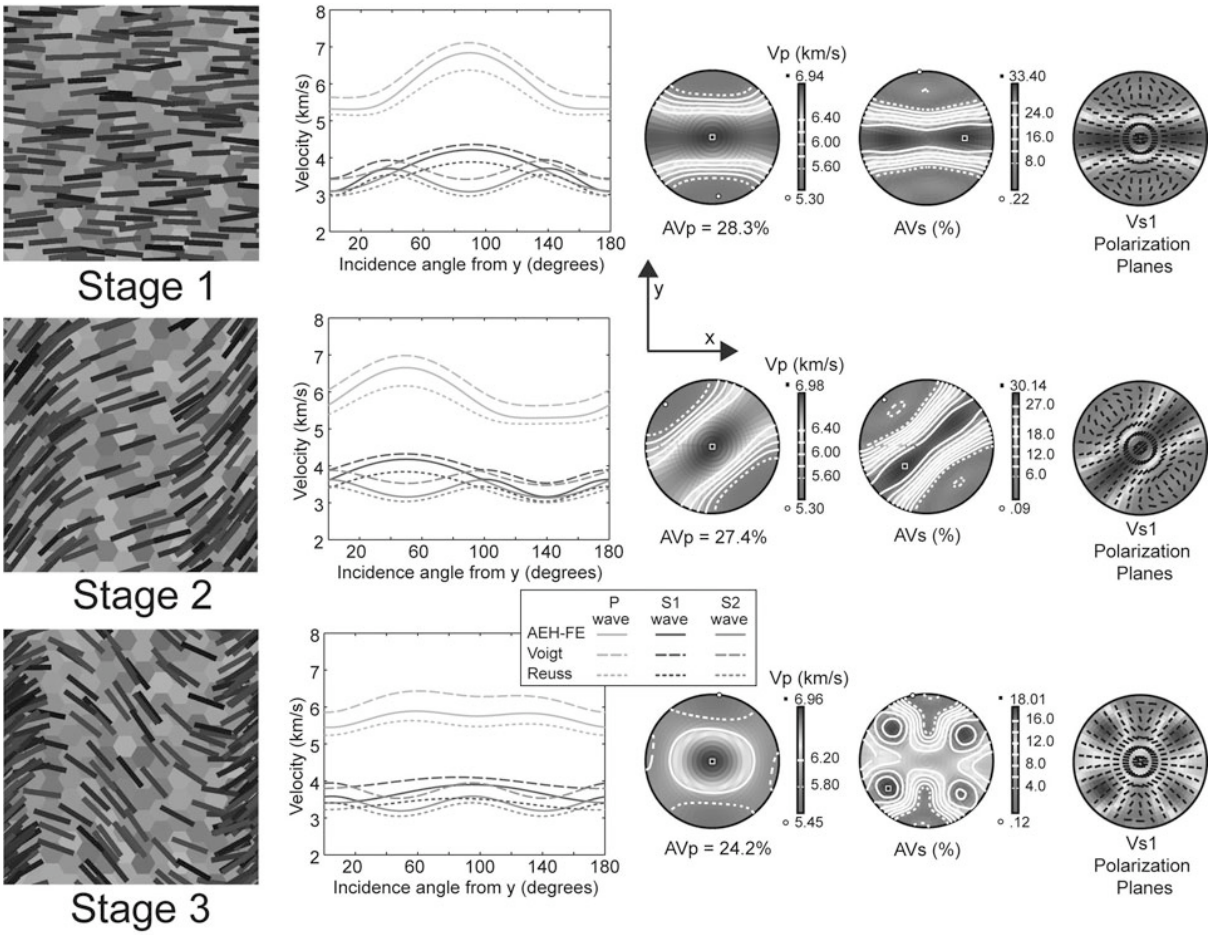

Figure 2. Analysis of three stages of crenulation cleavage development in a synthetic quartz, plagioclase and muscovite rock. Quartz and plagioclase are both represented as hexagons, and colors indicate crystallographic orientations. Muscovite grains are rectangular. The figure illustrates how development of this common rock fabric can modify both the seismic anisotropy and the geometry of the wave velocities relative to the kinematic reference frame. AEH-FE refers to the method of asymptotic expansion homogenization coupled with finite elements. Velocities plotted in the lower hemisphere.

References

Bons, P.D.D., Koehn, D., Jessell, M.W., eds., Microdynamics Simulation, Lecture Notes in Earth Science, v. 106.

Bunge, H.J., Kiewel, R., Reinert, T., Fritsche, L., 2000. Elastic properties of polycrystals - influence of texture and stereology, Journal of the Mechanics and Physics of Solids, 48, 29-66.

Griera, A., Bons, P.D., Jessell, M.W., Lenensohn, R.A., Evans, L., Gomez-Rivas, E., 2011. Strain localization and porphyroclast rotation. Geology, 39, 3, 275-278, doi: 10. 1130/G31549.1

Naus-Thijssen, F.M.J., Johnson, S.E., Koons, P.O., 2010. Modeling crenulation cleavage: a polymineralic approach. Journal of Structural Geology, 32, 330-341.

Naus-Thijssen, F. M. J., Goupee, A. J., Vel, S. S., Johnson, S. E., 2011. The influence of microstructure on seismic wave speed anisotropy in the crust: computational analysis of quartz-muscovite rocks. Geophysical Journal International, 185: 609–621. doi: 10.1111/j.1365-246X.2011.04978

Prakash, A., Lebensohn, R. A., 2009. Simulation of micromechanical behavior of polycrystals: finite elements versus fast Fourier transforms, Modelling and Simulation in Materials Science and Engineering, 17:064010.

Vel, S.S., Goupee A.J., 2010. Multiscale thermoelastic analysis of random heterogeneous materials. Part I: Microstructure characterization and homogenization of material properties. Computational Materials Science, 48: 22-38.

Wilson, C.J.L., Evans, L., Delle Piane, C., 2009. Modeling of porphyroclasts in simple shear and the role of stress variation at grain boundaries. Journal of Structural Geology, 31, 1350-1364. doi: 10.1016/j.jsg.2009.08.001

Development of Reaction Front During Experimental Dehydration of Gypsum: Role of Deformation

Sergio Llana-Fúnez*[1], John Wheeler[2], Dan Faulkner[2]

[1]Departamento de Geología, Universidad de Oviedo, Spain
[2]School of Enrivonmental Sciences, University of Liverpool, UK
*slf@geol.uniovi.es

Volterra gypsum is a good natural rock analogue to study the interaction between deformation and metamorphism in crystalline rocks. This natural polycrystalline material has very low porosity (~1 %) and has low permeability (10^{-16}-10^{-18} m^2): it is therefore very sensitive to small changes in pore volume. The partial dehydration of gypsum ($2H_2O{\cdot}CaSO_4$) to bassanite ($0.5H_2O{\cdot}CaSO_4$) involves a total volume increase of 9 % if the full 1.5 moles of water are expelled from the sample. The progress of the reaction at constant temperature and constant volume partly depends on the ability of excess water to leave the sample, otherwise pore fluid pressure increase would inhibit or slow down the progress of the reaction. In previous experimental studies of dehydration of natural intact rocks (serpentinite or gypsum) under drained conditions, the reaction initiated at locations in rock samples where pore fluid pressure was controlled and kept constant, i.e. the areas close to sample edges. The consequence of this configuration is the initiation of the reaction at the edges, forming a rim of reaction products. The progress of the reaction would involve the migration of this front towards the inside of the specimens. Evolution of pore fluid pressure inside the specimens during the dehydration experiments is unknown, because the pressure is not measurable from the outside.

We present dehydration experiments in gypsum in which we control pore fluid pressure at one end of the sample and we monitor pore fluid pressure at the opposite end of the sample, thereby simulating conditions from core to rim in previous experimental studies but with the ability of monitoring pore fluid pressure in the undrained parts of specimens. We observed that the drained end of the specimens dehydrates earlier and to a higher degree. Under certain experimental conditions of relative low temperature, the consequence of the initial configuration is the development of a planar reaction front, with the drained end of the sample substantially converted to bassanite, and the undrained end remaining exclusively made of gypsum.

We have found independently that gypsum is deformable at experimental conditions: permeability in gypsum decreases with time above certain effective pressure. The decrease in permeability is permanent, it does not recover fully when samples are unloaded, and the there is no change in porosity associated with this. We believe that the gypsum framework deforms viscously under relatively low effective pressure and room pressure, even in low porosity specimens. Deformation is at constant volume, but the pore space is modified as to affect permeability.

Our experimental work illustrates that crystalline rocks at effective pressure and undergoing devolatilization reactions are sensitive to viscous deformation of the reactant matrix and that deformation affects the progress of devolatilisation reactions.

The Tectonic Significance of Successive Horizontal and Vertical Foliation Orientations in High-Grade Metamorphic Terranes

Mark A. Munro*[1], Simon W. Richards[1]

[1]School of Earth & Environmental Sciences, James Cook University, Queensland, QLD 4811, Australia
*mark.munro@my.jcu.edu.au

Inclusion trails within cordierite, andalusite and K-feldspar porphyroblasts from samples within the famous High-Temperature Low-Pressure (HTLP) Cooma Metamorphic Complex of S.E. Australia exhibit a succession of sub-vertical and sub-horizontal fabrics. This sequence of multiple flat and steep foliations is found in many metamorphic complexes around the world and must reflect non-unique tectonic processes. Furthermore, porphyroblast growth and HTLP metamorphism in the Cooma Complex pre-dates magma generation and is interpreted to be associated with regional thermal processes. The porphyroblast-rich metapelites analysed exhibit a well-developed differentiated cleavage where non-, or very minor, rotation of the porphyroblasts can be demonstrated. Successive flat and steep foliations in these porphyroblasts are used here to interpret periods of switching in the orientation of the principal shortening direction from approximately vertical to approximately horizontal. Detailed overprinting relationships suggest up to eleven ductile deformation events preserved in rocks that have typically been interpreted to exhibit only five. These results suggest that switching between vertical and horizontal shortening may take place on much shorter timescales than previously considered (<2My).

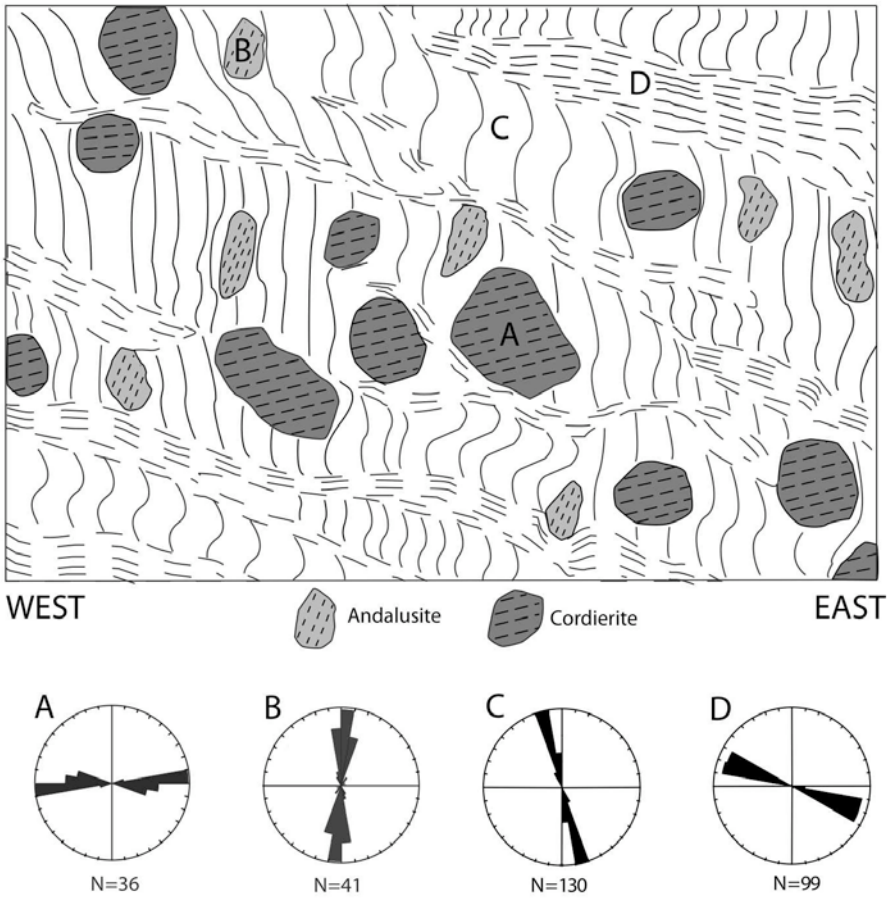

Representation of a typical vertical thin section from Slacks Creek in the Cooma Complex orientated at 090° (West-East) exhibiting how a number of sub-horizontal and sub-vertical foliations may be interpreted as present at the microscale within a single sample. Width = 4.3cm. The corresponding rose diagrams are also aligned West-East, with North-South representing the vertical. The first two record cordierite and andalusite inclusion trail pitches within a single slide, whereas the latter two field measurements of the dominant matrix foliations.

Metamorphism and Structural Control on the Cu-Co ore Deposits in the Central African Copperbelt

Philippe Muchez*[1], Hamdy A. El Desouky[1], David Banks[2], Adrian Boyce[3], Dieter Brems[1], Jacques L.H. Cailteux[4], An De Cleyn[1], Lennert Lammens[1], Osbert Sikazwe[5]

[1]Geodynamics and Geofluids Research Group, K.U.Leuven, Celestijnenlaan 200E, B-3001 Leuven, Belgium
[2]School of Earth and Environment, University of Leeds, UK
[3]SUERC, East Kilbride, Scotland, UK
[4]Group Forrest International, Lumbumbashi, D.R.Congo
[5]School of Mines, University of Zambia, Lusaka, Zambia
*philippe.muchez@ees.kuleuven.be

The Central African Copperbelt in the Democratic Republic of Congo (DRC) and Zambia is one of the world's largest and richest metallogenic provinces, characterized by stratiform Cu-Co ore deposits in the Neoproterozoic Katanga Supergoup (<880 to ± 500 Ma). These high grade deposits resulted from multiple mineralization and remobilization stages (Cailteux et al 2005, Selley et al 2005, Dewaele et al 2006). In the DRC, two main hypogene stages occur. During initial rifting, the first stage of Cu-Co sulphides formed due to convective circulation of brines in the underlying rock pile, including the pre-Katanga basement, from which metals were leached. Fluids associated with this Cu-Co stage had a moderate temperature (115° to ≤220°C) and salinity (11.3 to 20.9 eq.wt% NaCl. Interaction of these brines with bacteriogenic sulphide resulted in early diagenetic stratiform mineralization (Muchez et al. 2008). This stage occurs in the DRC, but is often obscured in Zambia. The second stage of Cu-Co sulphides formed during late diagenesis/metamorphism and the Lufilian orogeny. In the DRC, mineralizing fluids had a high temperature (>270°C) and salinity (35-45 eq. wt% NaCl, El Desouky et al 2009). The high molar Cl/Br ratios (1300-26000) indicate that the fluid originated from halite dissolution. Its bromine content varies from values that are lower than seawater to values typical for evaporated seawater, indicating that the ambient fluid already originated from mixing of fluids. Taking into account the geological setting and the high temperature of the mineralizing fluids, one component could have been (evaporated) seawater (Br-rich) trapped in the rock sequence and the other a Br-poor, low saline fluid likely released by metamorphic reactions. The fluid of the second stage is also characterized by low sodium and high calcium and potassium contents, indicating significant exchange between sodium and the other cations by fluid-rock interaction. Albitization, which is commonly observed in the Katanga Copperbelt, is likely the main reason for the significant Na depletion.

In the Zambian Copperbelt, which is characterized by a higher metamorphic grade and intense folding, the second Cu-Co mineralization stage can be further subdivided in multiple sub-stages (Brems et al. 2009). Detailed 2D and 3D geological mapping at the South and Central Orebody at Nkana indicates a relationship between the mineralization and the stratigraphy but also with compressional deformation. The location of the orebodies generally corresponds with the hinge zones of tight to isoclinal folds and with the contact between the sandstone and conglomerates of the footwall rocks and the overlying organic-rich shales. At least three successive vein generations occur at Nkana. Firstly, layer-parallel veins formed before folding and cleavage development during the onset of compression and thus the initial phase of basin inversion. Secondly, irregular veins crosscut the folds and cement the brecciated host rock. Remobilization of sulphides along cleavage planes could have occurred during this period of veining, which took place during the main phase of deformation. Thirdly, massive veins crosscut all earlier tectonic features. These veins may show evidence for both reverse and normal faulting and reflect a late phase of orogenesis and extensional tectonics. $\delta^{34}S$ increases from early diagenetic stratiform sulphides to sulphide derived from thermochemical sulphate reduction. Fluid inclusions measured in the different vein generations have a dominant H_2O-NaCl/KCl-$MgCl_2$ composition with the presence of gaseous component in some fluids. Fluid inclusions in the layer parallel veins suggest entrapment around 450°C at a depth of 8.4 km (2100 bars), i.e. during the main period of metamorphism. Secondary fluid inclusions in the layer parallel, irregular and massive veins have a high salinity (18.1 to >23.2

eq. wt% NaCl) and homogenization temperatures between 100 and 250°C. These fluids were trapped after formation of the veins, likely during retrograde metamorphism.

References

Brems et al. 2009, Journal of African Earth Sciences 55, 185-196.
Cailteux et al. 2005, Journal of African Earth Sciences 42, 134-158.
Dewaele et al. 2006, Journal of African Earth Sciences 46, 455-469.
El Desouky et al. 2009, Ore Geology Reviews 35, 315-332.
Muchez et al. 2008, Mineralium Deposita 43, 575-589.
Selley et al. 2005, Economic Geology 100th Anniversary Volume, pp. 965-1000.

Localised Folding and Axial Plane Structures

Alison Ord [1]

[1]Centre for Exploration Targeting, Earth and Environment, The University of Western Australia, WA, Australia
*aliup.oz@gmail.com

The development of folds in layered rocks is commonly analysed using Biot's theory of folding. This theory expresses the deflection, *w*, of a single layer embedded in a weaker medium in terms of the equation $\frac{\partial^4 w}{\partial x^4} + P\frac{\partial^2 w}{\partial x^2} + F\left(w, x\right) = 0$ where *x* is the distance measured along the layer, *P* is a function of the mechanical properties of the layer and *F*(*x*) is a function that represents the reaction force exerted by the embedding medium on the layer arising from the deflection of the layer. In Biot's theory *F*(*w*, *x*) is a linear function of *w* and is dependent on the wavelength of the deflection. The result is strictly sinusoidal folding even at high strains with, most importantly, no localised deformation in the embedding medium and hence no development of axial plane structures. However, if the embedding medium softens as the layer deflects or shows other more complicated deformation behaviour then *F* is no longer linear and can depend on the wavelength of the deflection in more complicated ways than in the Biot theory.

For a simple softening response of the embedding layer to deflection, the initiation of folds follows Biot's theory and the initial folding response is sinusoidal. However, as the folds grow and softening develops in the embedding material the fold profile ceases to be sinusoidal and the folds localise to form packets of folding along the layer. This behaviour is reflected in the embedding medium as a series of localised deformation zones parallel to the deflection direction, ***w***, that is, parallel to the axial plane of the folds. These zones constitute micro-lithons, or in an initially finely layered material, crenulation cleavages.

We also explore the situation where a layering arising from metamorphic differentiation forms oblique to folding multi-layers early in the folding history. Now the function *F* also depends on *x* and a variety of localised folds with associated axial plane structures develops. An important observation is that shear displacements form parallel to the axial plane structures during folding.

Our conclusion is that the response of the embedding medium to deflection of the layer(s) to be folded is fundamental in controlling the style of folding and the types of axial plane structures that form and future research should concentrate on the forms of these responses. Most importantly, these axial plane structures form parallel to the deflection vector, ***w***, and hence are controlled by the kinematics of the deformation and are not parallel to a principal plane of strain.

The Origin of a Fragment of the Iapetus-Torquist Ocean and its Accretion in the Variscan suture of NW Iberia: The Bazar Ophiolite

Sonia Sánchez Martínez*[1], Axel Gerdes [2], Ricardo Arenas [1], Jacobo Abati [1]

[1] Departamento de Petrología y Geoquímica e Instituto de Geología Económica (CSIC) Universidad Complutense, 28040 Madrid, Spain
[2] Institut für Geowissenschaften, Goethe Universität, D-6438 Frankfurt am Main, Germany
*s.sanchez@geo.ucm.es

The Bazar Ophiolite, one of the ophiolitic units involved in the Variscan suture of NW Iberia, is formed by metagabbroic amphibolites with N-MORB affinity with minor inclusions of low–to intermediate-P mafic granulites and some levels of ultramafic rocks. The ophiolite appears accreted under an arc–derived upper terrane affected by intermediate-P granulite facies metamorphism dated at 496–482 Ma. U-Th-Pb geochronology and Lu-Yb-Hf isotope geochemistry of zircons from an amphibolite sample allows to recognize two growth stages. The first occurred during crystallization of the gabbroic protolith and has been dated at 495 ± 2 Ma, while the second one interpreted as dating the high-T metamorphism yielded an age of 475 ± 2 Ma. The chronology of the Bazar Ophiolite and the accretionary history affecting this unit are not compatible with its generation within the Rheic Ocean realm, which is the most common interpretation for the setting of the ophiolites involved in the Variscan suture. On the contrary, the Bazar Ophiolite can be interpreted as a relic of the Cambrian peri–Gondwanan Ocean, the Iapetus–Tornquist Ocean, accreted to a dissected arc during or before the early stages in the opening of the Rheic Ocean. The features of the Bazar Ophiolite are unique and distinctive among the group of ophiolites described so far in the Variscan suture.

Antigorite microstrutures in HP-HT serpentinite from Cerro del Almirez (Betic Cordillera, Spain)

José Alberto Padrón-Navarta*[1], A. Tommasi[2], C.J. Garrido[3], V. López Sánchez-Vizcaíno[4], M.T. Gómez-Pugnaire[1,3].

[1] Departamento de Mineralogía y Petrología, Universidad de Granada (Spain) (padron@ugr.es)
[2] Géosciences Montpellier, Université Montpellier 2 & CNRS, 34095 Montpellier, France
[3] Instituto Andaluz de Ciencias de la Tierra (IACT), CSIC & UGR, Facultad de Ciencias. 18002 Granada, Spain,
[4] Universidad de Jaén, Escuela Politécnica Superior, Departamento de Geología, Linares, Spain
*padron@ugr.es

Because of the large pressure and temperature stability fields of serpentine minerals, serpentinite microstructures are an invaluable tool to decipher deformation mechanisms and kinematics during subduction and exhumation cycles (e.g. Hermann et al. 2000, Guillot et al. 2001). Moreover, the deformation of serpentinite minerals - particularly, antigorite; the serpentine-group minerals stable at high pressure and high temperature (HP-HT) - play a key role in the structure, rheology and dynamic of the subduction channel, as well as in the decoupling of the slab-mantle wedge interface (e.g. Wada et al., 2008, Chernak and Hirth, 2010).

Recent published work consistently points to the development of antigorite crystal preferred orientations (CPOs) by dislocation creep, but there is disagreement between the CPO observed in naturally deformed antigorite serpentinite and that of HP-HT deformation experiments. This suggests that slip systems activity in serpentinite may depend on PT conditions of deformation, but this has not been investigated in detail so far. Here we present a detailed microstructural study of naturally deformed HP-HT antigorite serpentinite from Cerro del Almirez (Betic Cordillera, SE Spain) (Trommsdorff et al., 1998, Garrido et al., 2005; López Sánchez-Vizcaíno, 2001, 2005, 2009; Padrón-Navarta et al., 2008; 2010a; 2010b).

We measured the serpentinite fabric by using high-resolution EBSD mapping (1-5 micron measurement steps) over representative areas from several samples in two orthogonal sections (XZ and XY sections). Antigorite in both sections shows a clear CPO, characterized by a strong alignment of [001] normal to the foliation plane and a weaker, but neat, parallelism between [100] axis and the macroscopic lineation defined by streched magnetite. Indexation rates in XY sections are lower than in XZ sections, but results are coherent. Alignment of [001] direction normal to the foliation plane is however overestimated in the more poorly indexed XY sections. Atg-serpentinite and Cpx-Tr-bearing serpentinite show similar antigorite CPO with a weak alignment of [100] axis parallel to the macroscopic lineation. In Ca-rich serpentinite a topotatic relationship between clinopyroxene and prograde tremolite has been observed being perturbed by solid rotation. In other samples, tremolite porphyroblasts cross cut the antigorite foliation indicating that deformation ceased in the tremolite stability field (~600-650ºC, probably at high pressure conditions). The syn- to post-kinematic character of tremolite suggests that the antigorite-serpentinite foliation was developed during prograde conditions and 'frozen' at high-pressure conditions. Static annealing at HP-HT conditions is further supported by the exceptionally ordered microstructure of the antigorite, consisting of the polysome m = 17 with no polysomatic defects (Padrón-Navarta et al., 2008)

Serpentinite foliation is characterized by a strong antigorite shape preferred orientation and also a well defined preferred crystallographic orientation with [100] axes dominantly subparallel to the lineation (which is horizontal in the texture component image, Fig. 1a & b). Analysis of the misorientation angles distribution highlights twins formed by a 180° rotation around [100] (marked by t in the histogram), whereas peaks at 60 and 120° are due to pseudosimetry around the [001] axis (marked with*, Fig. 1c). The main rotation axis for low angle misorientations (<15°) is [010] (Fig. 1d), suggesting that subgrain boundaries are mainly composed by (001)[100] edge dislocations. Two sets of subgrains in antigorite are exceptionally well-resolved in high resolution EBSD. They are most commonly oriented in two sets: (1) subgrain walls parallel to (001) planes, showing changes in orientation of up to 10° with [010] as the main rotation axis and (2) subgrain walls parallel to (100) showing smaller (~5°) rotations around [010]. Low-angle rotations around [100] are

also occasionally observed. Two slip systems can be inferred from these observations, namely (001)[100] and (001)[010].

In order to test the slip systems activities inferred from the analysis of the CPO we modelled the evolution of the antigorite CPO using a lower bound approach. We tested different critical resolved shear stresses (CRSS).

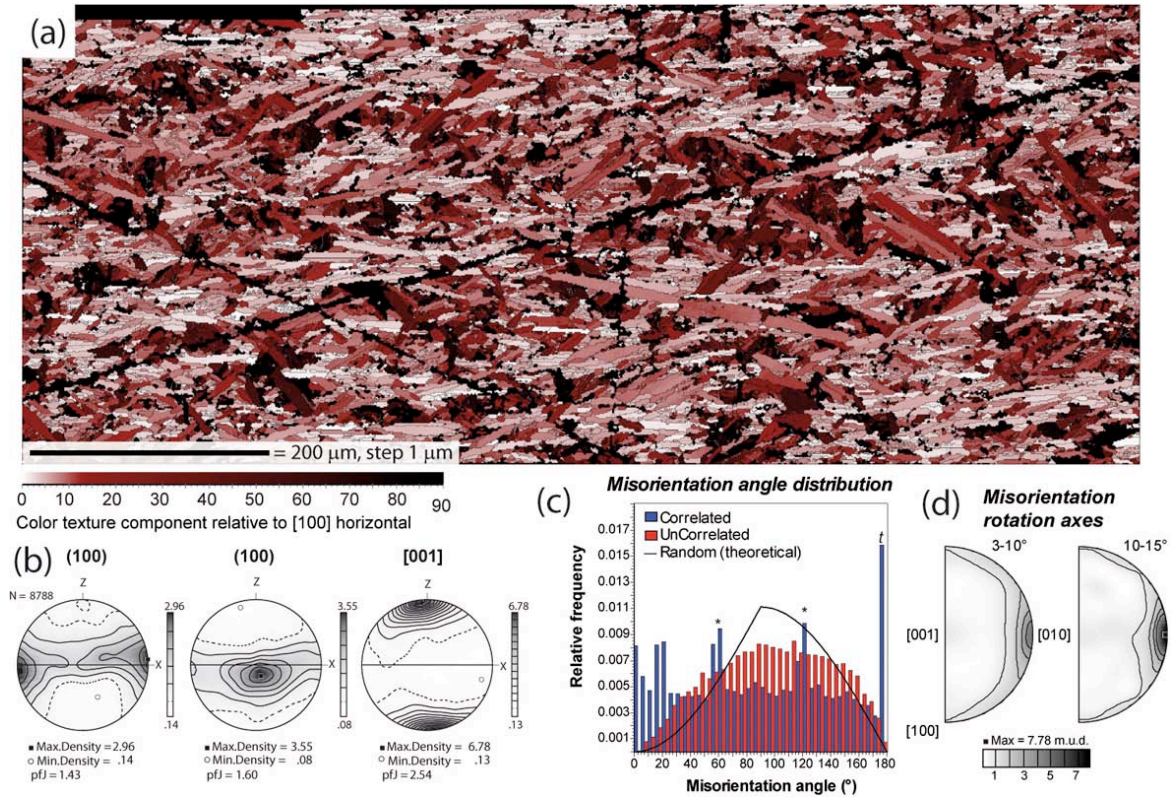

Figure 1: (a) High resolution EBSD map for a representative serpentinite showing in color the antigorite misorientation the relative to [100] horizontal (b) corresponding pole figures, (c) misorientation angle distribution and (d) misorientation rotation axes.

sets and deformation regimes. These models also indicate that simple shear cannot produce the observed fabric unless it is accompanied by a small amount of compression (transpression).

Analysis of the deformation microstructures, crystal preferred orientations and misorientations across low-angle boundaries of antigorite in a HT-HP serpentinite indicates deformation dislocation creep accommodated by slip on (001)[hk0] systems in antigorite, with (001)[100] being dominant. Transpression deformation suggested by CPO modelling is coherent with development of serpentinite foliation during subduction. These results are important to predict the deformation in the slab-mantle wedge interface and hydrated mantle wedge as well as the associated seismic anisotropy.

References

Chernak, L. J. Hirth, G. EPSL 296, 23-33 (2010).
Garrido C. J., López Sánchez-Vizcaíno, V. L. Gómez-Pugnaire, et al. G3 6, - (2005).
Guillot S., Hattori K. H., de Sigoyer J., et al. EPSL 193, 115-127 (2001).
Hermann J., Müntener O., Scambelluri M., Tectonophysics 327, 225-238 (2000).
López Sánchez-Vizcaíno V., Rubatto D., Gómez-Pugnaire M. T., et al., Terra Nova 13, 327-332 (2001).
López Sánchez-Vizcaíno V., Trommsdorff V., Gómez-Pugnaire M. T., et al., CMP 149, 627-646 (2005).
López Sánchez-Vizcaíno V., Gómez-Pugnaire, M. T. Garrido, C. J. et al., Lithos 107, 216-226 (2009).
Padrón-Navarta J. A., López Sánchez-Vizcaíno V., Garrido C. J., et al., CMP 156, 679-688 (2008).
Padrón-Navarta J. A., Hermann J., Garrido C.J., et al., CMP 159, 25-42 (2010).
Padrón-Navarta J. A. , Tommasi A., Garrido C.J., et al., EPSL 297, 271-286 (2010).
Trommsdorff, V. López Sánchez-Vizcaíno, V. L. Gómez-Pugnaire, et al., O. CMP 132, 139-148 (1998).
Wada I., Wang K. L., He J. G., Hyndman R. D, JGR-Solid Earth 113 (2008).

Paleozoic Extrusion Tectonics in Gondwanaland Forcing Large-Scale Strike Slip Motion in the Charters Towers Province, Northeastern Australia

Raphael Quentin de Gromard*[1]

[1] School of Earth and Environmental Sciences, James Cook University, QLD 4811, Australia
raphael.quentindegromard@my.jcu.edu.au

Abstract

The overall N-S trending Tasman Orogenic System that forms the eastern third of the Australian continent comprises, in its northeastern part, anomalous E-W structural and igneous trends presented in the Charters Towers Province (Fig. 1). The Tasman Orogen is interpreted to result from accretion and deformation of continental derived sediments and magmatic arcs due to the early to late Paleozoic west dipping subduction zone along the eastern coast of Gondwana. N-S compression contemporaneous with the development of the Tasman Orogen produced the ~450 to 300 Ma intracontinental E-W trending Alice Springs Orogen in central Australia whose effects propagated eastward to create the E-W trending Charters Towers Province (Fig. 2). The tectonic evolution of this Province in the Paleozoic resulted from the interaction between E-W and N-S bulk shortening. FIA data reveals several discrete deformation events of interspersed ~N-S and ~E-W shortening directions. The FIA ages were obtained through in-situ monazite dating and show N-S shortening events at ~475 Ma and ~415 Ma, followed by ~E-W shortening at ~400 Ma and N-S shortening at ~380 Ma in the Charters Towers Province. The magnetic anomaly map of Australia, used to locate the lateral extensions of shear zones and domain boundaries hidden by overlying sedimentary successions, allowed the linking of deformation structures from central to northeastern Australia. N-S continent-wide compression resulted in eastward extrusion of the Thomson Orogen forcing large scale sinistral strike-slip motion contemporaneous with granite emplacement in the Charters Towers Province.

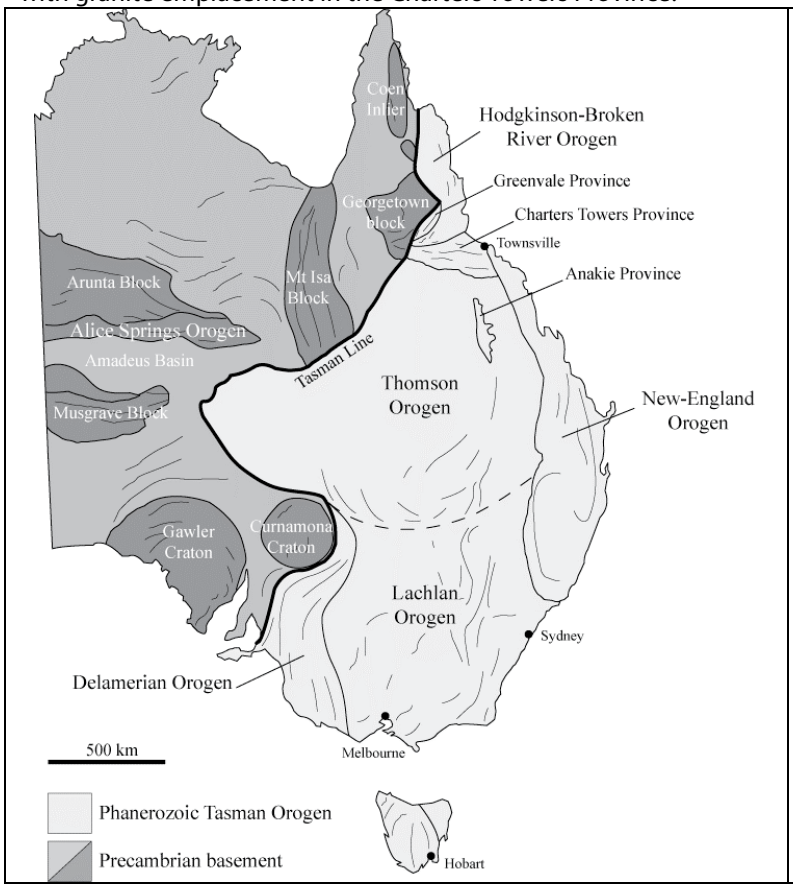

Figure 1: Simplified geological map of central and eastern Australia showing the overall N-S trending Tasman Orogenic System to the East separated from the Precambrian cratonic basement by the Tasman Line (thick line). Note the E-W trends of the Charters Towers Province. Thin lines show magnetic trends.

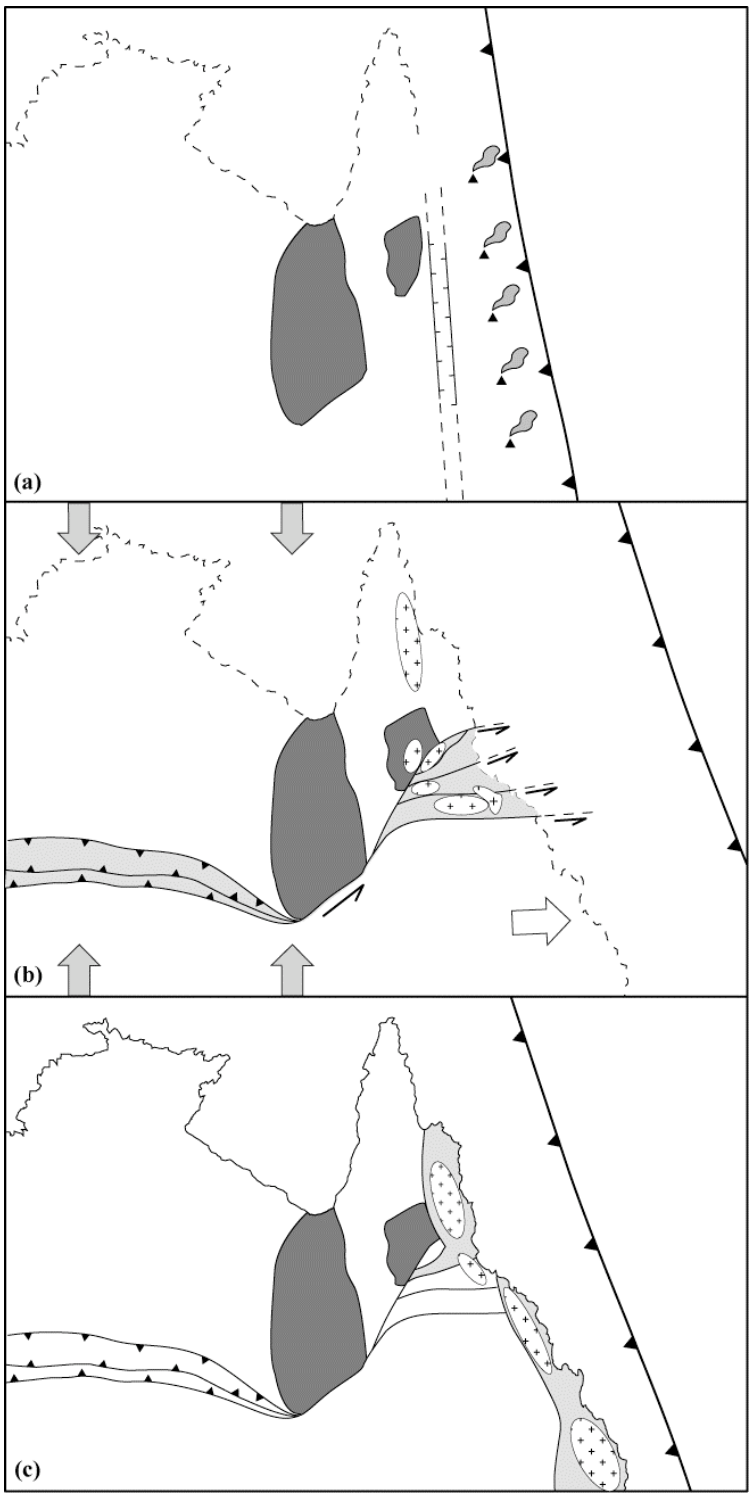

Figure 2: Simplified tectonic evolution of north central and northeastern Australia. (a) Cambrian-early Ordovician N-S trending arc/back-arc system. (b) Mid Ordovician-Mid Devonian N-S shortening in Central and northeastern Australia and eastward extrusion of the Thomson Orogen forcing sinistral strike-slip faults in the Charters Towers Province. This period also experiences short E-W compressional episodes. (c) Carboniferous-Permian accretion and deformation of the New-England Orogen during advance of the slab, overprinting the E-W structural trends of the Charters Towers Province; subsequent slab retreat and NNW-SSE granitoid belt emplacement.

Paleozoic Extrusion TInteraction Between Deformation and Metamorpism During the Exhumation of Subducted Hydrated Oceanic Mantle: Insights From the Western Alps

Gisella Rebay*[1], Maria Iole Spalla[2]

[1]Dipartimento di Scienze della Terra e dell'ambiente, Università di Pavia, Via Ferrata, 1- 27100 Pavia, Italy.
[2] Dipartimento di Scienze della Terra dell'Università degli Studi di Milano and CNR-IDPA,
Via Mangiagalli, 34 - 20133 Milano, Italy
*gisella.rebay@unipv.it

Deformation-metamorphism relationships in serpentinites are not a classsic tool used to unravel the tectonic evolution of the axial portion of collisional belts. The widespread occurrence of eclogitised serpentinite in the Zermatt-Saas Zone of the Western Alps and their poliphased sin-metamorphic deformations makes these rocks a key to infer the structural and metamoprhic history of a significant portion of the northern Western Alps.

The Zermatt-Saas Zone is the widely eclogitised portion of the Thethyan oceanic suture in the Western European Alps buried during Alpine subduction. The presence of pre-Alpine relics shows that this oceanic crust was variously affected by oceanic metamorphism before subduction (Dal Piaz et al., 1980, Li et al., 2004).

Serpentinites of upper Valtournenche, with lenses and dykes of metagabbro and meta-rodingite, display an Alpine poliphasic metamorphic evolution from eclogite to greenschist facies conditions associated with the development of superposed structures. Three successive foliations associated with different parageneses in all these rocks, followed by D4 folding, has been recognised. In metabasites, S1 and S2 foliations are associated to high-pressure low-temperature parageneses, whereas S3 is associated to a later re-equilibration in the greenschist facies. In serpentinite S2 is the pervasive foliation, and it may be parallel to bands rich in clinopyroxene2 + amphibole2. S1 is recognised where S2 is less pervasive: here relic Ti-clinohumite –olivine veins, up to 4 cm thick, boudinaged and folded in S2 foliation, are found. Sometimes they have a white clinopyroxene rim toward serpentinite.

Serpentinite mainly consists of serpentine with minor magnetite, but where S1 and S2 foliations are pervasive, metamorphic olivine is found, together with Ti-clinohumite and clinopyroxene.

The stable mineral assemblage associated with D1 is Srp1, Cpx1, opaques, titanite $\pm$ amphibole 1, chlorite1 olivine1, Ti-Clinohumite1, ilmenite. The assemblage stable with D2 is serpentine2, clinopyroxene2, opaques, Ti-clinohumite2, olivine2, + chlorite2, amphibole2, titanite.

The assemblage associated with D3 structures is serpentine3, opaques, $\pm$ chlorite3, ilmenite and amphibole3.

Mineral compositional variations are investigated with respect to microstructural positions of single grains in superposed fabrics: serpentine associated to D1 structures is more Mg-rich than that associated to D2 structures; olivine and chlorite do not have large chemical changes, though when associated to D1 structures they may be more Mg-rich than when associated to D2 structures; Ti-chumite1 is slightly Fe-richer than Ti-clinohumite2 and may have less Ti.

Successive veining episodes can predate or be contemporaneous to D2 structures and in this case they are filled by olivine, pyroxene, Ti-clinohumite. Post-D2 veins never contain Ti-clinohumite, olivine and pyroxene. This observation validated at the regional scale by the detailed structural mapping, allows to constrain the timing of Ti-clinohumite growth to S1 and S2 foliations, contradicting the conclusion of Li et al., (2004) that interpret the veins as post D3 or linked to ocean-metamorphism predating Alpine metamorphism. On the other hand this result is coherent with what observed by Scambelluri & Rampone (1999) and Groppo & Compagnoni (2007) in other parts of the western Alps.

The multidisciplinary structural and petrological approach allowed the reconstruction of a PTtd path suggesting that these rocks underwent pressures > 2.2 GPa for temperatures partially

exceeding 600°. PT conditions estimated for S1 and S2 parageneses have been evaluated with preliminary calculations of a PT grid in the MASH system and a PT pseudosection. The late greenschist facies re-equilibration develops during late sin-exhumation deformation: it is characterised by a small T-decrease. Radiometric ages (Rubatto et al., 1998 and Lapen et al., 2003) suggest ages of 50-43 Ma for the P peak and ages of 36-40 Ma for the greenschist facies retrogression, suggesting exhumations rates between 0.6 and 2.7 cm/y for this part of the Zermatt-Saas unit.

References

Dal Piaz, G.V., Di Battistini, G., Gosso, G. & Venturelli, G. (1980). Arch. Sc. Geneve, 33, 161-179.
Groppo, C. & Compagnoni, R. (2007). Per. Mineral. 76, 127-153.
Lapen, T.J., Jhonson, C.M., Baumgartner, L.P., Mahlen, N.J., Beard, B.L. & Amato, J.M. (2003). Earth.Plan.Sci.Lett., 215, 57-72
Li, X-P., Rahn, M. & Bucher, K. (2004). J. Metam. Geol., 22, 158-177.
Rubatto, D., , Gebauer, D. & Fanning, M. (1998). Geochim. Cosmochim. Acta, 132, 269-287.
Scambelluri, M. & Rampone, E. (1999). Contrib. Min. Pet., 135, 1-17.

Thickening and Exhumation of the Variscan Roots in the Spanish Central System: Tectonothermal Processes and 40Ar/39Ar Ages

F.J. Rubio Pascual*[1], R. Arenas[2], J.R. Martínez Catalán[3] ,
L.R. Rodríguez Fernández[1], J. Wijbrans[4]

[1]Instituto Geológico y Minero de España, Spain (f.rubio@igme.es)
[2]Dpto. de Petrología y Geoquímica, Universidad Complutense de Madrid, Spain
[3]Dpto. de Geología, Universidad de Salamanca, Spain
[4]Faculty of Earth and Life Sciences, Vrije Universiteit, The Netherlands
*f.rubio@igme.es

$^{40}Ar/^{39}Ar$ dating of white mica concentrates in metapelites, thermobarometric calculations, and a revision of the structural and geological mapping data have been carried out in the Somosierra region (Spanish Central System). The results can be integrated in a model that explains the whole Variscan tectonothermal evolution of this key region forming part of the Central Iberian Zone.

Three distinct tectonometamorphic units can be defined in the area. According to the evolution deduced for the Upper Unit (Fig. 1), the most important Variscan thickening took place between 354 and 347 Ma. Burial occurred under an intermediate P/T Barrovian gradient (23 ºC/km), reaching more than 7 Kbar at a structural level which roughly coincides with the Armorican Quartzite. The P conditions imply an overburden around 15 km thicker than the outcropping lithological succession. So, a 70% of the deduced thickness may be explained by a nappe stack similar to the NW Iberian allochthons (emplaced around 340-330 Ma ago), by a thick apron of synorogenic deposits or by a combination of both.

Contractional D_1 deformation in the Upper Unit continued until 327 Ma, when a large D_2 ductile shear zone developed in the Intermediate Unit (Berzosa Shear Zone, BSZ). The first stages of D_2 activity represent a thermal relaxation coeval to weak decompression in a subhorizontal shear zone. The areas located to the E and W of Somosierra developed the same M_1 Barrovian zonation but affecting lower stratigraphic levels, suggesting a more important thickening in the Somosierra axis. This thermal structure can be explained by the original presence of a NW-SE-directed tongue shaped overburden which, if it were an allochthonous nappe, would be compatible with D_2 stretching lineations with systematic top-to-the SE kinematic indicators. Peak conditions are calculated in 7.2 Kbar and 494 ºC at the Armorican Quartzite level (garnet zone); 8.9 Kbar and 658 ºC in the M_1 staurolite zone and 9.4 Kbar and 687 ºC for kyanite zone. The metamorphic field gradient in the shear zone at the end of M_1 is around 29 ºC/km, already close to HT/LP conditions.

Continuation of syn-D_2 activity in the BSZ enhanced decompression and produced retrogression until c. 316 Ma. During M_2 the quartz-feldspathic rocks in the Lower Unit underwent partial melting, kyanite was replaced by sillimanite and the staurolite M_2 isograd rose obliquely to M_1 structure, defining a "ramp" inclined 25º to the SE which is interpreted as the frontal slope of the domal uplift of the orogenic roots during D_2 decompression. Some late thrusts dated at c. 319 Ma, may correspond to frontal ramps of gravitational nappes. The calculated P-T conditions in the Lower Unit are 7.5 Kbar and 746 ºC, which represent an average gradient of 33 ºC/Km for the whole crustal section at the end of M_2. The M_2 overprinting on M_1 mineral assemblages is more important in the Somosierra area than in regions located towards the E or W, where rocks can bear stable kyanite.

Buoyant uplift of the orogenic roots was accompanied with D_3 thickening of the previously thinned crustal section. In this way, large upright folds affecting to M_1 and M_2 metamorphic isograde developed. D_3 folding and initial D_4 gravitational collapse, driven by radial extensional detachments, caused a new HT/LP M_3 metamorphic zonation coeval to the generation and emplacement of large massifs of syn-kinematic anatectic granitoids.

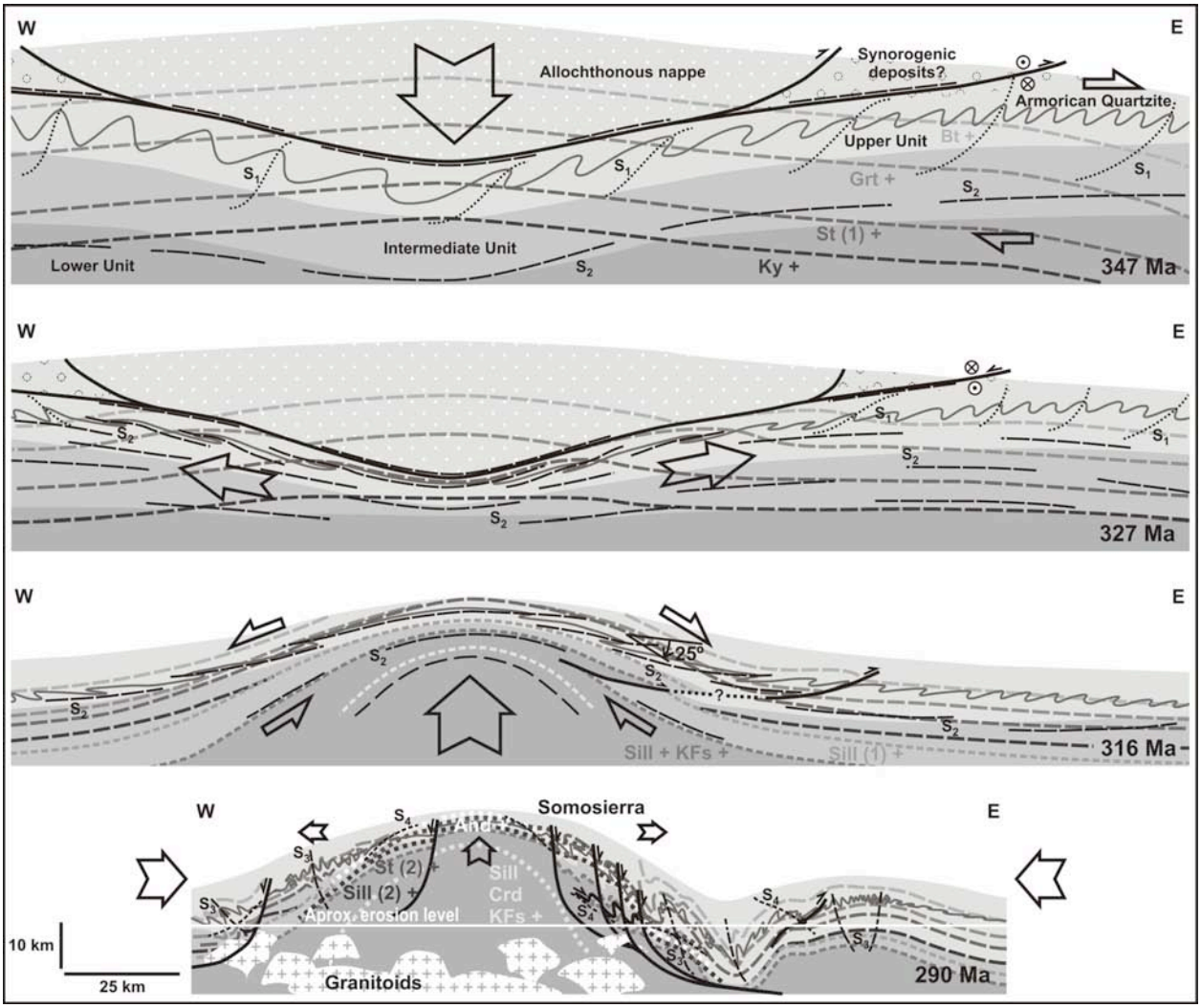

Fig. 1. Sketch showing the model suggested to explain the Variscan tectonothermal evolution of the Somosierra region.

Unravelling Orogenic Processes Using Microstructural and Petrological Records in Garnet Porphyroblasts

Etienne Skrzypek*[1], K. Schulmann[1], P. Štípská[1], O. Lexa[2]

[1]Université de Strasbourg, 1, rue Blessig, 67084 Strasbourg, France
[2]Institute of Petrology and Structural Geology, Charles University, Albertov 6, 128 43 Prague, Czech Republic
*etienne.skrzypek@eost.u-strasbg.fr

The Variscan orogenic root exposed in the Orlica-Śnieżnik Dome (West Sudetes) preserves a heterogeneous succession of three sub-orthogonal fabrics: subhorizontal S1, subvertical S2, and subhorizontal S3. In mica schists from the orogenic middle crust, this succession is also observed on the microscopic scale, especially in garnet porphyroblasts with curved, staircase or straight inclusion trail patterns. The internal records of the different garnet porphyroblasts have been investigated using in situ electron backscatter diffraction (EBSD) measurements of ilmenite inclusions and thermodynamic modelling of garnet zoning. EBSD data reveal that garnet porphyroblasts preserve planar structures that have nearly similar orientations to the S1 and S2 macroscopic foliations. In addition, the internal foliations define NE–SW and N–S trending foliation intersection axis sets (FIA) that are well correlated with the major structural trends of the dome. In polyphase garnet crystals, two distinct trends of Mn decrease are observed in both zones preserving the S1 and S2 internal foliations, whereas the S3 foliation is associated with sillimanite and biotite growth after garnet. The modelled garnet zoning indicates a prograde evolution from 4–4.5 kbar/490–510 °C to 5–6 kbar/520–550 °C in the earliest S1 fabric progressing towards 6.5–7.5 kbar/560–590 °C in the subsequent S2 foliation, while garnet resorption in the S3 fabric points to retrograde metamorphic conditions.

Coupling the orientation of internal fabric sets with *P–T* estimates suggests that the subhorizontal S1 and subvertical S2 fabrics are associated with a progressive burial of the mid-crustal metasediments during coeval exhumation of lower-crustal high-grade rocks. The apparent lack of porphyroblast rotation during the development of the subsequent S3 foliation additionally indicates that, although moderate buckling is evidenced, pure shear deformation was probably dominant during exhumation. These results illustrate that garnet microstructural and petrological records can significantly help constraining the orogenic evolution of polydeformed and polymetamorphosed areas.

Structural vs Metamorphic Hetherogeneities in the HP Metagabbros From the Western Alps Austroalpine Continental Crust

M. Iole Spalla*[1,2], Gisella Rebay[3], Davide Zanoni[3], Guido Gosso[1,2], Luca Baletti[1]

[1]Dipartimento di Scienze della Terra "A. Desio", Università degli Studi di Milano, Via Mangiagalli 34, 20133 Milano, Italy
[2]C.N.R.-I.D.P.A., Sezione di Milano, Via Mangiagalli 34, 20133 Milano, Italy
[3]Dipartimento di Scienze della Terra e dell'Ambiente, Università di Pavia, Via Ferrata, 1- 27100 Pavia, Italy
**iole.spalla@unimi.it*

Deformation heterogeneity may control progress of metamorphic reactions in high pressure-low temperature conditions (e.g.: Gosso et al., 2010; Salvi et al., 2010) and investigations on interaction between deformation and metamorphism indicate that strain enhance the reaction rates (e.g.: Hobbs et al., 2010). The polyphase Alpine deformation of huge Permian gabbro bodies emplaced in the continental crust of the Dent Blanche nappe is highly heterogeneous and responsible for superposed fabric gradients superposition in space and time. The Alpine deformation history has been recorded under low temperature – high pressure conditions, during late stages of Alpine subduction (Roda & Zucali, 2008 and refs. therein). The Dent Blanche nappe is the part of the Austroalpine Domain of the Western Alps containing the highest density of Permian gabbro bodies, mainly hosted in metagranitoids (e.g. Dal Piaz et alii, 1977; Monjoie et alii, 2005); the contact between gabbros and surrounding metagranitoids consists of a thick and persistent mylonitic horizons.

A detailed structural analysis of the gabbroic complex of Cima della Sassa reconstructed their Alpine and pre-Alpine history: three Alpine superposed groups of structures developed under PT conditions evolving from blueschist to greenschist facies. The weakly deformed volumes, preserved during the structural overprinting of the Alpine convergence, maintain at best the igneous and metamorphic pre-Alpine features (≤ 60% in volume of structural and mineral relicts), whereas normal LS tectonites and mylonites are associated with a diffuse Alpine metamorphic re-equilibration (≥ 70% in volume).

The detailed study of the interaction between fabrics development and reaction progress allows to highlight the role of deformation as reaction catalyst and is a fundamental support to perform PT estimates for successive Alpine deformation stages, in different structural and compositional domains.

Moreover the Alpine deformation heterogeneity allows exploiting to a great extent the memory of the gabbros, which offers details on Permian igneous and pre-Alpine metamorphic structures and mineral associations. This analytical approach provides data leading to the interpretation of the igneous emplacement conditions and successive subsolidus evolution, predating Alpine subduction and collision, and is fundamental to refine the comprehension of the Alpine geodynamic scenario.

References

DAL PIAZ G.V., DE VECCHI G., HUNZIKER J.C. (1977) - The Austroalpine layered gabbros of the Matterhorn and Mt. Collon-Dents de Bertol. Schweiz. Mineral. Petrogr. Mitt., 57: 59-88.

GOSSO G., MESSIGA B., REBAY G., SPALLA M.I. (2010) - Amphibolite eclogitisation in Sesia-Lanzo Zone (Western Alps): deformation and rock chemistry as controllers of metamorphic reactions. Int. Geol. Rev., 52: 1193-1219.

HOBBS B.E., ORD A., SPALLA M.I., GOSSO G., ZUCALI M. (2010) - The interaction of deformation and metamorphic reactions. Geol. Soc. London Spec. Pub., 332: 189-222.

MONJOIE P., BUSSY F., LAPIERRE H., PFEIFER H.R. (2005) - Modeling of in-situ crystallization processes in the Permian mafic layered intrusion of Mont Collon (Dent Blanche nappe, western Alps). Lithos, 83: 317-346.

RODA M., ZUCALI M. (2008) - Meso and microstructural evolution of the Mont Morion metaintrusive complex (Dent-Blanche nappe, Austroalpine domain, Valpelline, Western Italian Alps). Boll. Soc. Geol. Ital., 127: 105-123.

SALVI F., SPALLA M.I., ZUCALI M., GOSSO G. (2010) - 3D-evaluation of fabric evolution and metamorphic reaction progress in polycyclic and polymetamorphic terrains: a case from the Central Italian Alps. Geol. Soc. London Spec. Pub., 332: 173-187.

Structural Controls on Fluid Migration and Orogenic Gold Deposition in the Birimian of West Mali and East Senegal, West Africa

Peter J. Treloar*[1], James Lambert-Smith[1], David M. Lawrence[1], Paul Harbidge[2]

[1]Centre for Earth and Environmental Science Research, Kingston University, Kingston-upon-Thames, KT1 2EE, UK
[2]Randgold Resources, La Motte Street, St Helier, Jersey, JE1 1BJ, Channel Islands
*p.treloar@kingston.ac.uk

The Birimian-aged (2.3 Ga) Palaeo-Proterozoic rocks of the Kedougou-Kenieba inlier (KKI) of West Mali and East Senegal are remarkably prospective in terms of orogenic gold. On the eastern side of the KKI, in Western Mali, the Senegal-Mali shear zone (SMSZ) hosts a number of world class orogenic gold deposits. These include the 14 Moz Sadiola deposit in the north. The Loulo permit includes three major deposits – the 6.5 Moz Yalea deposit, the 6 Moz Gounkoto deposit and the 4.5 Moz Gara deposit. This paper discusses the evolution of the Loulo deposits.

The SMSZ strikes c.005° through the Loulo permit area and adjacent permits on the Senegalese side of the Faleme River. We identify a series of important structures. Due to poor exposure these were initially mapped by satellite imagery. Subsequent river section mapping, open-pit, and underground mapping has allowed the development of a rigorous structural model. Our new structural data (lineation data and S-C' fabrics) show the SMSZ to be a sinistral strike slip shear zone with an overall sub-horizontal displacement.

As with most orogenic gold deposits, those on the Loulo permit are not hosted within the first order structures – in this case the SMSZ. We identify a series of higher order structures that control the ore bodies. Second order structures are NNE-trending, steeply dipping transpressional, sinistral faults which pass into tight folds with vertical, NNE-trending axial planes. These second order structures have a Reidel geometry with respect to the SMSZ. They were subsequently mineralized during a later phase of transtensional deformation during which third order, N-trending sinistral faults developed. These have a Reidel geometry with respect to the second order structures. At this stage, both the second order and third order structures were mineralized. Fourth order, NNW-trending, steeply dipping brittle shears developed during continued transtensional during uplift. Also mineralized, these show a higher level mineralization with telluride phases present that are absent in the second and third order structures.

The Loulo permit area shows a complex, yet tractable, structural evolution that moves from sinistral transpression to sinistral transtension. Early second order transpressive structures were re-activated during transtension to provide space for mineralization.

Into this complex structural evolution we need to factor the evolving mineralogy and fluid chemistry of the ore bodies. The SMSZ itself is characterized by a regional Boron anomaly which isotopic data suggest has an igneous source. Different ore bodies within the Loulo permit have different chemical signatures. Gara has a Fe-Cu-REE-Au-Ni-W-As metal association, and abundant tourmaline and sodic alteration and is characterized by hypersaline fluid inclusions. This shows a clear magmatic signature which is atypical of orogenc gold deposits. By contrast, the Yalea body , has a Fe-As-Cu-W-Au-Ag-Pb-Sb-U metal signature with saline poor fluid inclusions. This has a more standard metamorphic signature.

There is a clear change in fluid chemistry across the SMSZ. To the west, in Senegal, the fluids are hypersaline and mineral assemblages often carry tourmaline. To the east, in Mali, the fluids are generally less saline with a lower Boron content. There is, though, a zone of mixing where low-temperature, high pH metamorphic fluids interact with high temperature low-pH fluids. Mixing of these fluids triggers rapid ore deposition as is clearly seen at Gara.

A key test for exploration structural geologists is to identify the extent to which the SMSZ acts as a barrier which separates dominantly igneous fluids to the east from metamorphic fluids to the

west. A second key question for exploration structural geologists is to identify the structures along which these diverse fluids might mix.

The SMSZ is probably best characterized as an atypical orogenic gold belt. Although atypical, understanding the relationships here between a temporally evolving structural system and a synchronously evolving fluid system should underpin future models for orogenic gold exploration in a variety of more or less complex systems.

Structural Control of high grade Au-shoots at Hill End, NSW, Australia

Colin Wilkins*[1]

[1]Geology, School of Geography, Earth and Environmental Sciences, University of Plymouth, Devon, UK
*C.Wilkins@plymouth.ac.uk

Economic quantities of Au were first discovered at Hill End in 1851 and were famed for their richness and coarse grained nature. During the early history of the Hill End goldfield as much as 50 t Au were produced together with the Holtermann Nugget, at 268 Kgs the largest non-alluvial nugget ever mined. Recent mining operations by Hill End Gold Limited (The Reward Mine) allowed underground access to un-mined mineralized vein systems for the first time in +100 years. A good body of work exists on the geology of the Hill End goldfield but, until now, no studies could explain the sporadic and very localized nature of high grade Au mineralization at Hill End. In particular, no structural work had been completed during active mining until the present study. Critically, developing and mining along any of up to +10 regularly spaced bedding parallel veins is no guarantee of profitability as zones containing economic grades are difficult to locate.

Bedding parallel laminated quartz veins (BPLQVs) host structurally controlled orogenic gold mineralization in the Hill End goldfield of New South Wales. The mineralized veins are contained within the turbidite-dominated Hill End Trough (HET) of mid Silurian to mid Devonian age in the Palaeozoic Lachlan Orogen of NSW. Regionally, the HET was deformed by two major events with synchronous metamorphism to chorite and biotite grade. D1 consists of SW-directed thrusting and associated S1 cleavage (usually only recognized as a bedding parallel fissility at the mine). The principal structures are D2 in age and formed during the Lower Carboniferous Kanimblan Orogeny. D2 formed tight N-S trending macroscopic folds (and associated BPLQVs) and faults, with a well developed S2 slaty cleavage prominent throughout the mine sequence.

The Reward Mine is located on the eastern limb of the doubly plunging N-S trending D2 Hill End Anticline where prominent BPLQVs were preferentially located within slate units, during folding of the Chesleigh Formation (a well bedded package of meta-mudstones and meta-greywackes). The Reward Mine was initially developed to mine sections of the Paxtons vein system to the north of areas of previously stoped-out BPLQVs. A detailed structural analysis in the Reward Mine indicated the following six stage structural and mineralization history during D2 fold development:

(1) Flexural slip folding of a turbidite-dominated sequence initiated bedding-parallel movement zones (BPMZ) with associated BPLQVs, saddle reefs and flexural-slip duplexes.

(2) In places, movement horizons with or without BPLQVs are marked by prominent gently-dipping extension veins (leaders), and as folds continued to develop duplexes and BPLQVs were folded in some cases.

(3) Continued shortening and limb rotation caused an axial planar cleavage (S2) to form, initially in the hinge areas and in finer grained lithologies (e.g. shale). Earlier formed extension veins were folded and subsequently cross-cut by later extension veins due to continued thrusting along BPMZs.

(4) S2 Axial planar cleavage intensified and formed in the limbs as well as the hinges of folds, and is now present in most lithologies. Saddle Reefs and BPLQVs can also develop a cross-cutting fracture cleavage. Earlier formed BPLQVs are folded or boudinaged during continued fold-related flattening. During these earlier stages in fold development (1-4), fluid flow and Au mineralization was restricted. It occurred mostly along bedding, BPMZs and BPLQVs. Au is associated with Po, Py and Cpy and Au grades range from 0-5 g/t (un-economic).

(5) The D2 folds locked up when interlimb angles reached ~60°, with subsequent E-dipping faults initiated along new or pre-existing weak zones (bedding, BPMZs, BPLQVs). This caused increased vein dilation and the introduction of massive quartz, i.e. veins are "pumped-up".

(6) After fold lock-up, continued shortening resulted in late W-dipping reverse faults that cross-cut and offset E-dipping BPLQVs (e.g. Paxtons). These discordant fault systems transected bedding and allowed larger volumes of ascending mineralizing fluids to contribute to elevated Au-grades in specific zones. For example the economic Au mineralization in Paxtons (+10 g/t and now associated with galena and sphalerite) forms discrete gently S-plunging Au-shoots that plunge in the same orientation as the W-dipping reverse fault – BPLQV intersection lineation.

Hence late W-dipping reverse faults displace, fracture and mineralize pre-existing BPLQVs, producing localized high-grade Au ore shoots in otherwise un-economic low-grade BPLQVs.

POSTER PRESENTATIONS

Linking Reaction and Deformation Paths Using Chemical Zoning in Amphiboles

Stokes, M. Rebecca*[1], Wintsch, R. P.[1]

[1]Indiana University, Bloomington
*mrstokes@indiana.edu

Chemical zoning preserved in individual amphibole grains from lineated amphibolites in the Eastern Blue Ridge, NC provides evidence that the dominant deformation mechanism in these rocks is solution-creep. The preservation of chemical zoning in the amphibole grains as well as in plagioclase and clinozoisite grains suggests that little lattice-diffusion induced homogenization has taken place, despite reaching metamorphic temperatures of ~750°C. Most amphibole grains display the chemical zoning along their lengths, and only moderate to no zoning is preserved orthogonal to the long-axis of the grains. The Si concentrations along the lengths amphiboles can range from 6.2-7.9 p.f.u., which correspond to compositions varying between the tschermakite and actinolite fields. Using the amphibole-plagioclase geothermometer (Holland and Blundy, 1994) crystallization temperatures were calculated for zoned amphibole grains and range between ~450°C and ~750°C. Also, temperature profile shapes from different samples preserve prograde and retrograde patterns. One sample in particular preserves both types of zoning, where the prograde population contains brecciated actinolite cores (~450°C) that have been healed by high-Si magnesiohornblende (~500°C) and lastly overgrown by low-Si magnesiohornblende and tschermakite. Conversely, the population of retrograde amphiboles within the same sample defines a different lineation and has low-Si magnesiohornblende cores (~750°C) and high-Si magnesiohornblende rims (~600°C). The elongated and aligned texture of the amphibole grains identified indicates crystallization of the grains during deformation and the pervasive chemical zoning patterns preserve the thermal evolution during fabric development.

Core and rim temperature and pressure estimates calculated using the garnet + amphibole + plagioclase thermobarometer constrain the pressure at peak temperature to be ~13 kbars at 750°C along a clockwise pressure-temperature-time path and in addition, corroborates peak temperatures obtained from the amphibole-plagioclase geothermometer. This information in addition to Ti-bearing mineral textures can be used to construct a semi-quantitative pressure temperature path along which the evolution of fabric forming amphiboles in equilibrium with the respective metamorphic conditions can be plotted. The lack of zoning parallel the short axis of the amphibole grains indicates that there has been dissolution of the grain orthogonal to the principal shortening direction in contrast to the significant amount of precipitation of new amphibole on the host grain in the extension direction. The dissolved ions migrate down chemical potential gradients to the end of the grains and precipitate a new, stable amphibole in equilibrium with the evolving metamorphic conditions. Thus the chemical zoning preserves the reaction path and also fossilizes the deformation path.

Tectonothermal Evolution of an Eclogite Facies Gneissic Formation at the Cabo Ortegal Complex: an Overview

Richard Albert*[1], Ricardo Arenas[1], Sonia Sánchez Martínez[1]

[1]Departamento de Petrología y Geoquímica e Instituto de Geociencias (UCM-CSIC), Universidad Complutense de Madrid, 28040 Madrid, Spain
*(r.albert@geo.ucm.es)

Field and petrologic studies have been recently archived at the Eclogite Facies Gneissic Formation of the HP-HT Upper Units in the Cabo Ortegal Complex (Galicia, Spain), also called "Banded Gneisses" by D.E. Vogel (1967). These studies represent the starting point of a more detailed research, the objective of which is to unravel certain aspects, as yet not well understood, about the origin of this formation and its tectonothermal evolution. This formation probably represents the only gneisses of all the Upper Units in the complex that really reached eclogite facies conditions, taking into account the mineralogical association of its basic inclusions, this is the evidence of coexistence of Omp+Grt before the intense retrogradation took place. The eclogite gneisses are made up from pelitic and greywackic sediments intruded by two main types of magmatic rocks, the first type, much more abundant than the second one, was formed by diabasic dikes and gabbros now displayed as retro-eclogites and rare coronitic metagabbros, and the second type shows granitic and tonalitic compositions and it is now recognized as thin inclusions of orthogneisses. This formation belongs to the Upper Units and, as all of these units, has been interpreted as a part of a peri-Gondwanan volcanic-arc with a Cambrian tectonothermal evolution (Abati et al., 1999; Fernández-Suárez et al., 2002; Fuenlabrada et al., 2010, and references therein). The studies carried out have shown no evidence of this Cambrian event but Fernández-Suárez et al. (2002) have described U-Pb ages of 500-480 Ma in HP-HT formations at the Órdenes and Cabo Ortegal complexes and so this event will be established as D0. Structurally under the eclogite gneisses a c. 300 m thick band of massive eclogites exists, and over it the Cariño Gneiss Formation which belongs to the so called Intermediate Pressure Upper Units. Between this formation and the studied gneisses there is a metamorphic gap of about 10 kbar and 100 ºC.

In the region where the eclogite gneisses appear, the Masanteo Peninsula is a locality of special interest where two geological sections have been studied and represented with detail. Here the gneisses show strong deformation and migmatization with many inclusions of mafic and felsic rocks. The mafic ones are mainly retrogressed eclogites always displayed as boudins of many sizes, from millimetres to decametres, with a not evident foliation different from the regional one. The felsic rocks do not show this boudinage process, but they are intensively foliated with the same imprint as the regional foliation. Both lithologies are also found tectonically imbricated even at millimetric scale. The main regional foliation (SR) is a pervasive mylonitc fabric that wraps around the boudins, and appears slightly folded with an approximately N-S orientation, dipping to the West or to the East. Associated to SR there is a lineation (LR) with top-to-north sense of movement that is defined as mineral stretching and mineral line up by Ábalos et al., 2004. The first type of rocks to mention is a gneiss bearing Qtz+Grt+Pl+Bt+Ky as primary minerals, considered a metasediment, which has been divided into two lithologies. One has high aluminium content and so it is defined as metapelitic and the other one lacks Ky and potasic feldspar, its aluminium minerals are scarce and therefore it is thought to be metagreywackic. Within these gneisses two types of basic rocks exist, variably retrogressed eclogites with Grt+Cpx+Hbl+Pl+Czo+Rt+Ilm+Spn and what it is thought to be a prograde pre-eclogitic type, coronitic metagabbros bearing Ol+Grt+Pl+Czo+Rt+Ilm+Spn. Two types of ortogneisses can be distinguished, a granitic one with Qtz+Grt+Pl+Mc+Bt and a tonalitic one with Qtz+Grt+Pl+Hbl+Czo. The foliation mentioned before in the mafic boudins is interpreted to be S1, and it is probably related to the eclogitic burial of the formation in a subduction process (D1), and on the other hand SR is interpreted as S2, linked to a strong decompression, and therefore to an exhumation (D2) after subduction.

We have found within the eclogite gneisses a huge mafic boudin intensively intruded by a mesocratic melt of tonalitic composition. The relationships observed in the field between both

lithologies are outstanding, being very similar to those seen in a mingling of basic and felsic rocks. The boudin shows in the internal parts little deformation associated to D2. Instead of the common tight foliation generally observed, this sector exhibits brecciated forms and rounded shapes. Its mafic parts are truly eclogitic, but the metamorphic conditions of the melts are not so clear. Its origin could be an original pre-metamorphic mingling, or it could be the result of a wide partial melting process after the eclogitic facies metamorphic event that intensively intruded and brecciated the formation supposedly during an important decompression. Until now the studies of its mineralogical associations haven't clarified its metamorphic evolution and its origin remains unclear. We hope that further analysis in this sector will give important clues to understand the tectonothermal evolution of the eclogite gneisses.

The macroscopic structure of the formation is a recumbent East-vergent synform of kilometric scale, of which its axial plane dips to the west with a N-S direction. It affects not only the eclogite gneisses but all of the Upper Units, and it produces an axial plane foliation which is only recognisable in the Cariño Gneiss Formation. The age of the fold is not accurately known, but it's certainly younger than the emplacement of the Intermediate Pressure Upper Units over the HP-HT Upper Units, because the limit between them is also folded with the same geometry. Even so, its age could be equivalent to the recumbent folding affecting the basal units, which is younger than 370 Ma. We have not found any geological evidence of other deformations between this structure and the regional foliation (S2), which is also affected by the recumbent synform, and so this kilometric fold is assigned to D3. This synform is also affected by an upright open folding of kilometric scale which is ascribed to D4.

We assume that a subduction process took place to give the eclogite facies imprint to the formation and we link this event (D1) to the accretion of the peri-gondwanan volcanic arc to Laurrusia 404 to 390 Ma ago (SHRIMP in zircons; Ordóñez Casado et al., 2001; Fernández-Suárez et al., 2007). This arc previously drifted away from Gondwana opening the Rheic Ocean and closing the pre-existing Iapetus-Tornquist Ocean (Arenas et al., 2007; Martínez Catalán et al., 2007). Immediately after the maximum pressure was attained (T-P values: 780-800ºC and 22 kbar, according to Mendia, 2000) the gneissic formation was exhumed (D2) suffering decompression and partial melting at c. 390–380 Ma (Ordóñez Casado et al., 2001). We also considerer that the recumbent folding (D3) could possibly be formed when the Rheic Ocean was consumed when Gondwana and Laurrusia collided in what is considered to be in a strict sense the Variscan Orogeny, of which its last stages produced the structures assigned to (D4). New investigations in process at the Eclogite Gneisses Formation are trying to contribute with new data to enrich and to confirm or even to modify this geological history.

References:

Ábalos, B. et al. (2004). Laboratorio Xeolóxico de Laxe, Serie Nova Terra, 24, 89 pp.
Abati, J. et al. (1999). Earth Planetary Science Letters, 165, 213-228.
Arenas, R. et al. (2007). Journal of Geology, 115, 129-148.
Fernández-Suárez, J. et al. (2002). Contributions to Mineralogy and Petrology, 143, 236-253.
Fernández-Suárez, J. et al. (2007). The Geological Society of America Memoir, 200, 469-488.
Fuenlabrada, J.M. et al. (2010). Gondwana Research, 17, 338-351.
Martínez Catalán, J.R. et al. (2007). Geological Society of America Memoir 200, 403-423.
Mendia Aranguren, M.S. (2000). Laboratorio Xeolóxico de Laxe, Serie Nova Terra, 16, 424 pp.
Ordóñez Casado, B., et al. (2001). Tectonophysics, 332, 359-385.
Vogel, D.E. (1967). Leidse Geologische Mededelingen, 40, 121-213.

Deformation Signatures Arrested by the Porphyroblast-Matrix Duo

Manua Banerjee

Indian Institute of Science Education and Research-Kolkata, India

A spectacular display of contrasting matrix grain size and porphyroblast grain size is manifested in the pelitic schists of the North Singhbhum Fold Belt (NSFB), Eastern India. A characteristic feature of the pelitic rocks of this region is that they occur in two distinct bulk compositions – the alumina rich component or the High Aluminous Pelite (HAP) and the alumina poor component or the Low Aluminous Pelites (LAP). The mineral assemblage of the LAP schist is quartz + muscovite + chlorite + biotite + garnet + staurolite + opaque minerals, where garnet, staurolite and opaque (magnetite?) occur as the porphyroblastic phases. The HAP schist comprises quartz + muscovite + chlorite (few) with kyanite, staurolite, chloritoid and pseudomorphs after andalusite (*shimmer aggregate*) as the porphyroblastic phases. These rocks are devoid of biotite.

Deformation recorded in this region is of the order 3 (i.e., D1, D2 and D3). The regional schistosity (D2) is a pervasive crenulation cleavage which is mylonitic at several places. The shearing responsible for the mylonitization is broadly coeval with D2 deformation. Evidences of this shearing, post dating D2, is also present in the rocks. D1 deformation has preserved its signature in tight rootless isoclinal fold hinges preserved in the pressure shadow regions of pre-D2 porphyroblasts as well as in the interfolia of D2 fabric (Mukhopadhyay et. al., 2004). D3 deformation has produced large scale warps on D2 and mylonitic foliations.

The disposition of porphyroblasts on a variedly deformed matrix, reveal an interesting history of formation of the pelitic schists of the NSFB. The ratio of porphyroblast size to matrix grain size (Ps:Ms) of the LAP is much less than the Ps:Ms ratio of the HAP. This work focuses primarily on the Ps:Ms ratio of the HAP schists. The high Al content in the bulk composition of the HAP has enhanced the stabilization of large high Al porphyroblasts.

Kyanite haphazardly overgrows the shimmer aggregates and D2 fabric. There is a continuity in the Si-Se trails (Fig.1). Often larger kyanite crystals are kinked by later deformations. Staurolite also overgrows haphazardly on the crenulated D2 schistosity and often has garnet with sigmoidal trail as inclusions. Staurolite crystals vary from 0.5cm to 24cm in length with maximum cross section of 6cm X 4cm. Garnet, besides being superimposed on D2 fabric, is pre mylonitization. It is also pre staurolite as it occurs as an included phase in staurolite (Fig.2). The andalusite porphyroblasts or the shimmer aggregates have a typical dipyramidal crystal form with orthorhombic symmetry. In section they show rectangular to rhombic and oval outlines often with internal zonal structure. The porphyroblasts are flanked and warped by D2 schistosity which is necessarily a crenulation cleavage, mylonitized at some places owing to the effect of post D2 shearing. Simple shear on D2 has modified the rectangular forms of the porphyroblasts to parallelograms and spindle shapes which parallel the pervasive foliation (Fig.3).

The matrix-grain size reduction is a typical case of deformation partitioning (Bell et. al 1986). Here in East Singhbhum, the matrix grain size reduction owes its cause to tectonic processes of shearing. These shearing forces and its consequent shear fractures introduced the rock to a huge fluid influx. This fine grained phyllitic rock, produced as a result of tectonism, is referred to as phyllonite (Naha 1965). The grain size refinement in mylonitic rocks is related to the replacement of large strained grains by small ones through the process of recovery & recrystallization. It is suggested that the development of mylonitic foliation parallel to axial planes of D2 folds is related to high stress condition in certain zones. The reduction in grain size leads to strain softening.

The large or extra large grain size of the porphyroblasts address not only a rapid growth rate but also indicate that the supply of porphyroblast-nutrients were remarkably large. Eventhough nucleation may have initiated in the Q-domains (Bell et. al 1986), several micro Q and M domains were encompassed and incorporated in the growth of such large grains (Fig.4). The shear stress that was subjected to these rocks was of the progressive shortening type (after Bell et. al 1983).

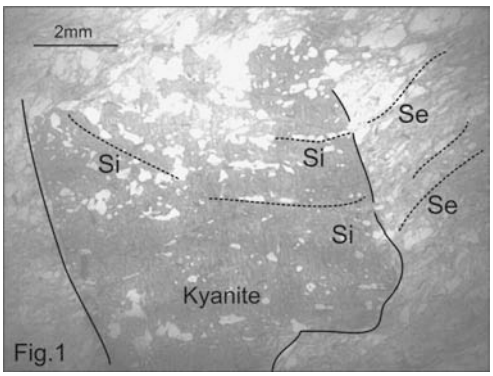

Fig.1 (Ghosh et.al 2006)

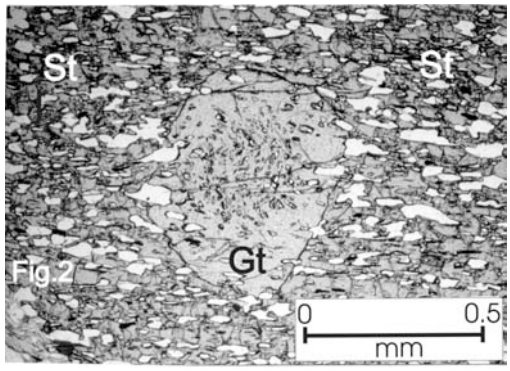

Fig.2

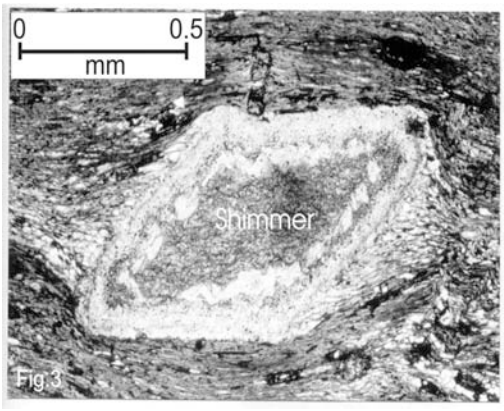

Fig.3 (Ghosh et. al 2006)

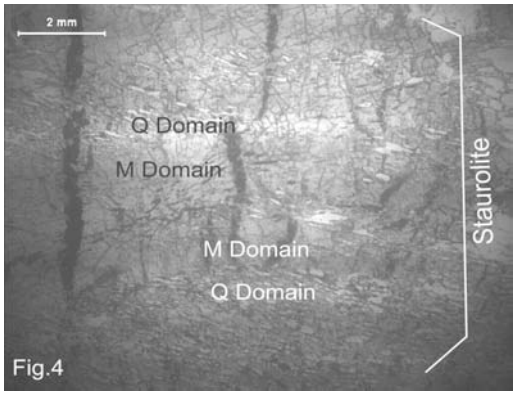

Fig.4

References:

Bell, T. H., Rubenach, M. J. and Flemming, P. D.,(1986). Porphyroblast nucleation, growth and dissolution in regional metamorphic rocks as a function of deformation partitioning during foliation development. Journal of Metamorphic Geology, 4, 37-67.

Bell, T.H. and Rubenach, M. L.,(1983). Sequential porphyroblast growth and crenulation cleavage development during progressive deformation. Tectonophysics, 92, 171-194.

Mukhopadhyay D, Banerjee M, and Chattopadhyay A (2004) Structural pattern in the Dhalbhumgarh-Kokpara Region and its bearing on the tectonics of the Proterozoic Fold Belt of North Singhbhum, Eastern India. GSI special publication No.84, pp.43-60.

Ghosh,M, Mukhopadhyay D, Sengupta, P. (2006) Pressure–temperature-deformation history for a part of the Mesoproterozoic fold belt in North Singhbhum, Eastern India. Journal of Asian Earth Sciences 26, 555–574.

Naha, K.M., (1965)Metamorphism in relation to stratigraphy, structure and movements in part of East Singhbhum, Eastern India. Quarterly Journal of Geology, Mining and Metallurgical Society of India, 37, 41-81.

Preliminary Results of the EDSB Study of Felsic Granulite Associated with the Beni Bousera Peridotite (Rif belt, N. Morocco)

Barich Amel *[1], Garrido C. J.[1], Vauchez A.[2], Tommasi A.[2], Smith B.[2], Camps P.[2], Bodinier J.L.[2], Bouybaouene M.[3]

[1] Instituto Andaluz de Ciencias de la Tierra (IACT), CSIC-UGR, Granada, Spain (*abarich@iact.ugr-csic.es)
[2]Geoscience Montpellier, Univ. Montpellier II – France
[3]Université Mohammed V Agdal – Rabat, Morocco

The internal Rif represent is the southern limb of the arcuate Betic-Rif alpine belt in the westernmost Mediterranean. The Sebtide metamorphic unit occurs in internal parts of the Rif. This unit is associated to the Beni Bousera subcontinental peridotite massif and, in their southern part, is composed by HP-HT granulites. Outcrops of mantle rocks in this massif are among the largest in the Alboran alongside their counterparts from Ronda in the Betic Cordillera in Spain.

In the Sebtides, two types of granulites occur rimming the Beni Bousera peridotite: (1) garnet-sillimanite-feldspar ± Kyanite ± graphite-bearing felsic granulites ("kinzigites"); and (2) garnet(pyrope)-kyanite-clinopyroxene-plagioclase-bearing mafic granulites, which occur mostly as lenses within the kinzigites. Thermobarometric estimations suggest the overprint of LP-HT metamorphism (10-13 kbar/850°C) related to crustal thinning, which is assumed to be the metamorphic peak related to the emplacement of mantle rocks. The kinzigites show a granoblastic texture consisting of centimetric garnets (almandine) associated to plagioclase and feldspar. Garnet and plagioclase are surrounded by symplectites mainly formed by cordierite. Sillimanite occurs as oriented fibers into a well-marked with quartz and biotite.

We have carried out a combined EBSD and ASM fabric study on kinzigites to better constraint the kinematic of these HP-HT lower crust granulites. Preliminary EBSD results show a well lattice preferred orientation of sillimanite (Fig. 1) that reveals synkinematic growth of this mineral during decompression. On the other hand, first investigations of Anisotropy of Magnetic Susceptibility in some granulite samples have shown a well-defined magnetic fabric. Further investigations will be carried out to compare the correlation between EBSD and magnetic fabrics and how they constrain the kinematic of kinzigites during lithospheric thinning and emplacement.

Granulites

[100] [010] [001]

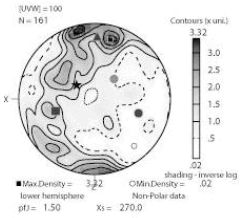

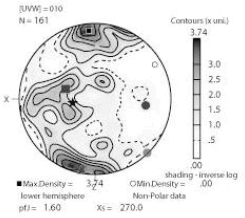

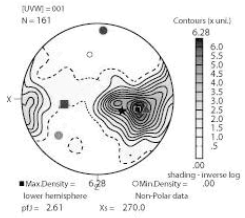

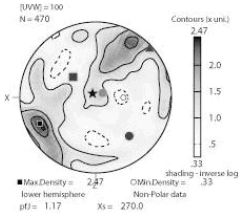

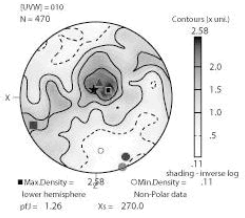

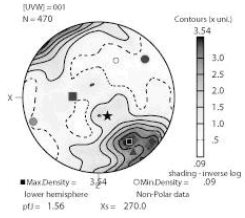

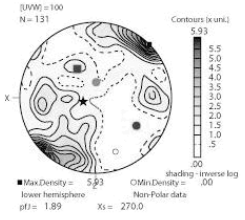

8BA106-2-W-oppg-Sil-pf.ai

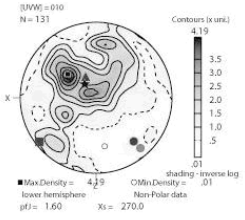

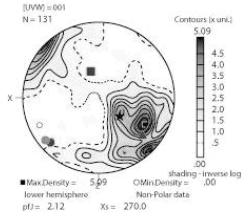

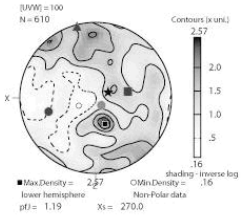

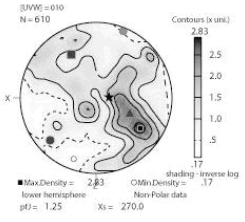

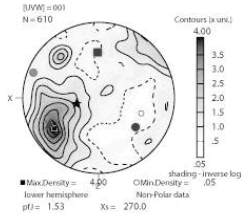

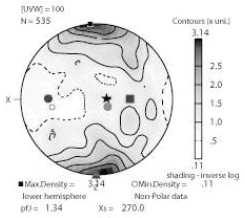

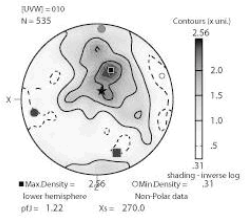

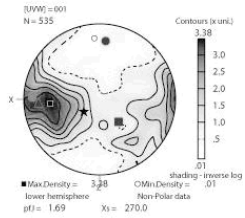

Mylonites

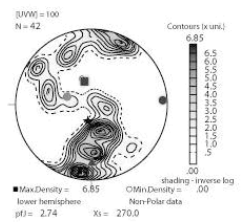

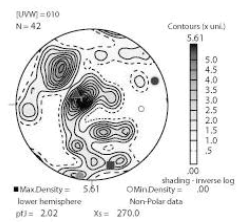

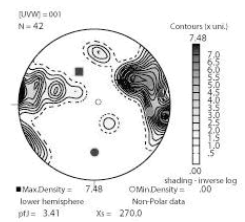

Garnet zoning in high grade granulite from Beni Bousera (internal Rif mountains, Morocco)

M. L. Belhassan*[1], R. Alami[1]

[1] Département des Sciences de la Terre, Faculté des Sciences, BP 1014 Rabat, Morocco
*bouybaouene@yahoo.fr

Rocks at the top of the peridotite body of Beni Bousera (internal Rif mountains, Morocco) are characterised by a granulite facies metamorphism. Up to now, only the retrograde metamorphic P-T evolution has been described. In our study, we present a more detailed P-T evolution based on thermobarometry as derived from microstructural features, mineral parageneses and compositional data of phases.

In zoned garnet of acide granulite, the analysed core composition is alm63, pyr33, gros3 (mole%). In the inner rim, the composition is alm60-61, pyr33-30and gros5-9. A narrow outer rim shows a lower Mg-content: alm61-67, pyr30-27, gros8-5. This chemical zoning corresponds to a zoning of mineral inclusion in garnet. Garnet cores contain inclusions of biotite, quartz, plagioclase, hercynite and sillimanite. Only kyanite can be found in the rim zone. The data are interpreted to reflect a three-stage metamorphic P-T evolution: the garnet core is formed at 6 to 7 kbar pressure at 680-750°C (M1). The inner rim reflects a significant pressure increase up to peak conditions of 13 to 14.5 kbar, 800 to 850°C (M2). The composition of the outer rim of garnet corresponds to decompression and cooling resulting in P-T conditions of about 6.5 kbar, 570°C (M3). A contemporaneous formation of symplectite around garnet and kyanite containing minerals such as cordierite, plagioclase, hercynite can be observed. The final exhumation of the rock unit is reflected by late stage shearing and extensive deformation (M4).

The data show that in the Rif mountains the granulite and formerly diamond bearing ultrabasic mantle rocks were uplifted in the same geodynamic environment.

Could low a(SiO_2) Enlarge the Stability Field of Staurolite?

Fetherston, Daniel*[1], Wintsch, Robert[1]

[1]Department of Geological Sciences, Indiana University;
*dfethers@indiana.edu

During prograde metamorphism, metamorphic differentiation can lead to the development of quartz-rich (Q) domains and phyllosilicate-rich, quartz-poor, (P) domains. The removal of quartz from P domains could lower the a(SiO_2) which could expand the stability field of Al-rich minerals. The common concentration of staurolite on the shoulders of quartz veins might be explained by this differentiation. Pressure gradients cause the diffusive transfer of SiO_2 out of the matrix and into the vein site, thus lowering the a(SiO_2) in the matrix (e.g. Ague, 2011).

A preliminary petrographic analysis of staurolite bearing samples collected from the Narragansett Basin of Rhode Island show metamorphic differentiation of argillaceous protoliths into quartz-rich Q domains and muscovite-biotite-rich (quartz-absent) P domains. Here, subhedral staurolite porphyroblasts up to 2 mm long occur only within the P domains. Staurolites contain small amounts of quartz inclusions parallel with micas in the matrix foliation. The staurolite truncates both the strongly aligned muscovite flakes in the enclosing schist as well as larger biotite porphyroblasts. However, there is a conspicuous lack of quartz at the interface between the muscovite-biotite matrix and the staurolite that would be expected given the replacement reaction:

$$\mathbf{25\ KAl_3Si_3O_{10}(OH)_2 + 6\ KFe_3AlSi_3O_{10}(OH)_2 + 31\ H^+ = 9\ Fe_2Al_9Si_4O_{23}(OH) + 57\ SiO_2 + 31K^+ + 42H_2O}$$

In fact, this reaction, supported by these replacement textures, predicts a 2 : 3 volume ratio of quartz to staurolite. The lack of quartz at the reaction site suggests that SiO_2 was continuously being removed during porphyroblast growth; otherwise the quartz byproduct would accumulate along the staurolite interface. Therefore, it is likely that staurolite growth occurred concomitantly with differentiation and SiO_2 loss at the reaction site.

This hypothesis of differentiation driven reaction is further supported the volumetric change taking place during the above reaction. The reaction of muscovite + biotite to staurolite + quartz produces a volume reduction of 75%. If SiO_2 is removed from the reaction site, this volume reduction drops to ~45% of original muscovite + biotite volume. Such Volume loss identifies locally high stress as another potential force driving the reaction producing staurolite. Thus differentiation could drive this reaction by both establishing an a(SiO_2) gradient away from the shoulders of veins by maintaining a local high stress to favor the smaller volume products.

Intragrain Oxygen Isotope Zoning in Titanite by Ion Microprobe: Cooling and Uplift Rates Along the Carthage-Colton Mylonite Zone, Adirondack Mountains, New York

Chloë Bonamici*[1], Rienhard Kozdon[1], Takayuki Ushikubo[1], John W. Valley[1]

[1]WiscSIMS Lab, Department of Geoscience, University of Wisconsin-Madison
*bonamici@geology.wisc.edu

Ion microprobe analyses of late Grenville-aged (ca. 1050 Ma) titanite from the Carthage-Colton Mylonite Zone (CCMZ) in the Adirondack Mountains, NY, reveal microscale variations in oxygen isotope ratios (Fig. 1A). The character of this $d^{18}O$ zoning varies systematically with the structural context of the titanite grain. By combining the microscale titanite $d^{18}O$ record with the micro- and mesostructural records of deformation, we reconstruct an integrated chronology of sequential fabric development, fluid infiltration, and uplift along the CCMZ.

The CCMZ is a long-lived, multiply reactivated, crustal-scale shear zone that defines the boundary between the granulite facies Adirondack Highlands and amphibolite facies Adirondack Lowlands (Mezger et al., 1992). The relative position of the Highlands and Lowlands during the Ottawan phase (1090-1000 Ma) of the Grenville orogeny and the timing of their current structural juxtaposition remain controversial; however, the CCMZ ultimately accommodated NW-directed displacement of the Adirondack Lowlands and consequent exhumation of the Adirondack Highlands (Mezger et al., 1992; Streepey et al., 2001).

We investigate outcrops of the Diana metasyenite in the south-central CCMZ near Harrisville, NY. Based on crosscutting relations, three deformational fabrics are recognized: the earliest fabric is a locally preserved protomylonite; the intermediate, a spaced network of steeply dipping ultramylonitic shear zones that crosscut the early protomylonite; and the latest, a well-developed mylonite/ultramylonite that overprints both earlier fabrics. Titanite porphyro*blasts* overgrowing the oldest fabric and porphyro*clasts* deformed within intermediate-age shear zones retain evidence for high-T diffusive exchange of oxygen; syn-shear zone titanite with transitional porphyroclastic/blastic microstructures show evidence of diffusion-modulated growth zoning; and titanite porphyroblasts overgrowing the latest fabric preserve symmetric growth zoning (Fig. 1B). The changing character of $d^{18}O$ zoning from the earliest to the latest formed titanite is consistent with cooling from above Dodson's temperature for titanite closure to oxygen exchange (650-700°C) during protomylonite and shear zone formation to temperatures of <550°C during the latest mylonitic overprinting.

Overall, titanite $d^{18}O$ increases systematically during the transition from shear zone formation to late ultramylonitic overprint, signaling a concomitant change in whole-rock $d^{18}O$ composition, related to high-$d^{18}O$ fluid infiltration from adjacent marbles (Cartwright et al., 1993). Late-syn-shearing transitional grains with elevated $d^{18}O$ (relative to pre-shearing grains) grew in the presence of fluids but decreasing $d^{18}O$ rims indicate subsequent isolation from fluids and modification of $d^{18}O$ at grain margins by diffusive exchange. Growth-zoned titanite that overgrew the latest mylonitic overprint records the highest $d^{18}O$, consistent with continued and perhaps even increased fluid infiltration during development of the last fabric. These relations suggest a shift in the locus of active fluid infiltration with the locus of active deformation from the intermediate-aged shear zone network to the mylonitic/ultramylonitic overprint.

Modeling the steep titanite $d^{18}O$ diffusion profiles measured by ion microprobe, we calculate cooling rates of 30-60°C/my along the CCMZ during late stage exhumation of the Ottawan orogen (Fig. 1A). This is significantly faster than the time-averaged, 1-5°C/m.y. cooling rate determined by regional thermochronology studies (Mezger et al., 1991; Streepey et al., 2001) and likely reflects rapid uplift accommodated by episodic movement on the CCMZ (Bonamici et al., 2011). Thus, $d^{18}O$ zoning in titanite captures previously unresolved detail along the late Grenville P-T-t-fluids path and suggests punctuated (non-steady-state) collapse of the Ottawan orogen.

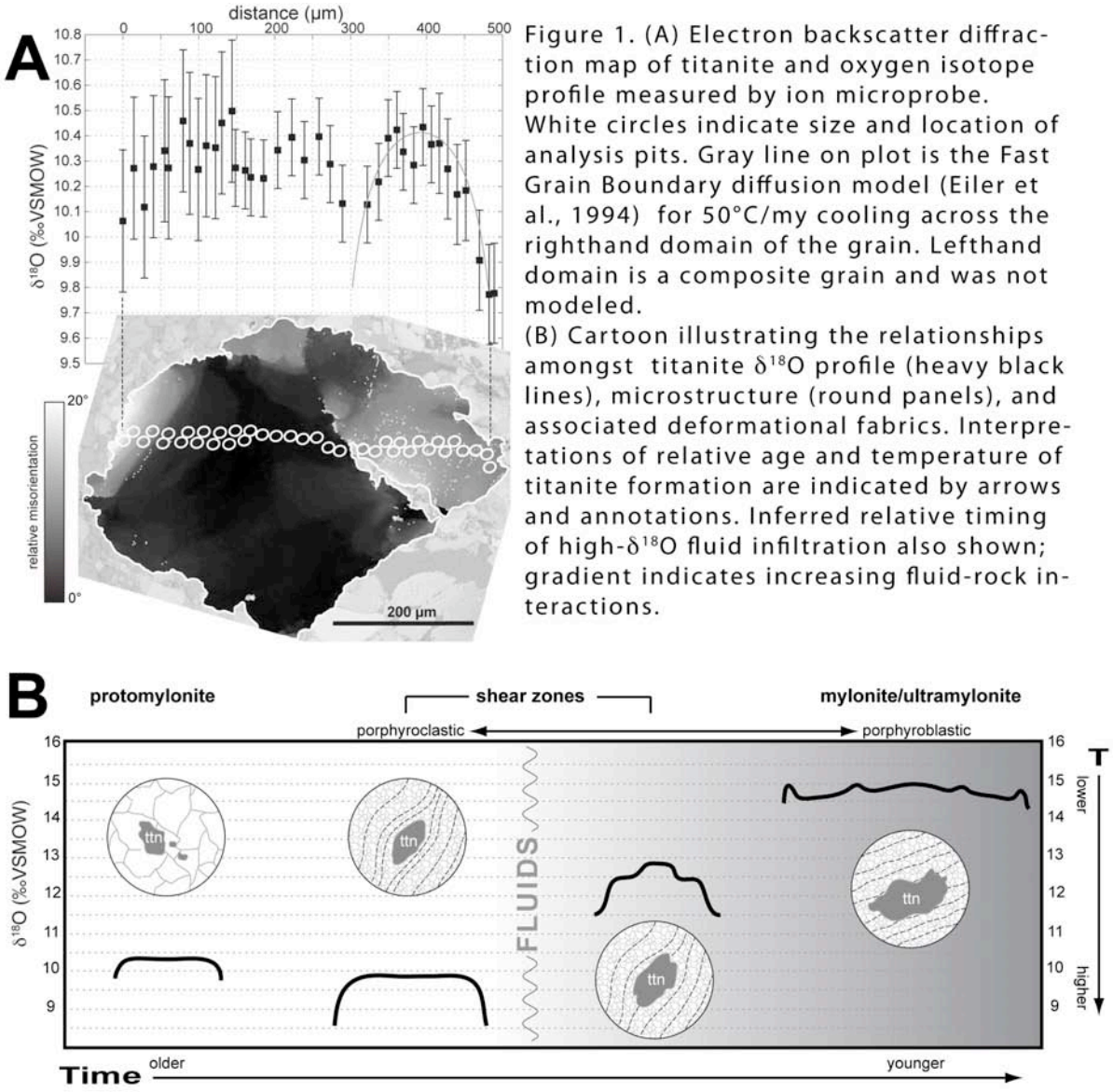

Figure 1. (A) Electron backscatter diffraction map of titanite and oxygen isotope profile measured by ion microprobe. White circles indicate size and location of analysis pits. Gray line on plot is the Fast Grain Boundary diffusion model (Eiler et al., 1994) for 50°C/my cooling across the righthand domain of the grain. Lefthand domain is a composite grain and was not modeled.
(B) Cartoon illustrating the relationships amongst titanite $\delta^{18}O$ profile (heavy black lines), microstructure (round panels), and associated deformational fabrics. Interpretations of relative age and temperature of titanite formation are indicated by arrows and annotations. Inferred relative timing of high-$\delta^{18}O$ fluid infiltration also shown; gradient indicates increasing fluid-rock interactions.

Bonamici, C.E., Kozdon, R., Ushikubo, T., and Valley, J.W., 2011, High-resolution P-T-t paths from d^{18}O zoning in titanite: A snapshot of late-orogenic collapse in the Grenville of New York: Geology, *(in review)*.

Cartwright, I., Valley, J.W., and Hazelwood, A.-M., 1993, Resetting of oxybarometers and oxygen isotope ratios in granulite facies orthogneisses during cooling and shearing, Adirondack Mountains, New York: Contributions to Mineralogy and Petrology, v. 113, p. 208-225.

Eiler, J.M., Baumgartner, L.P., and Valley, J.W., 1994, Fast Grain Boundary: A Fortran-77 program for calculating the effects of retrograde interdiffusion of stable isotopes: Computers & Geosciences, v. 20, p. 1415-1434.

Mezger, K., van der Pluijm, B.A., Essene, E.J., and Halliday, A.N., 1992, The Carthage-Colton mylonite zone (Adirondack Mountains, New York): the site of a cryptic suture in the Grenville orogen: Journal of Geology, v. 100, p. 630-638.

Streepey, M.M., Johnson, E.L., Mezger, K., and van der Pluijm, B.A., 2001, Early history of the Carthage-Colton shear zone, Grenville Province, Northwest Adirondacks, New York (U.S.A.): Journal of Geology, v. 109, p. 479-492.

Metamorphic Evolution and P-T Pseudosection Modelling of Chloritoid-bearing Schists From the Variscan Chain of NE Sardinia, Italy

Gabriele Cruciani*[1], Marcello Franceschelli[1], Luca Giacomo Costamagna[1]

[1]Dipartimento di Scienze della Terra Università degli Studi di Cagliari, via Trentino 51, 09127 Cagliari Italy
*gcrucian@unica.it

The studied samples, collected a few km north of Lula village, belong to the Low to Medium Grade Metamorphic Complex (LMGMC) of the Variscan chain, located in NE Sardinia. The LMGMC consists of an igneous-sedimentary sequence made up of quartzite, mylonitic schist and paragneiss, and Ordovician orthogneiss and augen gneiss. Five Variscan deformations (D_1 to D_5), showing different fold style, have been recognized in the LMGMC. In the studied samples three foliations (S_1,S_2,S_3) related to the D_1, D_2, D_3 deformation phases described in the LMGMC (Elter et al., 1986, Carosi and Palmeri, 2002) can be identified. The S_1 foliation is still well recognizable in the hinges of the D_2 folds. The S_1 foliation is defined by the orientation of muscovite, paragonite, chloritoid, quartz, and Fe-oxides in microlithons.

Garnet occurs in porphyroblasts up to 3-4 mm in size surrounded by S_2 schistosity. Inclusion trails in garnet are rectilinear, gently or strongly folded. Several curved trails of quartz inclusions in garnet seem to identify the S_1 schistosity. Inclusions in garnet also consist of rutile, Fe-oxides, apatite, paragonite, and chloritoid.

Strain shadows are also very common on both sides of garnet porphyroblasts. They consist of medium-grained quartz and chlorite or of a fine-grained intergrowth of quartz, phyllosilicates (muscovite and chlorite) and carbonaceous matter. Sometimes quartz crystals of the strain shadows are incorporated as slightly elongated inclusions into the rim of garnet porphyroblasts.

S_2-oriented minerals are muscovite, paragonite, chlorite, and carbonaceous matter.

Margarite is the less abundant between the phyllosilicates. It grows on chloritoid lath included in garnet. In this laths margarite grows on chloritoid near to the rim of garnet. Margarite has never been observed in chloritoid lath from the matrix. This observation strongly supports the role of the grossularite component in the formation of margarite.

Garnet is almandine-rich with high grossularite, spessartine and low pyrope content (Alm=53-70 mol%, Pyr=4-6, Grs=15-24, Sps=8-20). All garnets show slight variation in pyrope content and systematic increase in almandine content, counterbalanced by a decrease in spessartine and grossularite from core to rim. The X_{Mg} ($Mg/Mg+Fe^{2+}$) ratio slightly increases from core to rim.

Chloritoid is Fe-rich (Fe^{2+}_{tot}=0.82-0.84 a.p.f.u., Mg=0.14-0.16 a.p.f.u.) with X_{Mg} in the range 0.15-0.17 and low Mn content (<0.02 ap.f.u.).

Chlorite shows Al^{IV} content in the range 2.5-2.8 a.p.f.u., Al^{VI} =2.5-2.8 a.p.f.u. and X_{Mg} ratio between 0.41 and 0.48.

S_1 muscovite is characterized by Si=6.2-6.3 a.p.f.u., X_{Mg}~0.48, Na/(Na+K)=0.17-0.19. Paragonite (Si: 6.06 a.p.f.u., X_{Mg}=0.25, Na/(Na+K)= 0.9) contains small amount of Ca an K (0.05 and 0.16 a.p.f.u., respectively).

S_2 muscovite has Si=6.4-6.5 a.p.f.u., X_{Mg}=0.5-0.6, Na/(Na+K)=0.13-0.17.

Margarite contains small amounts of Fe, Mg, and Na (Fe^{2+}_{tot}=0.10, Mg=0.02, Na=0.42 a.p.f.u.) and yielded an X_{Mg} value of about 0.17.

The metamorphic history of chloritoid-bearing schists has been investigated by *P-T* pseudosection calculated in the NCKFMASH+Ti model system using the approach of Connolly (1990) and the internally consistent thermodynamic data set and equation of state for H_2O by Holland and Powell (1998, revised 2004). The P-T pseudosection was calculated within the P-T range 1-20 kbar, 400-800°C at a_{H2O}=1.

The phases considered in the calculation were: plagioclase, quartz (Qtz), K-feldspar, cordierite, staurolite, garnet (Gt), biotite, phengite (Phe), chlorite (Chl), chloritoid (Ctd), paragonite (Pa),

margarite (Marg), andalusite, kyanite, sillimanite, epidote (Ep), rutile (Rt), titanite, ilmenite, and magnetite (Mt). Solid-solution models are those of Holland and Powell (1998) for garnet, biotite, phengite, chlorite, staurolite, cordierite, chloritoid and epidote, and Newton et al. (1981) for plagioclase.

The prograde part of the P-T path, characterized by the mineral assemblage paragonite, muscovite, chloritoid, quartz, rutile and Fe-oxide match the paragenesis of the garnet-, staurolite- and margarite-free fields stable at temperatures below 560°C and pressure above 6 kbar (Chl±Ep+Phe+Ctd+Pa+Qtz+Rt+Mt multivariant fields). Further constrains for the prograde stage can be obtained by the intersection between compositional isopleths for Si content in S_1-oriented muscovite and X_{Mg} isopleths for chloritoid included in garnet that point to P-T conditions of 10.5 kbar and ~ 480-500°C.

The metamorphic peak assemblage consisting of garnet and S_2-oriented minerals (muscovite, paragonite, chlorite, chloritoid) match the paragenesis of the multivariant field Chl+Ep+Phe+Ctd+Pa+Gt+Qtz+Rt+Mt stable at T~560°C and P comprised between 8.6 and 15kbar. Intersection between isopleths representing the pyrope and grossularite content observed in garnet rim allow to estimate P-T conditions of the metamorphic peak at, or near to, $T \leq 560$-570°C and P = 7.5-9.5kbar. These P-T conditions are in agreement with the decrease of grossularite and increase in pyrope content from garnet core to rim suggesting that, the pressure peak was followed by an increase in temperature accompanied by a slight decrease in pressure up to the thermal peak.

Finally, the retrograde assemblage characterized by the entry of margarite corresponds to the Chl+Phe+Ctd+ Marg+Pa+Qtz+Rt+Mt field stable at T below 560°C and P lower than about 7-7.5 kbar. Pressure estimation for the retrograde stage has been obtained from X_{Mg} of coarse-grained, retrograde chlorite which indicate re-equilibration at about 2-3 kbar. The P-T path of the chloritoid-bearing schists from NE Sardinia have significant analogies with that described by Ricci et al. (2004) for the upper garnet zone of the Variscan chain of Sardinia. The P-T path of the studied rocks is loop-shaped and clockwise, typical of continental orogenic belts having undergone crustal thickening.

Carosi R., Palmeri R. (2002) Orogen-parallel tectonic transport in the Variscan belt of northeastern Sardinia (Italy): implications for the exhumation of medium-pressure metamorphic rocks. Geological Magazine, 139, 497–511.

Connolly J.A.D. (1990) Multivariable phase diagrams: an algorithm based on generalized thermodynamics. American Journal of Science, 290, 666–718.

Elter F.M., Franceschelli M., Ghezzo C., Memmi I., Ricci C.A. (1986) The geology of northern Sardinia. In: Carmignani, L., Cocozza, T., Ghezzo, C., Pertusati, P.C., Ricci, C.A. (Eds.), Guide-Book to the Excursion on the Paleozoic Basement of Sardinia. IGCP Project. Newsletter, vol. 5, pp. 87–102. special issue.

Holland T.J.B., Powell R. (1998) An internally consistent thermodynamic data set for phases of petrologic interest. Journal of Metamorphic Geology, 16, 309–343.

Newton R.C., Charlu T.V., Kleppa O.J. (1981) Thermochemistry of the high structural state plagioclases. Geochimica et Cosmochimica Acta, 44, 933–941.

Ricci C.A., Carosi R., Di Vincenzo G., Franceschelli M., Palmeri R. (2004) Unravelling the tectono-metamorphic evolution of medium-pressure rocks from collision to exhumation of the Variscan basement of NE Sardinia (Italy): a review. Periodico di Mineralogia, 73, 73-83.

Mylonitic Staurolite-bearing Schists From the Variscan Chain of NE Sardinia, Italy

Gabriele Cruciani [1], **Marcello Franceschelli*[1]**, Luca Giacomo Costamagna[1], Franco Marco Elter[2], Matteo Padovano[2]

[1]Dipartimento di Scienze della Terra Università degli Studi di Cagliari Cagliari Italy.
[2]Dipartimento per lo Studio del Territorio e delle sue Risorse Università degli Studi di Genova, Italy.
*francmar@unica.it

Staurolite-bearing schists were collected in the Low- to Medium-Grade Metamorphic Complex in the southern flank of the Posada Valley, along a 5 km wide and 100 km long late Variscan shear zone (the so called Posada-Asinara line) running from Posada village in NE Sardinia to the Asinara Island in NW Sardinia.

From south to north the rocks of the Posada Valley are characterized by a prograde increase in metamorphic grade, from the staurolite+biotite zone, through the kyanite+biotite zone up to the sillimanite zone.

The Posada Valley rocks were involved in the polyphase history of the Variscan orogeny and were affected by at least five deformation phases. The D_1 event, associated to a S_1 foliation, is only visible at the microscopic scale; the D_2 event is marked by a well defined S_2 mylonitic foliation (Franceschelli et al., 1989), which strikes WNW-ESE, with WNW-ESE plunging mineral lineations. The kinematic indicators relative to the D_2 event reveal a dextral sense of shear, while the thermobaric estimations point to lower amphibolite-greenschist facies conditions; the D_3 and D_4 events are characterized by different fold types, not associated to axial plane schistosity; D_5 phase produced kilometre-sized flexure with a sub- horizontal axis (Elter et al., 1986, Carosi and Palmeri, 2002, Helbing et al., 2006, Elter et al., 2010).

The staurolite-bearing schists consist of a mylonitic matrix, with well developed S-C planes, hosting garnet, staurolite, ± kyanite, and plagioclase porphyroblasts. The volume ratio between the matrix and the porphyroblasts, as well as the grain size of the mylonitic matrix are strongly variable.

In the mylonitic matrix millimeter-thick phyllosilicate-rich domains irregularly alternate with quartz-feldspathic domains. Biotite, chlorite, and quartz often form strain shadow on both sides of garnet and staurolite porphyroblasts. Ilmenite, tourmaline and Ti-oxide occur as accessory phases in the matrix, and/or as inclusions in staurolite and garnet.

Staurolite occurs as elongated, sometimes prismatic porphyroblasts of about 0.5mm in size containing garnet, biotite and ilmenite inclusions. Staurolite crystals are also characterized by gently to tightly folded curved graphite trails defining an older S_1 schistosity. In a few grains, in the limbs of the graphite trails tight folds the development of a new foliation is recorded.

Garnet, up to a few mm in size, is fractured and contain several inclusions of anhedral quartz. Garnet is almandine-rich with lower grossularite, spessartine and pyrope content (Alm=70-84 mol%, Pyr=9-12, Grs=2-12, Sps=2-14). An increase in almandine and pyrope content, counterbalanced by a decrease in spessartine has been observed from core to rim. The X_{Mg} ($Mg/Mg+Fe^{2+}$) ratio in garnets slightly increases from core to rim. Staurolite (X_{Mg} ratio ~ 0.15) contains low amounts of Mn (~ 0.08 a.p.f.u.) and Ti (~ 0.13 a.p.f.u.). No compositional zoning has ever been detected in staurolite porphyroblasts. Plagioclase composition ranges between $Ab_{75\text{-}89}$. Biotite (X_{Mg}=0.36-0.51) contains Ti up to 0.15-0.16 a.p.f.u., Mn up to 0.02 a.p.f.u. and Cr up to 0.011 a.p.f.u. Chlorite has X_{Mg} ratio between 0.42 and 0.54 and Al^{VI} ~2.9 a.p.f.u. S_2-muscovite is characterized by Si~6.2 a.p.f.u., X_{Mg}=0.42-0.54, Na/(Na+K)=0.19-0.25. Muscovite growing around staurolite and kyanite shows slightly lower Si content, lower X_{Mg} (0.37) and lower Na/(Na+K) ratio (0.11).

The metamorphic P-T conditions of the staurolite-bearing schists have been investigated by *P-T* pseudosection calculated in the NCKFMASH model system using the approach of Connolly (1990) and the internally consistent thermodynamic data set and equation of state for H_2O by Holland and

Powell (1998, revised 2004). The P-T pseudosection was calculated within the P-T range 1-20 kbar, 400-800°C at a_{H2O}=1.

The porphyroblastic mineral assemblage and the chemical composition of garnet and staurolite are consistent with P-T conditions of about 600°C and 8-9 kbar, corresponding to the garnet+staurolite± kyanite-bearing multivariant fields of the P-T pseudosection. Microstructural observations suggest that these P-T conditions are probably very near to those of the thermal peak.

The mylonitic assemblage records lower temperature and pressure conditions. Comparison between compositional isopleths of X_{Mg} in chlorite and Si content in muscovite with the observed values, suggests that S_2-oriented muscovite and chlorite are compatible with post-peak temperatures of about 520-570°C and pressures ~2 kbar lower than those determined for the peak conditions. In summary, the staurolite porphyroblasts, developed during the early D_2 deformation, record P-T conditions very near to the metamorphic peak whereas the mylonitic matrix reflect shear strain under amphibolite facies P-T conditions before the late reactivation of the shear zone in greenschist facies P-T conditions.

Carosi R., Palmeri R. (2002) Orogen-parallel tectonic transport in the Variscan belt of northeastern Sardinia (Italy): implications for the exhumation of medium-pressure metamorphic rocks. Geological Magazine, 139, 497-511.

Connolly J.A.D. (1990) Multivariable phase diagrams: an algorithm based on generalized thermodynamics. American Journal of Science, 290, 666-718.

Elter F.M., Franceschelli M., Ghezzo C., Memmi I., Ricci C.A. (1986) The geology of northern Sardinia. In: Carmignani, L., Cocozza, T., Ghezzo, C., Pertusati, P.C., Ricci, C.A. (Eds.), Guide-Book to the Excursion on the Paleozoic Basement of Sardinia. IGCP Project. Newsletter, 5, 87-102.

Elter FM.,Padovano M.,Kraus R.K. (2010) The emplacement of Variscan HT metamorphic rocks linked to the interaction between Gondwana and Laurussia: structural contraints in NE Sardinia (Italy). Terra Nova, 22, 369-377.

Franceschelli M., Memmi I., Pannuti F., Ricci C.A. (1989) Diachronous metamorphic equilibria in the Hercynian basement of northern Sardinia, Italy. In: Daly J.S., Cliff R.A., Yardley B.W.D. (Eds.) Evolution of metamorphic belts. Geological Society Special Publications, 43, 371-375.

Helbing H., Frisch W., Bons P.D. (2006) South Variscan terrane accretion: Sardinian constraints on the intra-Alpine Variscides. Journal of Structural Geology, 28, 1277-1291.

Holland T.J.B., Powell R. (1998) An internally consistent thermodynamic data set for phases of petrologic interest. Journal of Metamorphic Geology, 16, 309–343.

The Effects of Deformation Partitioning on Metamorphic Re-equilibrations in the Subducted Continental Crust of Western Alps: the Structural map of Monte Mucrone Metagranitoid

Francesco Delleani[1], M. Iole Spalla[1,2], Daniele Castelli[3], Guido Gosso[1,2]

[1.]Dipartimento di Scienza della Terra "A. Desio", Università di Milano, Via Mangiagalli 34, 20133, Milano, Italy
[2.]C.N.R.-I.D.P.A., Sezione di Milano, Via Mangiagalli 34, 20133, Milano, Italy
[3.]Dipartimento di Scienze Mineralogiche e Petrologiche, Università di Torino, Via Valperga Caluso 35, 10125, Torino, Italy
*francesco.delleani@unimi.it

The Mt. Mucrone metagranitoid is one of the most-studied Permian intrusives belonging to the Eclogitic Micaschists Complex (EMC) of Sesia-Lanzo Zone (SLZ) within the HP metamorphic belt of Western Alps (e.g. Compagnoni et al. 1977). An integrated structural and petrological study has been focused on the still poorly-known southern slope of Mt. Mucrone, in order to complete the available data and to correlate with the structural and metamorphic history inferred in the Mombarone-Mt. Mars-Mt. Mucrone area to NW (Zucali et al., 2002). The result is a 1:5,000 interpretative structural map integrated with new chemical data on mineral assemblages supporting successive fabrics.

Rocks constituting EMC are: micaschists, paragneisses, metagranitoids, eclogites and impure marbles (Compagnoni et al., 1977). Protolites of metagranitoids are Permian in age, whereas the early Alpine metamorphism has been dated at 60-70 Ma (e.g. Rubatto et al., 1999).

Six phases of deformations (D1 to D6) generating superposed folds, foliations and shear zones, have been recognized.

All lithologies are eclogitized and typically show a foliated fabric marked by Qtz, Pg, Phe, Grt, Gln, Jd (or Omp), Rt and Zo. This fabric is the axial plane foliation (S1) of the oldest recognized fold (D1). Minor volumes of eclogites, metagranitoids and paragneisses escaped deformation during the growth of the eclogite-facies minerals, and only display coronitic reaction textures. The D1 deformation is highly heterogeneous in metagranitoids where domains fully preserving the igneous texture (the so-called grey-type metagranite) are juxtaposed to foliated domains (green-type metagranite).

During D2, isoclinal folds occur that are associated with coronitic reactions producing Qtz, Phe, Pg, Omp, Aeg, Gln, Grt, Czo and Rt; a foliated S2 fabric locally develops in some metapelites.

D3 is responsible for the development of meter-thick mylonitic shear bands in which the S3 foliation is marked by Qtz, Phe, Pg, Rit, Brs, Win, Grt, Na-Agt, Mg-Chl, Czo and Ttn.

The last three phases develop either open to gentle folds (D4 and D6) or centimeter-thick shear zones (D5), with partial replacement of the preexisting minerals by Ab, Qtz, Phe, Pg, Act, Ep, Chl and Bt.

The main differences in the microfabrics developed under eclogite-facies conditions (D1 and D2 deformation stages) are between the two types of metagranite. The grey-type metagranite occurs as rock volumes that largely escaped the D1 stage and were deformed only during D2-D6. During D1 only coronitic and/or pseudomorphic reactions occurred, including: replacement of the igneous Pl by fine-grained aggregates of whitish Jd, Zo and Qtz; partial replacement of Bt by fine-grained Phe with the formation of Grt rims; development of fine-grained Phe after magmatic Kfs. During D2, the grey-type metagranite still preserved the widespread relics of primary Bt, and also the fine-grained, pseudomorphic aggregates of whitish Jd+Zo+Qtz that were only partially replaced by Aeg and/or Omp. In the green-type metagranite, the combined effect of deformation/recrystallization and fluid migration during D1 allowed the complete substitution of the igneous Bt by coarse-grained Phe, and the formation of euhedral, coarse grained, greenish Jd.

Folding and metamorphic evolution point to the development of D1 and D2 deformations under Qtz-eclogite facies conditions, of D3 deformation under blueschist-facies conditions, and of D4 to D6 deformations under greenschist-facies conditions.

Compositional variations of minerals at different microstructural sites support quantitative PT estimates during successive deformation stages suggesting T = 580° ± 65° C for the D1 stage and T = 500° ± 65° C for the D2 stage, for a P interval between 2.0 and 1.5 GPa (Zucali et al. 2002), respectively. During D1, the effects of strain gradients on re-equilibration progress drive the compositional variations of Grt in the mylonitic (green-type) metagranitoids with respect to those observed in Grt from the poorly deformed (grey-type) ones.

As proposed for the metagranitoids of the eastern face of Mt. Mucrone (Castelli et al., 1994), the distinction between the two types of metagranitoids, the green- and grey-type metagranite, respectively, is mainly due to the different degree of deformation recorded during the eclogite-facies re-equilibration. Contrary to the grey-type, the occurrence of the green-type metagranite is related to pervasive deformation/recrystallization and fluid migration during D1 that favoured the almost complete replacement of igneous Bt by large Phe and the formation of euhedral, coarse-grained crystals of greenish, Jd-rich Cpx.

CASTELLI D., COMPAGNONI R. & NIETO J.M., 1994. High pressure metamorphism in the continental crust: eclogites and eclogitized metagranitoids and paraschists of the Monte Mucroen area, Sesia Zone. In: Compagnoni R., Messiga B. & Castelli D. (Eds.): High pressure metamorphism in the Western Alps. Guide-book to the B1 field excursion of the 16th Gen. IMA Meeting, Pisa, 4-9 settembre 1994, 107-116.

COMPAGNONI R., DAL PIAZ G.V., HUNZIKER J.C., GOSSO G., LOMBARDO B. & WILLIAMS P.F. 1977. The Sesia-Lanzo Zone, a slice of continental crust with Alpine HP-LT assemblages in the Western Alps. Rend. Soc. It. Mineral. Petrol., 33, 281-334.

RUBATTO D., GEBAUER D. & COMPAGNONI R., 1999. Dating of eclogite-facies zircons: the age of Alpine metamorphism in the Sesia-Lanzo Zone (Western Alps). Earth Planet. Sci. Lett., 167, 141-158.

ZUCALI M., SPALLA M.I. & GOSSO G., 2002. Strain partitioning and fabric evolution as a correlation tool: the example of the eclogitic micaschists complex in the Sesia-Lanzo Zone (Monte Mucrone – Monte Mars, Western Alps Italy). Schweiz. Mineral. Petrogr. Mitt., 82, 429-454.

Deformation of Mantle Pyroxenites From the Beni Bousera Peridotite Massif (Northern Morocco)

Erwin Frets*[1,2], Carlos J. Garrido[1], Andrea Tommasi[2], José Alberto Padrón-Navarta[3]

[1]Instituto Andaluz de Ciencias de la Tierra, CSIC-UGR, Granada, Spain
[2]Géosciences Montpellier, Université de Montpellier 2 & CNRS, Montpellier, France
[3]Dep. Mineralogía y Petrología, Univ. Granada, Granada, Spain
*erwin.frets@iact.ugr-csic.es

Mantle pyroxenites are an important constituent of the upper mantle, corresponding to recycled oceanic material incorporated in the lithosphere, either directly as eclogites derived from subducted oceanic crust or as recycled materials in mantle plumes (Sobolev et al., 2005; Sobolev et al., 1997) and, in a lesser extent, mid-ocean ridges (Hirschmann and Stolper, 1996).

The abundance of garnet pyroxenites, some of which contain pseudomorphs after diamond, has been responsible for the large interest given to the Beni Bousera peridotite massif, which is exposed in the Rifean belt, northern Morocco (Pearson et al., 1992; Pearson et al., 1991; Pearson et al., 1989; Kornprobst, 1969; El Atrassi et al., 2011). A large variety of pyroxenites may nevertheless be observed in Beni Bousera; garnet clinopyroxenites, garnet websterites, garnet-spinel websterites and (olivine-) spinel websterites are among the most common. This massif constitutes therefore a unique opportunity to investigate the rheology of pyroxenites equilibrated at variable p-T conditions during the polyphase exhumation of the subcontinentental lithospheric mantle.

Microstructural observations show that pyroxenite textures are mainly porphyroclastic in garnet clinopyroxenites, garnet websterites and garnet-spinel webstrerites, but tend to be intermediate to granoblastic for spinel websterites.

In the porphyroclastic pyroxenites, the average recrystallized grain size shows a wide range of variation that is correlated with mineralogy. Much smaller recrystallized grain sizes are observed in garnet clinopyroxenites, which contain a matrix of very fine grained neoblasts (50-250 microns). In these rocks, garnet porphyroclasts show a strong shape preferred orientation, which indicates that garnet deformed plastically under high deviatoric stresses.

Recrystallised grain sizes in the spinel websterites are much coarser, around 1-5 mm. Triple junctions at grain boundaries between diopside and enstatite are often observed, and spinel, although aligned in the foliation, is undeformed, displaying interstitial shapes. Undeformed cpx-opx-spl symplectites are interpreted as product reactions of the breakdown of former garnets (Garrido & Bodinier, 1999). Pyroxene porphyroclasts, nevertheless, still show evidence for plastic deformation such as undulose extinction, suggesting that static recrystallisation affected only the smaller matrix grains.

CPO of diopside is characterized by concentration of [001] axes parallel or slightly oblique to the lineation and of [010] normal to the foliation, suggesting dominant activation of {110} [001] glide. Enstatite shows always [001] parallel to the lineation, but when enstatite is a major component [100] tends to align normal to the foliation, while when it is a minor phase [010] aligns preferentially normal to the foliation. In pyroxenites with a garnet SPO, a weak CPO is also present, suggesting deformation by ½ {111} {110} glide. Misorientations within porphyroclasts also indicate that dislocation creep was the dominant deformation mechanism for garnet in these samples.

Preliminary pressure-temperature calculations were performed to determine primary deformation conditions using PerpleX. Garnet clinopyroxenites equilibrium conditions yield minimum pressures above 2.2 GPa and temperatures of at least 1100 ºC. For spinel websterites, considering higher equilibrium temperatures of 1200 – 1300 ºC, similar to those evidenced in peridotites from Ronda (Soustelle, 2009), maximum equilibrium pressures must not have exceeded 1.5 -1.6 GPa. Intermediate pressure of about 1.9 – 2.0 GPa and temperatures of 1200 ºC were determined for garnet – spinel websterites, as these rocks lie per definition on the Seiland – Ariegite transition curve of the p – T diagram.

Considering microstructures, CPOs and preliminary thermobarometrical data we conclude that the decrease in the synkinematic stress conditions recorded from the garnet pyroxenites to the

spinel websterites is probably due to a transient temperature increase at the base of the lithosphere (asthenospheric upwelling?) that occurred before final emplacement of the peridotite massif into the crust.

El Atrassi F., Brunet F., Bouybaouene M., Chopin C., Chazot G. (2011) : Melting textures and microdiamonds preserved in graphite pseudomorphs from the Beni Bousera peridotite massif, Morocco. European Journal of Mineralogy, 23, in press.

Garrido C.J. and Bodinier J.-L. 1999. Diversity of mafic rocks in the Ronda peridotite. Evidence of Pervasive melt-rock reaction during heating of subcontinental lithosphere by upwelling astenosphere. Journal of Petrology 40, 729-754.

Hirschmann, M.M., Stolper, E.M., 1996. A possible role for garnet pyroxenite in the origin of the "garnet signature" in MORB. Contributions to Mineralogy and Petrology 124, 185-208.

Kornprobst, J., 1969. Le massif ultrabasique des Beni Bouchera (Rif Interne, Maroc): Etude des péridotites de haute température et de haute pression, et des pyroxénolites, à grenat ou sans grenat, qui leur sont associées. Contributions to Mineralogy and Petrology 23, 283-322.

Pearson, D.G., Davies, G.R., Nixon, P.H., 1992. Geochemical Constraints on the Petrogenesis of Diamond Facies Pyroxenites from the Beni Bousera Peridotite Massif, North Morocco. Journal of Petrology 34, 48.

Pearson, D.G., Davies, G.R., Nixon, P.H., Greenwood, P.B., Mattey, D.P., 1991. Oxygen isotope evidence for the origin of pyroxenites in the Beni Bousera peridotite massif, North Morocco: derivation from subducted oceanic lithosphere. Earth and Planetary Science Letters 102, 289-301.

Pearson, D.G., Davies, G.R., Nixon, P.H., Milledge, H.J., 1989. Graphitized diamonds from a peridotite massif in Morocco and implications for anomalous diamond occurrences. Nature 338, 60-62.

PEARSON, D.G., NOWELL, G.M., 2004. Re–Os and Lu–Hf Isotope Constraints on the Origin and Age of Pyroxenites from the Beni Bousera Peridotite Massif: Implications for Mixed Peridotite–Pyroxenite Mantle Sources. Journal of Petrology 45, 439-455.

Sobolev, A.V., Hofmann, A.W., Sobolev, S.V., Nikogosian, I.K., 2005. An olivine-free mantle source of Hawaiian shield basalts. Nature 434, 590-597.

Sobolev, S.V., Zeyen, H., Granet, M., Achauer, U., Bauer, C., Werling, F., Altherr, R., Fuchs, K., 1997. Upper mantle temperatures and lithosphere-asthenosphere system beneath the French Massif Central constrained by seismic, gravity, petrologic and thermal observations. Tectonophysics 275, 143-164.

Soustelle, V., Tommasi A., Bodinier, J. L., Garrido, C.J., Vauchez, A. (2009). Deformation and reactive melt transport in the mantle lithosphere above a large scale partial melting domain: the Ronda peridotite massif, southern Spain. Journal of Petrology 50, 1235-1266.

Reaction-Enhanced Strain Localization in Mantle Pyroxenite During Thinning of the Subcontinental Lithospheric Mantle

Hidas, Károly*[1], Garrido, C.J.[1], Tommasi, A.[2], Konc, Z.[1], Padrón-Navarta, J.A.[1], Booth-Rea, G.[1]

[1] Instituto Andaluz de Ciencias de la Tierra (IACT), CSIC-UGR, Granada, Spain /*karolyhidas@iact.ugr-csic.es
[2] Géosciences Montpellier, UM-2-CNRS, Montpellier, France
*karolyhidas@iact.ugr-csic.es

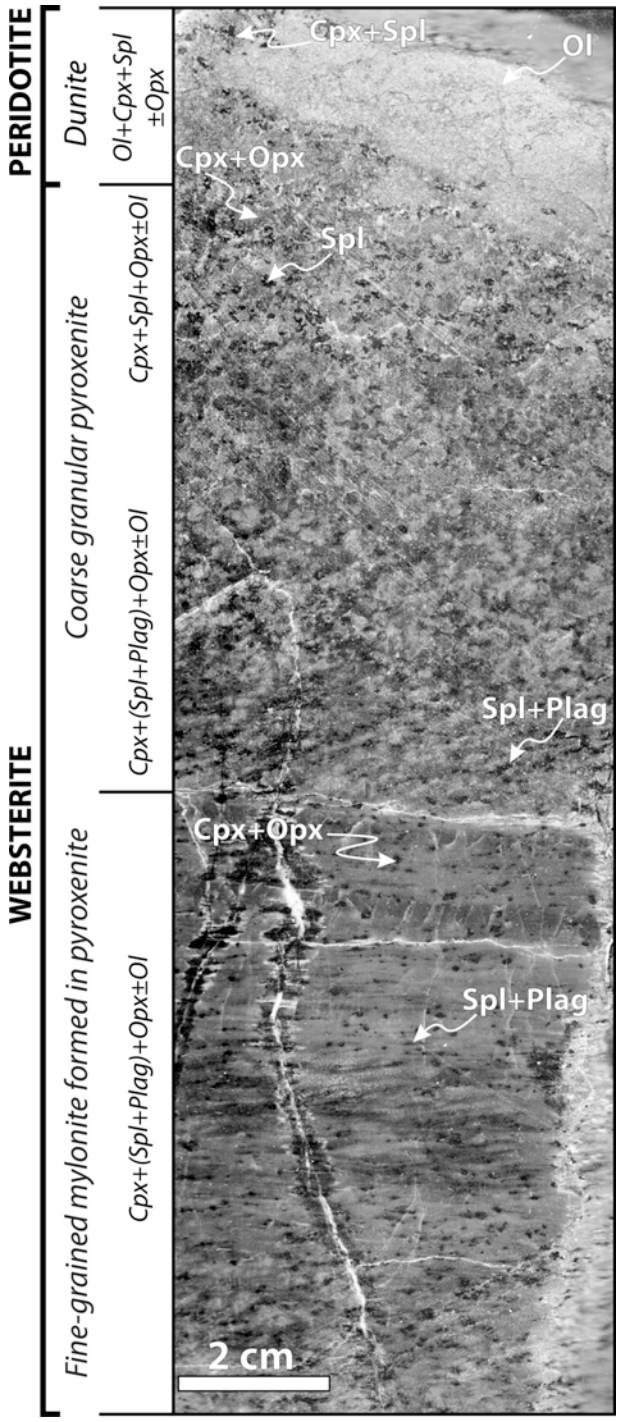

The deformation of rocks in response to forces in Earth's interior is governed by rock rheology, which varies as a function of a number of constitutive and environmental aspects including mineralogy, fluid content and chemistry, melt fraction, temperature, pressure, differential stress conditions and mineral grain size. The upper mantle consists predominantly of olivine (~55-60%) and pyroxenes (+aluminous minerals: garnet, spinel or plagioclase depending on the P-T conditions). In most of the cases, olivine is weaker than any other phases and, as a volumetrically dominant mineral, it is usually assumed to determine the rheological properties of the upper mantle. Therefore, it has been suggested that strain localization in the mantle occurs due to grain-size-sensitive creep of dynamically recrystallized fine-grained olivine, and pyroxenes in the upper mantle rocks are usually stronger than olivine, at least in the dislocation creep regime (Karato, 2008). However, if in an upper mantle rock the grain size of a stronger mineral becomes significantly smaller than that of olivine, it can control strain localization (Karato, 2008). Synkinematic net-transfer metamorphic reactions can result in fine-grained reaction products promoting positive feed-back between deformation and reaction, thus reaction-enhanced softening is a well recognized mechanism fostering strain localization.

Fig. 1 – Close-up view of the studied composite sample in which strain localization occurs in pyroxenite. Rock surface is perpendicular to the foliation and is parallel to the lineation. Cpx: clinopyroxene; Ol: olivine; Opx: orthopyroxene; Plag: plagioclase.

Here we report the study of strain localization in mantle pyroxenite from the spinel to plagioclase (sp-pl) websterite transition in the Ronda peridotite (southern Spain). Incipient strain localization in sp-pl pyroxenite occurs in the transition between coarse-grained peridotite to plagioclase-lherzolite tectonic domains of this

massif. Mapping shows that in this transition shear zones systematically occurred in thinned pyroxenites located at the tip of major shear zones extending towards the plagioclase tectonite. These observations indicate that pyroxenite was weaker than host peridotite and that strain localization in pyroxenite lithologies played a major role in nucleating intra-lithospheric shear zones in the shallow lithospheric mantle.

We have investigated strain localization in pyroxenite in a unique outcrop of dunite and sp-pl websterite from the Ronda Peridotite Massif, where a centimeter-sized fine-grained mylonitic shear zone occurs within coarse-granular, sp-pl websterite (Fig. 1). The host peridotite consists of virtually undeformed coarse granular (0.5-0.8 centimeter sized) olivine with minor clinopyroxene + spinel ± orthopyroxene and has a sharp yet transitional contact with the pyroxenite layer. The pyroxenite is composed of coarse granular (0.2-0.5 centimeter sized) clinopyroxene + spinel + orthopyroxene ± olivine (Fig. 1). Strain localization is defined by the abrupt decrease of grain size (down to 10-50 μm) in the pyroxenite layer (Fig. 1). Grain size reduction is correlated with the increase of metamorphic plagioclase around spinel in the coarse granular pyroxenite with decreasing distance to the shear zone, as well as in the fine-grained mylonitic shear zone itself (Fig. 1). The transformation of aluminous phases in the mantle is controlled by the P-T conditions and the bulk chemistry. Plagioclase is stable at higher pressure in a fertile, than in a depleted peridotite (e.g. Borghini et al., 2010). Similarly, during thinning of the lithospheric mantle spinel in a more fertile clinopyroxene-rich pyroxenite can disaggregate into plagioclase at higher pressures than in a relatively depleted olivine-rich peridotite. In this case, the spinel-plagioclase transition in pyroxenites can be a cause of nucleation of shear zones and these observations indicate that strain localization in larger lithospheric shear zones might initiate in pyroxenites during thinning of the subcontinental mantle. Further thinning and decompression can propagate these weak zones into larger shear zones that affect also mantle peridotites.

Borghini, G., Fumagalli, P., Rampone, E. (2010) The stability of plagioclase in the upper mantle: Subsolidus experiments on fertile and depleted lherzolite. Journal of Petrology 51, 229-254

Karato, S.-I. (2008) Deformation of Earth materials – An introduction to the rheology of solid Earth. Cambridge University Press, Cambridge, UK, pp. 474.

FIA trends along the PreCambrian Rocky Mountains: a new approach to timing continental docking

Hui Cao*[1,2], Chris Fletcher[1]

[1]School of Earth and Environmental Sciences, James Cook University, Townsville, Qld 4811, Australia
[2]Institute of Geology, Chinese Academy of Geological Sciences, Beijing 100037, China
*caohuicugb@gmail.com

A similar succession of Foliation Inflection/Intersection Axis trends preserved within porphyroblasts (FIAs) is present in two areas separated by 200 km along the Rocky Mountains. PreCambrian rocks in Central Colorado and Northern New Mexico were affected by deformation and metamorphism from approximately 1506 to 1370 Ma. A succession of five FIAs trending W-E, SSW-NNE, NNW-SSE, NW-SE and WSW-ENE has been distinguished in Central Colorado that have been dated at 1506±15Ma, 1467±23Ma, 1425±18 Ma, not dated and 1366±20 Ma, respectively. To the south in Northern New Mexico, a succession of five FIAs trending SSW-NNE, WNW-ESE, NNW-SSE, NW-SE and WSW-ENE have been distinguished dated at 1482±48Ma, 1448±12Ma, 1422±35Ma, not dated and 1394±22Ma. The excellent correlation of the sequence of FIA trends and their ages between regions reveals a six fold FIA succession across the region with the first developed FIA not being present in Northern New Mexico and the third not being present in Central Colorado. Preferential partitioning of W-E trending deformation into the Central Colorado region around 1506±15Ma was followed by SSW-NNE trending deformation that affected both regions at 1470±20 Ma. However, preferential partitioning of WNW-ESE trending deformation into Northern New Mexico at 1448±12 Ma left Central Colorado unaffected. Both regions were then affected by the three remaining periods of orogenesis, the first trending NNW-SSE at 1424±15 Ma followed by one trending NW-SE that has not yet been dated, and then one trending WSW-ENE at 1390±19 Ma. This suggests that the Yavapai terrain was tectonized at approximately 1506 Ma, prior to amalgamation with the Mazatzal terrain around 1470 Ma. Subsequent orogenesis was initially partitioned preferentially into the Mazatzal terrain, but the following three periods of tectonism affected both terrains in a similar manner.

Anomalous Structures Preserved Within Low-strain Zones Adjacent to Basement Highs and Their Significance for Orogenesis

Hyunwoo Lee*

Structural Systems and Site Evaluation Department, Korea Institute of Nuclear Safety
*heanu@kins.re.kr

The Chungju region, situated at the northeastern end of the Ogcheon Orogenic Belt, South Korea, preserves anomalous NW–SE-striking bedding and foliation. This region was only weakly affected by the deformation that produced the dominant NE–SW trend of the orogen. The anomalous NW–SE trends, which curve into the regional NE–SW trend to the south, were previously interpreted to have been formed by (1) overprinting by a much younger fold, (2) passive rotation of the pre-existing NE–SW trends by a sheath-like upheaval of basement gneiss, or (3) NE-directed extrusion of sediments at the belt margin during NW–SE shortening.

The NW–SE-trending structures and several sets of crenulations in the Chungju area formed prior to a major change in the direction of orogenic bulk shortening. NE–SW shortening during D_2 produced the NW–SE trend observed in the Chungju region. This was followed by gravitational collapse and NE–SW extension during D_3. These early foliations, which generally appear as a composite foliation, $S_{1,2,3}$, were folded around NE-trending D_4 and D_5 structures, and are locally folded around N–S-trending D_6 folds. Precambrian gneiss bodies in the northeastern Chungju region created a strain-shadow region that was protected from the effects of D_4/D_5, preserving the NW–SE strike of bedding and early foliations. However, in the rest of the Ogcheon Orogenic Belt the overall strike of bedding and foliations was rotated to NE–SW during D_4, with relic NW trends only preserved within porphyroblasts and quartzose strain shadows. The orientations of foliation inflexion/intersection axes (FIAs) resulting from this succession of foliations are consistent throughout the orogen.

Record of Tension and Shear Deformation of Andalusite Porphyroblasts within a Normal-Sense Shear Zone in the Sanandaj Sirjan area, Iran

Leili Izadikian*[1]

[1]Buali Sina University of IRAN
*l.izadi@basu.ac.ir

The Sanandaj-Sirjan zone is the metamorphic belt(figure1) of the Zagros Orogen in western Iran that uplifted during continental collision between the Afro-Arabian continent and the Iranian microcontinent. Five episodes of deformation were recognized in the ALS-bearing schists. The Simin- Darehmoradbeig (SD) shear zone is located in the Complexly-deformed sub-zone of Sanndaj sirjan zone in the south of Hamadan city. Field evidence shows tension, compression and shear stress in this area. The SD shear zone dips to northeast with normal sence of shear movement with dimension 2.5-3 width and at least 10 Km length. This shear zone developed in migmatites, granite and andalusite hornfels. Andalusite porphyroblasts in regional and contact metamorphic rocks in the studied area demonstrate tensional and shear deformations. Andalusites are broken or deformed and display deformation stages as kinematic indicators (Figure 2). Andalusite boudins have variable plunges with maximum extension to the northeast. Kinematics of the SD shear zones defined by deformed andalusite porhpyroblasts is concordant with other kinematic indicator such as mantled porphyroclasts (complex, σ, δ), oblique and sheath fold, S-C fabrics (Figure 3), stretching lineations, LPO of quartz and mylonitic foliation. According to deformation stages recorded in the Hamadan tectonites, this shear zone formed syn to post second deformation (D2) and mylonitic foliations are folded by the next deformation.

Fig.2: Evidence of tension and rotation of Andalusite porphyroblasts.

Fig3: S-C fabric by Andalusite boudin. Andalusite is extended in S direction.

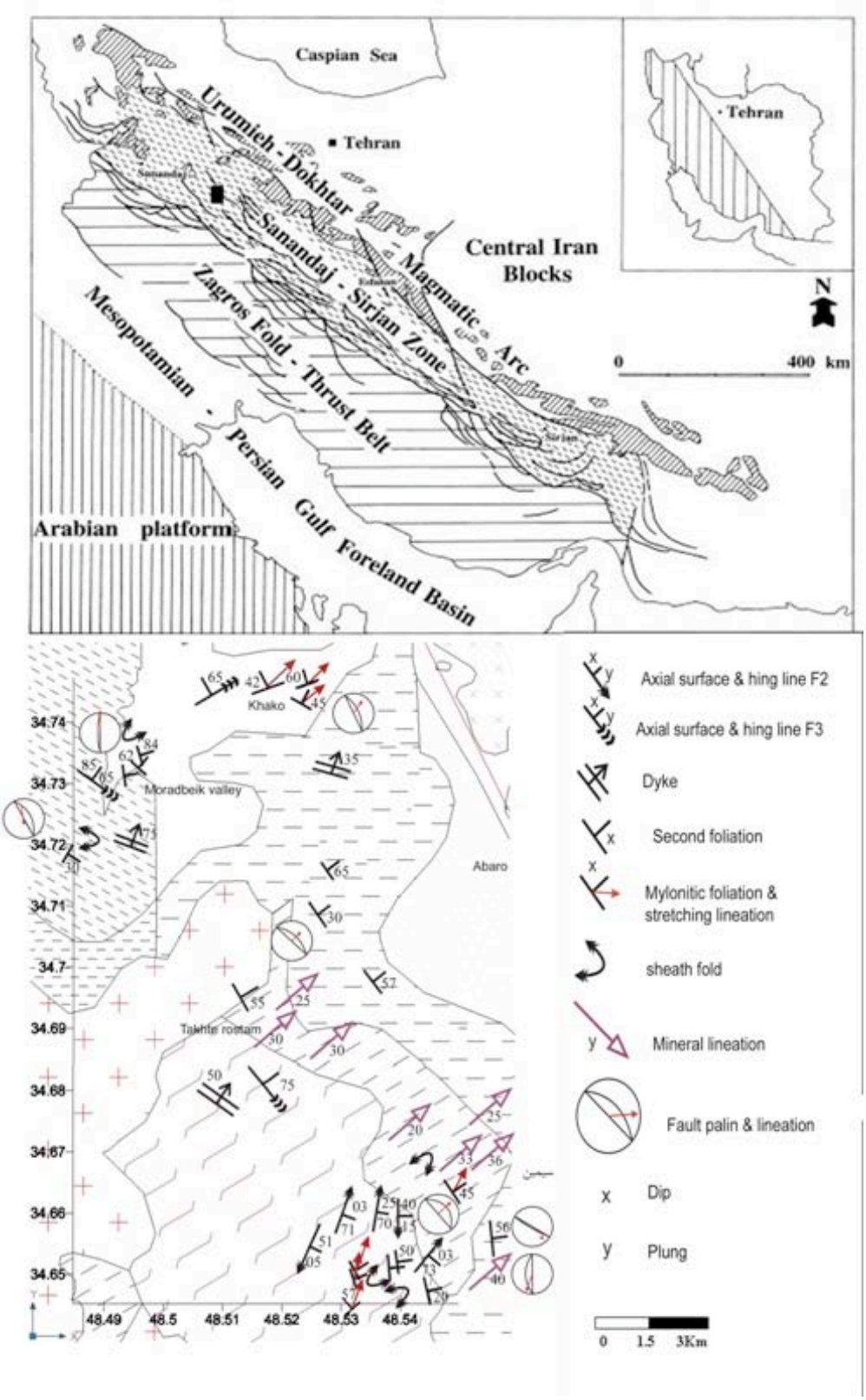

Fig.1: the regional and structural map of studied area.

Geochemistry, and P-T-t Evolution of the Abu-Barqa Metamorphic Suite, Northernmost Extremity of the Arabian-Nubian Shield in Central Wadi Araba, Jordan

Ghaleb H. Jarrar*[1], Thomas Theye[2], Najel Yaseen[1], Martin Whitehouse[3]

[1]Geology Department, University of Jordan, 11942 Amman, Jordan, P.O.Box 13633
[2]Institut für Mineralogie und Kristallchemie, Universität Stuttgart, Azenbergstr. 18, D-70174 Stuttgart, Germany
[3]Swedish Museum of Natural History, Box 50007SE-104 05 Stockholm, Sweden
*jarrargh@ju.edu.jo

The evolution of the Arabian-Nubian Shield evolution in south Jordan took place between ~ 800 and 542 Ma during the East African Orogen as revealed from age determinations on metamorphic and igneous rocks.

The investigated Abu Barqa Metamorphic Suite (ABMS) is sporadically exposed over an area that extends along the easter shoulder of Wadi Araba for a distance of about 40km. The major exposures are present in the form of EW trending belts in Wadi Huwar, Wadi um Saiyala, Wadi Abu-Barqa, and Wadi Rahma. The ABMS comprises, paragneisses, tonalitic gneisses, metasediments, and granitic gneisses.

Geochemically the great majority of the investigated metapelites plot in the shales field and the gneisses plot in the fields of greywackes. Thus the protolith of the ABMS rocks is of pelitic and psammitic character. Furthermore, the K_2O/ Na_2O vs. SiO_2 tectonic diagram of Roser and Korsch (1986) suggests that the precursor of the ABMS rocks was deposited at an active continental margin and island arc setting.

Single zircon dating of the tonalitic gneiss constrain its age at about 800 Ma; while the metasediments zircons show a wide age span from 1030 to about 700 Ma. A four points Rb/Sr isochron of the metasediments from the sillimanite zone yielded an age of about 693 with an initial ratio of 0.7044. The whole metamorphic complex has been intruded by calc-alkaline granitoids dated (625-608 Ma),

Petrographic and field investigation and microtextural analyses of the metasediments helped in differentiation of three metamorphic zones: I. andalusite-staurolite, II. sillimanite-garnet, and III. sillimanite-cordierite zones. The respective mineral parageneses are: I. andalusite + staurolite + biotite + muscovite + plagioclase ± garnet + quartz ± chlorite + fibrolitic sillimanite + accessories; II. sillimanite + garnet + biotite + plagioclase + quartz + K-feldspar + hercynite + cordierite (penitized); III. Sillimanite + biotite + plagioclase + cordierite + hercynite + quartz + accessories. Three deformational phases (M1, M2, and M3) have been identified.

Sillimanite occurs in prismatic and fibrolitic forms. The former is well developed as bundles of oriented prisms that are aligned and or inclined at up to 60° to the main regional penetration schistosity (S1).

Garnets are common as euhedral porphyroblasts ranging in size from 0.1 to 10 mm and are distributed in the three zones. They are, however, more common and larger in size in metapelitic lithologies poor in silica and rich in iron and aluminium i.e true shales. They occur as large idiomorphic crystals, almost free of inclusions; large sub- to euhedral snowball porphyroblasts with spiral, circular, or arch shaped quartz and opaques inclusions, small idiomorphic inclusion-free crystal aggregates, as well as relics within cordierites in the cordierite-sillimanite gneisses.In the staurolite andalusite zone postkinematic garnets have been observed. Rotation of the synkinematic snowball garnets as revealed from microtextural analyses reaches up to 270 °.

Frequently the garnets have inclusion rich cores and inclusion free outer rims and the size of the inclusions increases outwards, which implies garnet growth during matrix coarsening.

Staurolite occurs as typically highly pleochroic, colorless to pale golden yellow, sub- to anhedral poikiloblasts, several millimeters in diameter. Cruciform twins in particular in euhedral staurolite are common. Frequently staurolite porphyroblasts are built up from inclusions-poor and inclusions-rich bands. These bands reflect the original schistosity of the matrix, from which the

staurolite has developed. The internal schistosity (Si) is continuous with the external Se, and the staurolite poikiloblast were rotated during growth, though this rotation rarely exceed 90 ° .

Andalusite occurs as strongly poikiloblastic, almost colorless and up to 2 cm long lenticular porphyroblasts. Inclusions reach up to 40% by volume of resorbed quartz, biotite, muscovite, opaques, staurolite and rarely unresorbed garnet. These textural features indicate that andalusite has at least partially grown at the expense of staurolite.

The continuity of S_i and S_e , the retrograde growth of muscovite on andalusite, the deflection of biotite flakes around andalusite, and the alignment of andalusite parallel to the main regional schistosity (S_1) in addition to the staurolite relics are indication in favor of andalusite growth during the last stages of regional metamorphism.

Cordierite occurrence is restricted to the sillimanite zone in Wadi Abu Barqa and in the gneiss of Wadi Rahma. It occurs in ovoidal grains, which are up to 1 mm in size and dissected by curvilinear pinitized fractures. It is particular fresh and well developed in the cordierite gneisses in Wadi Rahma and highly pinitized in Wadi Abu Barqa. Cordierite growth as microtextural evidence suggest was postkinematic and associated with the granitoids intrusion.

P-T pseudosection calculations have been performed with the **Perplex** software package on selected samples from the three zones.

Accordingly, P-T conditions of the garnet and staurolite producing M1 a event are estimated to 550°C, 3.5 kbar. The andalusite growth took place at lower 2.5 kbar.

On the other hand, high Mg and low Ca content of garnet in the sillimanite zone indicate T in the range of 700°C at relatively low P of 5 to 6 kbar (M1). At such conditions, the rock was molten to c. 20%. This is supported by the abundant migmatization in this zone. Uplift and cooling led to the formation of cordierite and occasionally to complete disappearance of sillimanite. In the cordierite gneiss, likewise the garnet was resorbed during uplift from M1 to M2. The garnet relics are homogenous and relatively rich in Mn. From compositional garnet isopleths, P-T conditions of 3.5 kbar, 600°C results.

The widespread granitoid intrusions most probably were responsible for the retrograde growth of fibrolite and randomly oriented muscovite in the Staurolite zone and the extensive growth of cordierite and consumption of garnet in the sillimanite zone.

SHRIMP U-Pb zircon dating on garnet bearing gneiss from Banefo-Mvoutsaha area (NE Bafoussam). New evidence for 2.15 Ga magmatism within the Pan-African North-Equatorial Fold Belt of Cameroon

Gus Djibril Kouankap Nono*[1], Sylvestre Ganno[1], Jean Paul Nzenti[1], Emmanuel Suh Cheo[2], Richard Armstrong [3]

[1]Laboratory of Petrology and Structural Geology, Faculty of Science, University of Yaoundé I, PO Box 3412 MESSA-Yaoundé, Cameroon.
[2]Economic Geology Unit, Dept. of Geology and Environmental Science, University of Buea, P.O. Box 63 Buea, SW Province, Cameroon.
[3]Reseach School of Earth Sciences, The Australian National University, Mills Road, Canberra 0200, A.C.T. Australia
*kouankap@yahoo.fr

The Pan-African North-Equatorial Fold Belt which is linked to the Trans-Saharan Belt of western Africa and to the Brasiliano Orogen of NE Brazil affects the whole of the central Africa continent. In Cameroon many authors have subdivided it in into three geodynamic domains, the South, the Central and the North domains.

The Banefo-Mvoutsaha area belongs to the western central part of the central domain. The area comprises Neoproterozoic granitoid rocks which are intrusive as a series of sheets into the metamorphic basement. Granioids are made up of orthogneissified granite, quartz monzonite and granodiorite. The metamorphic basement, poorly surveyed, is made up of Amphibolites, Garnet bearing gneiss and migmatitic gneiss.

The microtexture of the garnet bearing gneiss is heterogranular and poeciloblastic with phenoblast of garnet showing quartz inclusions. The garnet bearing gneiss are relatively silica-rich and have granodioritic-dioritic protoliths. Negative Eu*anomalies are pronounced in all the rocks (Eu/Eu*= 0.29-0.85).

The SHRIMP U-Pb zircon dating reveals a magmatic event marked by plutonism occurred in the Paleoproterozoic (2161 ± 11 Ma). These protoliths were then affected by granulite metamorphism associated with migmatization at 599 ± 17 Ma.

This data in the western part of the central domain of Pan-African North-Equatorial Fold Belt are the first SHRIMP U-Pb zircon dating on panafrican rocks in Cameroon and they are new evidences for paleoproteroizoic magmatism residues within the central domain of neoproterozoic belt of Cameroon.

Local Equilibrium and P-T-Deformation-t(relative age)-Redox Mapping at the Thin Section Scale

Pierre Lanari*[1], Olivier Vidal [2], Benoit Dubac, Manuel Munoz, Eric Lewin

[1]ISTerre, Univ. of Grenoble, France
[2]Univ. Cambridge, UK
*pierre.lanari@ujf-grenoble.fr

Linking deformation with metamorphic conditions requires spatially continuous estimates of pressure (P) and temperature (T) conditions at least in two dimensions (P–T maps) that can be superposed to the observed structures of deformation.
We have developed an approach and a package of matlab scripts that can be used to quantify semi-quantitative EMP maps of composition acquired at 100 nA for counting times as low as 100 ms. The software is used to recognize automatically the nature of the analyzed phase on each pixel of the measured map of composition. The output results are maps of quantitative analyses or structural formula (one structural formula per pixel) for all phases occurring in the thin section.

These maps of composition can be used for thermodynamic modeling. In particular, the thermodynamic models of Vidal et al. (2006) and Dubacq et al. (2010) can be used to calculate equilibrium P–T conditions for each pixel of chlorite and mica occurring in metapelitic samples. The combination of quantitative X-ray maps of mineral composition with these models makes it possible to calculate P–T-deformation-t(relative age)-Fe^{2+}/Fe^{3+} maps at the thin section scale even for samples free of low variance parageneses. Various examples show that in rocks metamorphosed at < 550 °C, the composition of phyllosilicates does not change significantly by lattice diffusion with varying P and T. Different compositions of phyllosilicate grains coexisting metastably in the same thin section are therefore indicative of different P-T conditions of crystallization that were achieved at different times. The nucleation of new phyllosilicate grains with different compositions during P–T variation is activated by deformation, so that the location of the different phyllosilicate generations characteristic of different P–T conditions is correlated to the microstructures.

The P–T-deformation-t(relative age)-Fe^{2+}/Fe^{3+} maps (i) highlight historical information about the P–T and deformation history, (ii) they offer information about the evolution of redox condition and possibly the depth at which oxidation from externally derived fluid occurred during the sample history, and (iii) they provide information about the heterogeneity of rheology at the thin section scale.

Structural zonation at the core of a major crustal-scale shear zone (Malpica-Lamego Line, NW Iberia)

Sergio Llana-Fúnez*[1]

[1]Departamento de Geología, Universidad de Oviedo, Spain
*slf@geol.uniovi.es

The Malpica-Tui Line (MLL) is a major structure in the Variscan Orogen in northwestern Iberia. It runs parallel to the trend of the orogen for more than two hundred kilometres, from northern Portugal were offsets are at a minimum to the northern coast of Spain were offsets are at a maximum. The sense of movement along the MLL is predominantly dextral in the Spanish segment of the shear zone with a significant dip slip component, elevating the western block. The present level of erosion into the continental crust assembled in the Variscan orogeny allows the observation in the field of structures formed in lower to mid crustal conditions.

The coastal section of the shear zone in northern Spain shows an increase in accumulated strain in rocks at the core of the shear zone from east to west. The first few meters are characterised by intense quartz veining in subvertical quartz-feldspathic schists. To the west, the intense veining is followed by several meters of phyllonites and fine-grained schists. The phyllonitic bands are several cms in width and alternate with several cms of schists with abundant but very thin (1-5 mm) quartzfeldspathic bands. The decrease in grain size coincides with the disappearance of the quartzfeldspathic bands, and this is enhanced towards the west. Silica rich rocks to the west host several cataclastic bands, few cms in width. A range of cataclastic rocks has been observed, from fragment-supported cataclasite to matrix-dominated cataclasite with fragments of host rock floating in the matrix.

Strain accumulation during the operation of the MLL was accompanied by substantial fluid infiltration, as the intense veining activity at the core of the shear zone reflects. Crystallization of K-feldspar between fragments of large plagioclase crystals fractured during high strain and the mixing of feldspar and quartz grains during deformation indicate simultaneous operation of phase transformations and deformation processes.

Most of the structures observed in the field indicate that movement in the shear zone was accumulated aseismically. However, the presence of cataclasites cutting mostly phyllonitic and mylonitic fabrics, may point to late pulses of seismic deformation.

Microstructural Evolution in Quartz and Feldspar During Medium-T Deformation (Viveiro Fault, NW Spain)

Marco A. López-Sánchez*[1], Sergio Llana-Fúnez[1], Francisco J. Martínez[2], Alberto Marcos[1]

[1] Department of Geology, University of Oviedo, Spain
[2]Department of Geology, Autonomous University of Barcelona, Spain.
*malopez@geol.uniovi.es

We show microstructures at increasing degree of strain in a granitic rock affected by the development of a crustal-scale shear zone, the Viveiro fault (vf). The temperature of deformation inferred from syn-tectonic metamorphism developed in the hanging-wall of vf points to deformation occurring at medium t (400-550 ºc).

The Penedo Gordo (pg) granite is coarse-grained two-mica biotite-rich granite. Quartz, microcline, plagioclase (An_{0-20}), biotite and muscovite are the main constituents. It is located at the hanging-wall of the VF and shows a localized eastward increase of deformation, towards the core of the shear zone. On the other hand, the VF hanging-wall shows a staurolite and locally andalusite plus biotite growth during the development of VF. Andalusite growth took place after staurolite growth, and is related to the intrusion of syn-tectonic granitic bodies, such as Penedo Gordo granite.

The microstructures of deformed samples with grades I to IV, representing an increase of accumulated strain, indicate that the dominant deformation mechanisms are: i) intracrystalline plasticity in quartz; and ii) cataclasis accompanied by syn-tectonic crystallisation of very fine grains, probably with albitic composition, in feldspars.

In weakly deformed samples (grades I-II) the dominant mechanism for recrystallization in quartz was "slow" grain boundary migration (bulging or BLG-type). In contrast, the microstructures in grade III-IV samples clearly show that the dominant mechanism for recrystallization in quartz was sub-grain rotation (SGR-type). Feldspars show solid-state deformation microstructures in the case of grades I-II. In grades III-IV, however, feldspar fractures along two dominant planes. New very fine-grained feldspar grains crystallize along fractures as well as at the rim, sometimes accompanied by mica grains. Plagioclase shows a pervasive sericitic alteration.

Highly deformed (grade V) samples consist of a matrix containing feldspar, quartz and sericite with an average grain size < 15 µm, usually featuring some quartz pods and small feldspar porphyroclasts.

Based on pseudosections for representative hanging-wall pelite compositions hosting the PG granite, temperature conditions during deformation are estimated to be in the 400-550°C range. Because andalusite appears locally in the hanging-wall pelites a maximum pressure of 450 Mpa is expected, based on the Al_2SiO_5 triple point.

Petrological and structural thermobarometry data indicate that temperatures during deformation reached 400-550 ºC during fracturing and neocrystallisation of feldspars. Similar feldspar microstructures have been reported previously in rocks where the temperature was estimated between 250 to 400ºC.

In the grade III-IV samples, the microstructures observed in quartz are consistent with a SGR-type dynamic recrystallization. According to Stipp et al. (2002) this recrystallization takes place in the temperature range of 400-500ºC at natural strain rates, in agreement with temperatures inferred in this study.

The microstructures of highly deformed samples clearly indicate a change in the relative contributions of deformation mechanisms during deformation with more participation of mass transfer processes. Furthermore, we suggest that fluids were involved in the VF development, reflected in the increase in mica content with increasing deformation.

Hangingwall Metamorphism Related to an Extensional Orogen-scale Shear Zone: The Vivero Fault (NW Spain)

Marco A. López-Sánchez*[1], Alberto Marcos[1,] Francisco J. Martínez[2], Sergio Llana-Fúnez[1]

[1] Department of geology, University of Oviedo, Spain
[2]department of Geology, Autonomous university of Barcelona, Spain.
*malopez@geol.uniovi.es

The Vivero Fault (VF) is a large crustal-scale shear zone (length >140 km) that follows the main Variscan structures with an N-S trend. It represents the most important extensional shear zone indicating top-to-the-hinterland shear sense in the NW Iberian Variscan belt. It separates two major zones with different tectonostratigraphic features. The attitude of mineral/stretching lineations and foliations are different on each side of the fault. The movement accumulated during its tectonic history affects the major lithostratigraphic sequence of Iberian rocks but also the metamorphic facies developed during Variscan orogenesis. The minimum vertical offset estimated from petrological and mineralogical thermobarometry data is 5.5 km. Other remarkable features previously noted are: i) a related hangingwall metamorphism, with staurolite and kyanite and/or andalusite plus biotite, overprinting the regional greenschist facies metamorphism, and ii) the local presence of folded quartz veins with kyanite and andalusite. In addition, a local kyanite-chloritoid plus andalusite pseudomorphs assemblages were observed in the high-strain Al-rich pelites inside strike-slip shear zones.

The aim of this study is to establish the environment conditions and the metamorphic evolution of VF hanging-wall during its development.

Results

In the hangingwall, and locally, three main tectonic foliations are observed. The first one (S1) shows a pervasive development and is related with the development of tight to isoclinal folds which are currently in an upright position. The second one (S2) shows an uneven distribution and ranging from a gentle crenulation cleavage to a mylonitic foliation. In some cases this foliation shows a clear relation with the development of strike-slip shear zones. Both foliations (S1 and S2) exhibit a steeply dipping to subvertical attitude, except close to the core of VF. The third one (S3) is a low-dipping foliation related with the development of VF. Its development ranges from a gentle crenulation cleavage to mylonitic foliation and is related with the development of cylindrical to sub-cylincrical hinterland-vergent folds.

Matrix-porphyroblast relations show that staurolite, and locally, andalusite plus biotite grew during the VF development. Andalusite growth took place after staurolite growth, and is related to the intrusion of syn-tectonic granitic bodies. However, kyanite and previous andalusite grew before the development of low-dipping foliation related with the VF development. Andalusite-kyanite, staurolite-kyanite and kyanite quartz veins are observed close to the core of VF. In the case of andalusite-kyanite quartz veins, some microstructures show that andalusite grew after kyanite.

Related to regional metamorphism, matrix-porphyroblast relations show that chlorite growth is previous (less probably) and/or syn-tectonic with S1. On the other hand, andalusite and subsequent kyanite growth inside the strike-slip shear zones showing syn-tectonic relations with them. The presence of quartz-kyanite veins in these zones is also common.

Pseudosections for representative hangingwall pelite compositions show that the temperature conditions during VF development fall in the range 400-550ºC. Because andalusite appears locally, we have inferred a maximum pressure of 450 MPa based on the Al_2SiO_5 triple point. The minimum pressure estimated is around 390 MPa for a water activity of $aH_2O=1$. This temperature constraint is consistent with the structural thermometry based on dynamic recrystallisation mechanism in the hangingwall VF mylonites.

Deformed syn-VF granites have yielded crystallisation ages (LA-ICP-MS U-Pb zircon geochronology) that, within error, cluster at 291 My.

Concluding remarks

The observed matrix-porphyroblast relationships clearly indicate that the hanging-wall developed a MT-LP metamorphism during the development of the VF. It also shows that this metamorphic event is subsequent to kyanite growth, the latter probably related with the development of strike-slip shear zones. The inferred PTt path for hangingwall rocks affected by VF metamorphism is almost isobaric prograde path.

Structural, petrological and geochronological data show that a large-scale syn-collisional extensional collapse in the VF is difficult to prove, whereas the post-collisional extension is clearly exposed.

Tectonic- Metamorphic History of Deh-Salm Metamorphic Complex (DMC) in East of Iran

Shahryar Mahmoudi*[1], Farhad Shehki[1]

[1]Geology Department, Tarbiat Moallem University, 49 Mofateh Avenue, P.O. Box 15614, Tehran, Iran
*shahryar.mahmoudi@gmail.com

The Deh-Salm metamorphic Complex (DMC) of the Lut block in East Iran consists of metapelites, amphibolites, marbles, and metasandstones intruded by granite and pegmatites. The Lut block is one of the main tectono-stratigraphic terranes in the east of Iran (Fig. 1a). It is part of a set of terranes considered to have originated by rifting from the northern edge of Gondwana during opening of the Neotethys Ocean in the Permian (Crawford 1972; Stampfli and Borel 2002; Ramezani and Tucker 2003; Golonka 2004).

Some samples demonstrate the regional slaty cleavage and the primary deformation are contemporaneous with middle-grade metamorphism as mentioned above (mahmoudi, 2003). Mica clusters and elongated quartz and specially Andalousite grains define the L1 stretching lineation oriented NS in the meddle part of the area. This cleavage approximately observed in all study area. Few large isoclinal folds F1 display stretched limbs and slightly thickened hinges. Their axis orientation is NNW–SSE to NS. Macrostructure such as primary bedding indicate that the micaschiste series are regionally normal with folds F1 verging E to W. S0–S1 intersection lineation are parallel to local F1 fold hinges. In Andalousite schist, Andalousite porphyroblast show lineation and overprinted by F2 folding. Second folding (F2) deform the regional S1 slaty cleavage together with its L1 lineation in andalousite grains. F2 hinges are particularly well displayed by S1 parallel quartz vines. Ranging in scale from centimeter to meter, the F2 folds are typically non-cylindrical, tight to isoclinal. F2 folding affected L1 and overprinted with bond andalousite Crystal and this rotated about 30 to 45° of clockwise. The crenulation cleavage S2 is common in the shear zones and near granit body intruded in complex. Andalousite and sillimanite are syntectonic porphyroblast. This foliation is well developed in metapelites but is poorly evident, discontinuous, or absent in the metasandstones and marbels and amphibolite (spaced cleavage).

U–Pb dating of zircon, monazite, xenotime, and titanite by ID-TIMS show that the granitic rocks were emplaced at 166–163 Ma, confirming that the high temperature metamorphism was synchronous with the intrusive activity, and that the region cooled rapidly thereafter. Late- to post-magmatic hydrothermal activity was probably responsible for the late crystallization, at 159.5 Ma, of zircon and titanite in an amphibolite and of monazite in granite. Xenocrystic zircons yield indications for a Carboniferous component in the source, together with a variety of Precambrian ages, which indicate a provenance of the sedimentary protolith from mature continental crust. The timing and rapidity of the events are consistent with evolution of the DMC in a back-arc environment during the Jurassic subduction of the Neotethys OceanEditing the template:

The intrusive activity in the DMC was a rapid process that probably spanned just a few million years and was accompanied by high temperature–low pressure metamorphism of the hosting metasedimentary succession. Syeno-granite of the Shah Kuh Pluton yields an age of 165.9 ± 0.2 Ma and appears to be slightly older than leuco-granite from the Eastern Pluton dated at 165.1 ± 0.4 Ma. The sheet-like granitic intrusions found in the highest-grade central axis of the DMC yield somewhat younger ages of 163 ± 1 and 163 ± 4 Ma, the same age indicated by monazite in sillimanite schist. By contrast, zircon and titanite in an amphibolite yield a younger age of 159.5 ± 0.5 Ma, which probably dates a late to post magmatic event of hydrothermal activity. The high temperature–low pressure type of metamorphism, the short-lived nature of the granitic magmatism, and the petrological evidence for fast cooling support a back-arc type of setting for this activity, which can be related to subduction of the Neotethys Ocean below the Cimmerian block.

Overprinting Fabrics and Excess Argon in the Classic Barrovian Sequence of Dutchess County, N.Y.

Ryan J. McAleer*[1], B. P. Proctor [1], M. J. Kunk[2], R.P. Wintsch[1]

[1]Indiana University, [2]United States Geological Survey
*rjmcalee@indiana.edu

New structural, petrographic, and geochronologic data from rocks collected across the classic Taconic Barrovian sequence exposed in Dutchess County, N.Y. indicate that the sequence was affected both by later deformation and by incorporation of excess argon. Twenty white mica $^{40}Ar/^{39}Ar$ age spectra from rocks at chlorite to kyanite grade all produce age minima of ~380-390 Ma and are interpreted to reflect the a time of cooling through muscovite closure (~350°C) at ~380-390 Ma across the entire metamorphic field gradient. These ages suggest that by 380 Ma the white mica closure isotherm was approximately parallel to the present surface and that the tilting leading to the present field gradient exposure occurred before this time. However, these interpretations are complicated by what appears to be a component of excess argon affecting the $^{40}Ar/^{39}Ar$ data. The presence of excess argon is suggested by the U-shaped white mica age spectra recorded in most analyses. Further indicating excess argon are biotite plateau ages that are ubiquitously older than coexisting white mica ages, despite the higher nominal closure temperature of white mica, and disparate biotite plateau ages from rocks within the same outcrop. Adding still further complexity to age interpretation is the recognition of a shallowly dipping retrograde fabric that locally crosscuts the dominant foliation and truncates the porphyroblasts that define the Barrovian sequence. The cleavage is defined by muscovite + chlorite ± biotite suggesting that this retrograde, deformation-induced, fabric developed at or below white mica closure. Thus, an age recovered solely from white mica in this fabric should closely approximate the age of fabric formation, but age spectra from bulk white mica separates may record mixed white mica cooling and growth ages.

Work is underway to analyze samples where the retrograde fabric is most prevalent and where earlier fabrics are most pervasively recrystallized. Additionally, future work will attempt to evaluate how excess argon is lithologically distributed, at what temperature excess argon might have been incorporated, and how crystal-chemical variations might play a role in the variable excess incorporation that we see. In the ideal case we may be able to recover the cooling history of early (Taconic) fabrics, the crystallization age of the late fabric, and something about the fluid history in these complexly deformed rocks.

Gabbroic mylonites developed in a hydrated oceanic crust: an example from the Godzilla Megamullion, Philippine Sea

Katsuyoshi Michibayashi*[1], Yumiko Harigane[2]

[1]Institute of Geosciences, Shizuoka University, Shizuoka 422-8529 Japan
[2]Geological Survey of Japan/AIST, Tsukuba 305-8567, Japan
*sekmich@ipc.shizuoka.ac.jp

Microstructural and petrologic analyses of gabbroic rocks sampled from the Godzilla Megamullion, located along the Parece Vela Basin spreading ridge (Parece Vela Rift), Philippine Sea (Fig. 1), revealed the development of a high-temperature ductile shear zone associated with hydrothermal metamorphism in the lower crust.

The deformed gabbroic rocks are petrographically classified into mylonites and an ultramylonite, and are characterized by porphyroclastic textures consisting mainly of coarse plagioclase and clinopyroxene/amphibole porphyroclasts in a fine-grained matrix (Fig. 2). Plagioclase crystal-preferred orientations vary from (010)[100] and (001)[100] patterns in the mylonites to a weak (001)[100] pattern in the some mylonites and ultramylonite, suggesting a change in the deformation mechanism from dislocation creep to grain-size-sensitive creep with increasing intensity of deformation.

The chemical composition of matrix plagioclase is generally more sodic than that of porphyroclasts. Secondary amphibole is ubiquitous, consisting mainly of pargasite and magnesiohornblende (brown hornblende) and actinolite (green hornblende). The mineral assemblage is consistent with the hydrothermal metamorphic reaction: clinopyroxene + calcic plagioclase + fluid → amphibole + sodic plagioclase.

With reference to a deformation mechanism map for plagioclase, the grain size of plagioclase in the matrix and the estimated temperatures indicate a strain rate of 10^{-10}/s. Compared with deformed gabbroic rocks from the breakaway (Harigane et al., 2008) and termination (Harigane et al., 2010) areas of the Godzilla Megamullion, the samples record ductile shearing under high temperature conditions, possibly related to the development of the Godzilla Megamullion (Harigane et al., 2011).

Harigane, Y., Michibayashi, K. and Ohara, Y., 2011. Deformation and hydrothermal metamorphism of gabbroic rocks within the Godzilla Megamullion, Parece Vela Basin, Philippine Sea. Lithos, in press.

Harigane, Y., Michibayashi, K. and Ohara, Y., 2010. Amphibolitization within the lower crust in the termination area of the Godzilla Megamullion, an oceanic core complex in the Parece Vela Basin, Island Arc, 19, 718-730.

Harigane, Y., Michibayashi, K. and Ohara, Y., 2008. Shearing within lower crust during progressive retrogression: structural analyses of gabbroic rocks from the Godzilla Mullion, an oceanic core complex in the Parece Vela backarc basin. Tectonophysics, 457, 183-196.

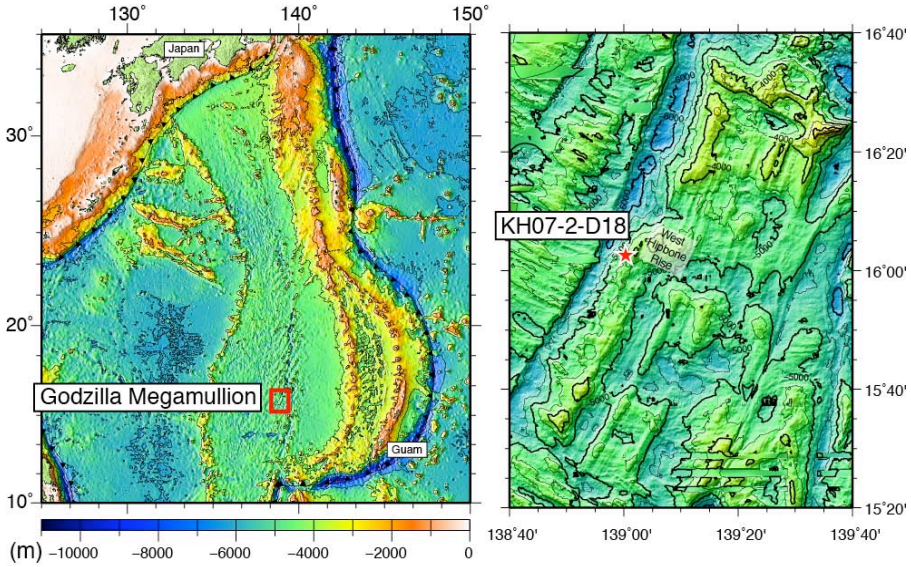

Fig. 1. Godzilla Megamullion, Parece Vela Basin, Philippine Sea.

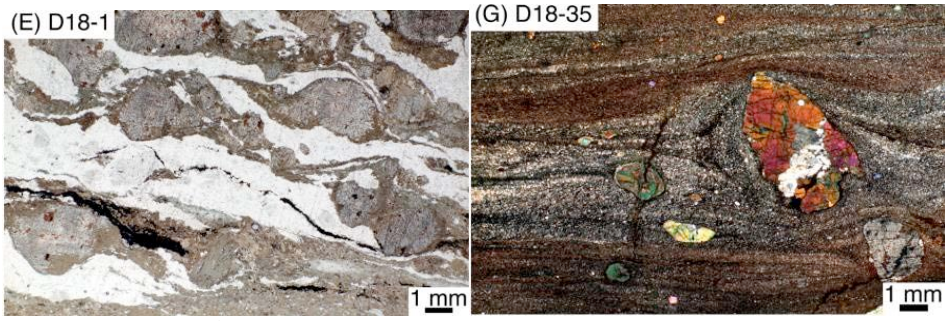

Fig. 2. Left panel: gabbro mylonite, Right panel: gabbro ultramylonite.

Deciphering the Early Variscan Collisional History of SW Iberia Through Quartz Microfabric in the Moura-Cubito Schists

Carlos Ponce[1], F. Simancas[2], **A. Azor*[2],** D. Martínez-Poyatos[2], G. Booth-Rea[2], I. Expósito[3]

[1]Departament de Geologia, Universitat Autònoma de Barcelona, Barcelona, Spain
[2]Departamento de Geodinámica, Universidad de Granada, Granada, Spain
[3]Departamento de Sistemas Físicos, Químicos y Naturales, Universidad Pablo de Olavide, Sevilla, Spain
*azor@ugr.es

The southwestern Iberian Massif is made up of three continental blocks (the southern part of the Central Iberian Zone, the Ossa-Morena Zone and the South Portuguese Zone) amalgamated during the Variscan Orogeny. Independently of the interpretation given to the different contacts between these three continental fragments, their collisional history is characterized by important left-lateral displacements occurred in Carboniferous times. This kinematics is a particular feature of SW Iberia with respect to the right-lateral displacements that prevailed elsewhere in the Orogen. Contrary to the Carboniferous evolution, the kinematics of the early (Devonian) stage of continental collision in SW Iberia is poorly documented. We have investigated this early collisional kinematics by studying the earliest deformation fabric (D_1) preserved in quartz veins of the Moura-Cubito Schists, which form part of an Allochthonous Complex presumed to be rooted in the suture between the Ossa-Morena and South Portuguese Zones. We interpret D_1 as related to the beginning of exhumation, after moderate subduction of the Ossa-Morena margin underneath the South Portuguese one. The most prominent D_1 microstructures are a stretching lineation (L_{m-e}) and a mylonitic foliation (S_1) deformed by subsequent D_2 folding. Once restored, L_{m-e} trends approximately towards N70ºE, forming a small angle with the N100ºE trend of the suture. The quartz microfabric of the early syn-metamorphic veins (preferred orientation of c-axes and subgrain boundaries) suggests top-to-the-east shearing, from which we infer that the Ossa-Morena / South Portuguese collision started as the result of oblique left-lateral convergence. Peak P-T conditions of 400-450º C and 1 GPa estimated for D_1, are in good agreement with the ones independently deduced from quartz microstructures. Minor activation of prism [c] slip in a few of the samples studied is attributed to the influence of P_{H20}, discarding high-temperature conditions. A mylonitic fabric has also been described in some metabasites of the Allochthonous Complex, with N-S to NNE-SSW stretching lineation and top-to-the-north sense of movement. This fabric might have the same tectonic meaning as the S_1 and L_{m-e} fabrics in the Cubito-Moura schists, i.e. both fabrics could be coeval and related to strain partitioning in a general context of oblique collision. However, the mylonitic fabric in the metabasites has also been interpreted as having formed during late extensional collapse subsequent to the collision. Despite remaining controversy regarding the precise meaning of the northerly-oriented stretching lineation, the top-to-the-east sense of movement determined here for D_1 in the Moura-Cubito Schists and, by extrapolation, for the whole Allochthonous Complex, suggests that this tectonic unit must be rooted WSW of its present-day location. Thus, the kinematic scenario in SW Iberia was one of continuous left-lateral convergence from the beginning to the end of the continental collision. In the general context of the Variscan Orogen, dominated by a dextral collision, the left-lateral convergence in SW Iberia all along its collisional history can be explained in terms of impingement of the Newfoundland salient between Iberia and Morocco.

Low grade metamorphosed sandstone-type ore deposits, central Iran

Khalil Rezaei*

Department of Geology, Tarbiat Moallem University of Tehran, Iran,
*khalil.rezaei@yahoo.com

Central Iran includes several potential sites from lead and uranium deposits point of view. The exposed rocks are ophiolitic mélange (consists of mafic-ultramafic fragments set in meta pelites matrix), metamorphosed sandstones, gabbros, granites and post-granite dykes (lamprophyres) and veins (quartz). The metamorphosed sandstone rocks (vary from greywacke to arkosic in composition) outcrop at central Iran at two studied locations. The first sandstone outcrop intruded by fertile porphyritic granite and lamprophyre dykes and second one intruded also by the fertile porphyritic granites. These rocks cut by two generation of quartz veins; a) barren quartz veins cross-cut the foliation planes of MSS and b) mineralized quartz veins -bearing visible mineralization (wolframite, cassiterite and xenotime) and extends parallel to the foliation planes. The MSS rocks show relics of primary bedding, banding and obvious foliation. The common alteration products are represented by kaolinitization, flouritization, hematitization, chloritization and manganese dendrites. The alterations are associated with visible greenish yellow U- minerals. The emplacement of both of lamprophyre dykes and porphyritic granites may be played an important role as a heat source, which lead to U-mobilization from hot granites, transported (along deep faults, foliation planes and banding) and redeposit in MSS rocks under suitable conditions.

Typology of Lozenges Developed in Shear Zones Affecting Foliated Rocks: Geometry and Kinematics

Carlos Ponce*[1], Jordi Carreras[1], Elena Druguet[1]

[1]MIET, Departament de Geologia, Universitat Autònoma de Barcelona
*Carlos.Ponce@uab.cat

Ductile shear zones develop anastomosing patterns no matter the mechanical properties of pre-existing rocks (i.e. isotropic/ anisotropic, homogeneous/inhomogeneous). The origin of this pattern can be a consequence of the presence of variable oriented sets of shears, connecting splays and/or secondary shears. Shear zone coalescences lead to the anastomosing pattern which is related to a high inhomogeneity of strain, with band-shaped high shear strain domains bounding less or undeformed lozenge-shaped domains. The two dimensional shape of lozenges can vary considerably from square or high angular rhomboidal shapes to highly elongated lensoid shapes. In rheological heterogeneous rocks the shape of the lozenge depends mainly on the initial shape of the more competent rock and the competence contrast. In isotropic homogeneous rocks the lozenge shapes depend on the orientation of the developing sets of shears. Usually, the initial shape of lozenges that are bounded by sets of shears with the same kinematics is more elongate than that of lozenges that result from the coalescence of conjugate sets of shears. However, in all cases, progression of deformation leads to the gradual elongation of the lozenges at the same time as the bounding shear zones tend to parallelize. This implies the internal deformation of the lozenges.

In rocks bearing pre-existing mechanical anisotropies, the geometry of lozenges is far more complex. There, the orientation of the shears is strongly influenced by the relative orientation of the pre-existing anisotropy with regard to the bulk strain field (Cobbold et al., 1971; Williams and Price, 1990). This contribution is a preliminary analysis of lozenge structures in foliated rocks, focusing on role of the orientation of the pre-existing foliation and on the kinematics of the bounding shear zones.

In isotropic rocks, the presence of two equally developed conjugate sets or the prevalence of one set (synthetic) over another (antithetic) depends on the bulk vorticity. However, this does not entirely apply to foliated rocks, because equally developed conjugate sets might appear in non-coaxial deformations (if the ISAs are orthogonal to the anisotropy), while a prevalent set can develop in coaxial deformation (if the ISAs are oblique to foliation). This leads to a situation where the shear zone pattern and, in consequence, the structure of the lozenges have a complex relation with the bulk vorticity.

The proposed analysis does not consider the proportion of shear zones with similar or opposite kinematics. Thus the presented typology is independent of the bulk vorticity of the flow, because each individual shape can form in all bulk vorticity spectrum ($0<Wk<1$). Shapes are drawn for profiles normal to the mean shear plane and parallel to the shear direction. As stated above, two variables are considered: (1) the orientation of the pre-shear foliation with regard to the enveloping surface of the mylonitic foliation and (2) the kinematics of the bounding shear zones, that is, shear zones of the same or opposite shear sense (Ponce et al., 2010). For the sake of simplicity, the typology assumes that (i) the bounding shear zones make originally an obtuse angle facing the bulk shortening, (ii) each individual shear zone satisfies the simple shear model and (iii) shears are active in a sequential way. Moreover, the presence of an internal deformation of the lozenge is neglected. The two examples shown in Fig. 1 evidence the marked differences in the structures formed at the lozenge margins, simpler when all shears are synthetic (Fig. 1b) and more complex when shears form conjugate sets (Fig. 1a).

These theoretical patterns are compared with real examples from the Northern Cap de Creus Shear Belt (Carreras, 2001). There, in spite of a prevalent dextral wrench regime, both dextral and sinistral shears are present, prevailing the dextral/reverse ones over the less abundant sinistral/normal ones. As stated in Carreras (2001) conjugate sets of shears zones form preferentially where the shortening ISA lies closely parallel to the pre-existing foliation, while dextral sets are prevalent where the ISA is oblique.

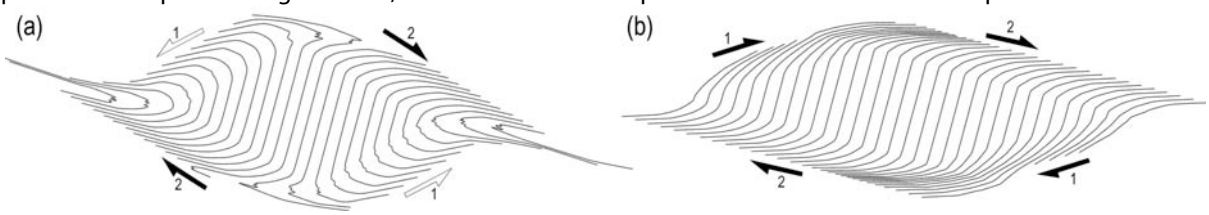

Fig. 1. Comparison of two lozenge structures formed in foliated rocks with the same initial orientation of the previous foliation (70º). (a) conjugate shears (1 followed by 2) giving rise to millipede-shaped lozenges (Bell, 1981). (b) synthetic shears (1 followed by 2) giving rise to sigmoidal lozenges.

The examples shown are from the Culleró area, where both, conjugate sets and dominant dextral sets occur in domains of differently oriented previous foliation. Where conjugate sets are present, the sinistral set predates the dextral one. Millipede-shaped lozenges (Bell, 1981) typically arise from conjugate sets of shears (Fig. 2a), while sigmoidal lozenges form in domains where the lozenges are wrapped by dextral shears (Fig. 2b).

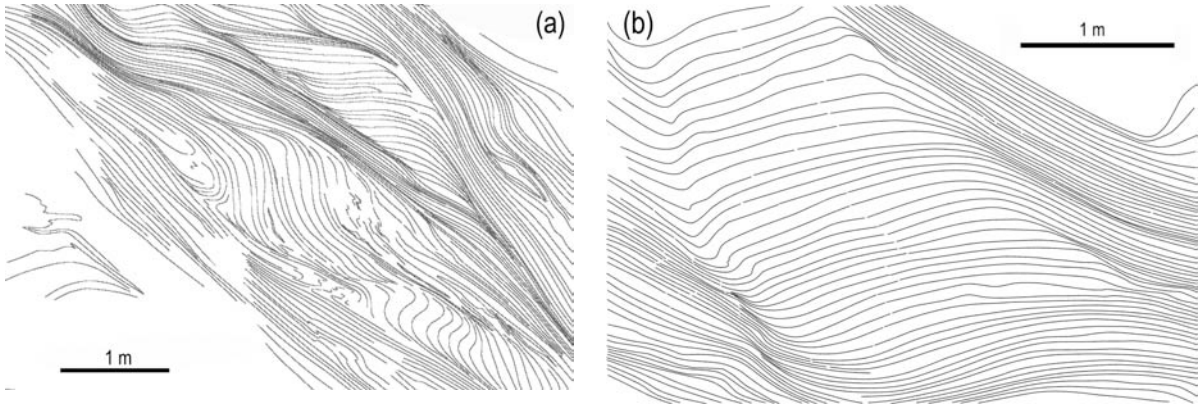

Fig. 2. Structures of lozenges arising from variable kinematics of the bounding shears. (a) The lozenge at the centre of the image was initially bounded by sinistral shear zones and subsequently sheared dextrally. Note the complex folds arising at domains of sinistral-dextral shear coalescence. (b) A typical sigmoidal lozenge bounded by dextral shears. In this situation, local foliation-parallel anthithetic shearing occurs to accommodate internal deformation and rotation of the lozenge.

A whole understanding of the geometry of lozenges and its relations with kinematics requires a three-dimensional approach. Concerning the 3D-shape of the studied lozenges this is generally fusiform, with the long axis closely parallel to the stretching lineation that in Cap de Creus is nearly coincident for dextral and sinistral shears. The relation between 3-D geometry and kinematics is complex due to the fact that the structure depends on the relative orientation of pre-existing foliation and the shear plane and independent of the shear direction (Carreras, 1997). This causes the angle between the bending/fold axis (B in Fig. 3) and the shear direction to vary between 0º and 90º. In consequence, some exposed asymmetries do not reflect the shear sense (Fig. 3).

Field observations indicate that, in foliated rocks, the prevailing shears does not depend so much on the bulk kinematics (degree of non-coaxiality) but on the angular relationship between the pre-existing foliation and the bulk kinematic axes. The fact that there is a great angular variability between initial foliation and shear zone patterns, the final geometry is not univocally related neither to strain type (oblate/prolate) nor to the degree of non-coaxiality. The complete understanding of lozenges requires further investigation in 3D.

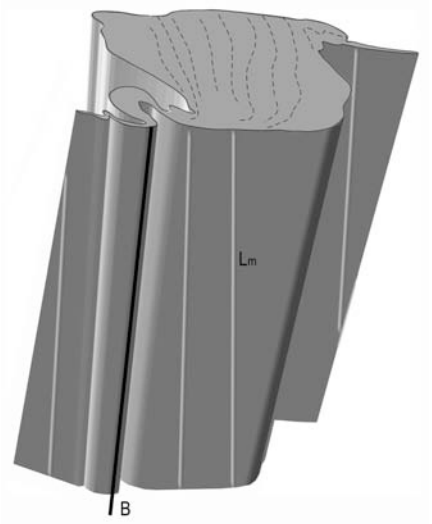

Fig. 3 Three-dimensional sketch of a lozenge developed in a dip-slip shear zone. Note that the rotation axis (B) is closely parallel to the shear direction and thus the observed asymmetric d-shaped structure is not kinematically indicative when observed on the shown section.

Bell, T.H., 1981 Foliation development. The contribution, geometry and significance of progressive, bulk, inhomogeneous shortening. Tectonophysics 75: 273-296.

Carreras, J. 1997. Shear zones in foliated rocks: geometry and kinematics. In: Sengupta, S. (Ed.), Evolution of geologic Structutres in Micro- to Macro-scales. Chapman and Hall. London, pp. 185-201.

Carreras, J. 2001. Zooming on Northern Cap de Creus shear zones. Journal of Structural Geology 23: 1457-1486.

Cobbold, P.R., Cosgrove, J.W., Summers, J.M., 1971. The development of internal structures in deformed anisotropic rocks. Tectonophysics 12: 23–53.

Ponce, C. Carreras, J. Druguet, E. 2010. Development of "lozenges" in anastomosing shear zone networks in foliated rocks. Geogaceta 48: 207-210.

Williams, P.F., Price, G.P., 1990. Origin of kinkbands and shear-band cleavage in shear zones: an experimental study. Journal of Structural Geology 12: 145–164.

The Betic Ophiolites: Relics of Jurassic Oceanic Slabs Tectonically Intercalated Between Crustal Units of the Mulhacen Complex after their Eo-Alpine Subduction and Exhumation

E. Puga*[1], C. M. Fanning [2], A. Díaz de Federico[1], J. A. Rodríguez Martínez-Conde[3], J. M. Nieto[4], M. A. Díaz Puga[5], J.A. Lozano[1], J. I. Manteca Martinez[3]

[1]Instituto Andaluz de Ciencias de la Tierra (CSIC-UGR). Fac. de Ciencias, Granada, Spain.
[2] Research School of Earth Sciences.The Australian National University, Mills Road, Canberra ACT 0200, Australia.
[3] Dpto. de Ingeniería Minera, Geológica y Cartográfica, Universidad Politécnica de Cartagena, Murcia, Spain.
[4]Dpto. de Geología, Facultad de Ciencias Experimentales, Universidad de Huelva, Spain.
[5]Dpto. de Hidrogeología, Universidad de Almeria, Spain.
*epuga@ugr.es

The Betic Ophiolite Unit forms part of the Mulhacén Complex, and crops out discontinuously over approximately 250 km in the central and eastern sectors of the Nevadofilábride Domain in the Betic Cordillera (Fig. 1). It comprises numerous metre- to kilometre-sized lenses of metamorphic rocks, deriving from basic, ultramafic and/or sedimentary rock types, representing very important relics of the ocean floor from the westernmost end of the Jurassic Tethys. This ocean floor almost completely disappeared through subduction during the Upper Cretaceous collision of the European and African plates. However, some rare slices of it were exhumed and incorporated into the continental margin, forming the Betic Ophiolites.

We recently determined the absolute age of zircons from the cumulitic olivine gabbros forming the basal layers of these ophiolites, using the U-Pb method by SHRIMP (Sensitive High Resolution Ion Micro Probe) with cathodoluminescence images, yielding an average value of 185±3 Ma. Some of these radiometric ages and their geodynamic meaning have been recently published by Puga et al., (2011). The Pliensbachian age obtained for the Betic Ophiolites suggests that they derive from the first oceanic basin that developed in the westernmost Tethys Ocean, the Betic Tethys (Fig. 2). During continued break-up of Pangaea the other Western Tethys oceanic basins formed propagating from the Betic Tethys towards the northeast (Schettino & Turco, 2010). The uniqueness of the Betic Ophiolites as the only preserved relics of the earliest formed western Tethys oceanic floor make them of great value for palaeogeographical studies. Moreover, the late-orogenic emplacement of the Betic ophiolitic relics between nappes of continental origin, the Caldera and Sabinas units of the Mulhacen Complex (Fig. 2), following their earlier subduction and eclogitization during the Eo-Alpine event, is key evidence for elucidating the timing and tectonic significance of the present nappe pile that constitutes the Nevadofilabride Domain of the Betic Cordillera (Fig. 1).

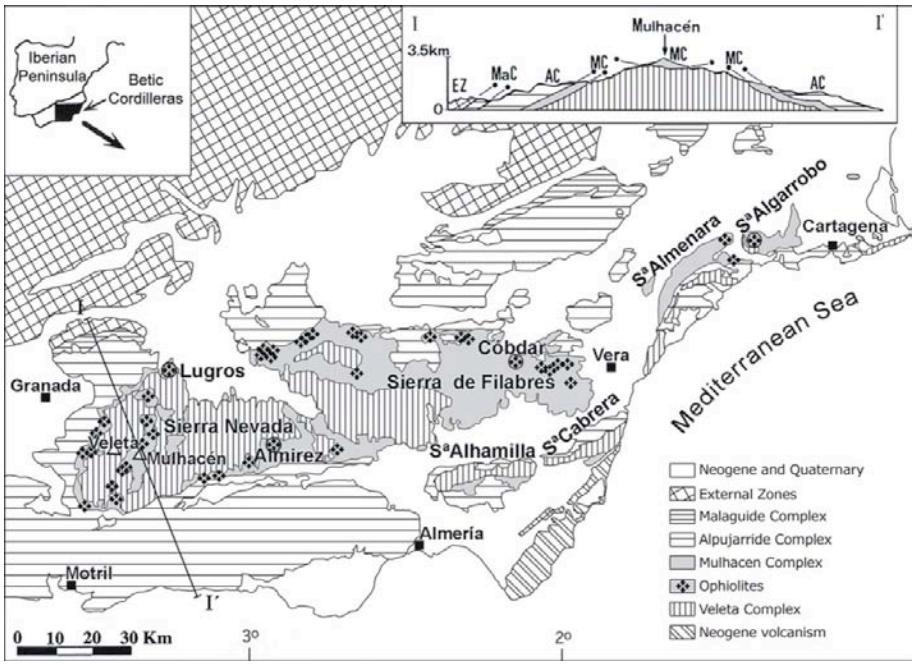

Fig. 1: Geological sketch of the central-eastern sector of the Betic Cordilleras. Black four-pointed stars on the Mulhacen Complex represent the location of the main outcrops of the Betic Ophiolites. Encircled stars indicate the outcrops that contain the U-Pb dated zircons.

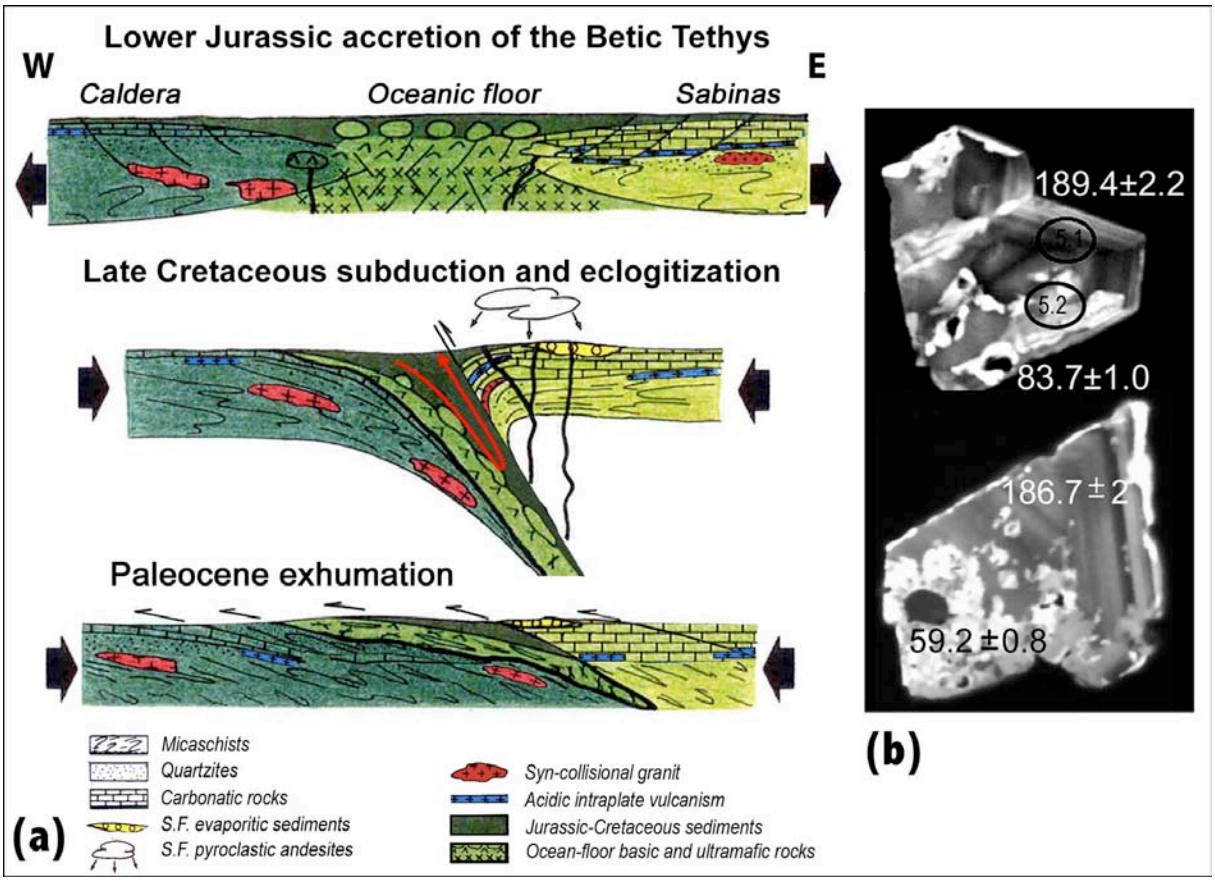

Fig. 2: (a) Tentative sketch of Jurassic to Paleocene geodynamic evolution of the Betic oceanic floor according to radiometric data and paragenetic succession in the Betic Ophiolites (modified after Puga et al., 2011). (b) Cathodoluminescence images of zircons from the eclogitized gabbros of the Betic Ophiolites, dated by U/Pb method with SHRIMP, evidencing Lower Jurassic ages for their oscilatory zoned igneous rims and late Cretaceous to Paleocene ages for their recrystallized areas during the subduction and Eo-Alpine metamorphic event.

References:

Puga, E., Fanning, C. M., Díaz de Federico, A., Nieto, J. M., Beccaluva, L., Bianchini, G., Diaz Puga, M. A. (2011). Petrology, geochemistry and U-Pb geochronology of the Betic Ophiolites: inferences for Pangea break-up and birth of the Westernmost Tethys Ocean. Lithos, doi: org/10.1016/j.lithos.2011.01.002

Schettino, A., Turco, E. (2009). Breakup of Pangaea and Plate Kinematics of the central Atlantic and Atlas regions. Geophysical Journal International 178, 1078–1097.

Microstructural Analysis of Shearband Boudin – Preliminary Results

Benedito C. Rodrigues*[1], Mark Peternell[2], António Moura[1], Jorge Pamplona[3]

[1] Centro de Geologia da Universidade do Porto, Rua do Campo Alegre, 687, 4169-007 Porto, Portugal, [2]Tektonophysik, Johannes-Gutenberg Universität Mainz, 55099 Mainz, Germany (*bjc.rodrigues@gmail.com)
[3]Centro de Investigação Geológica, Ordenamento e Valorização de Recursos, Universidade do Minho, Campus de Gualtar, 4710-057 Braga, Portugal

Introduction - The internal structure of a shearband boudin resulting from an original igneous, hydrothermal or metamorphic segregation tabular rigid body is a subject of scientific interest. It allows understanding the deformation mechanisms acting on homogeneous quartz aggregate activated during simple shear progressive deformation. This communication is focused on the characterization of two main structural aspects: (i) the existence of different internal domains in shearband boudins; (ii) the development of internal structures related with its genesis and evolution, namely, secondary shear planes c' type-I and c' type-II, parameter B-t (mass accumulation sector on blunt tip of shearband boudin) and S-t (sharp tip of shearband boudin) (Pamplona & Rodrigues, 2011a, Pamplona and Rodrigues, 2011b), internal migration of mass (rotation and translation) and mechanisms of ductile deformation activated on the process.

Methodology - The obtained results come fundamentally from inputs of five methodologies: (i) Quartz microtextural analysis (classical optical microscopy appointing to the identification to textural features related with internal quartz domains and internal shearband boudin microstructures; (ii) Quartz *c*-axis preferred orientation measurements by the use of an automated fabric analyzer system (Wilson et al., 2007; Peternell et al., 2009; 2010); (iii) Quantification of quartz microstructures by the use of the PolyLx toolbox (Lexa, 2003); (iv) Fractal geometry based analysis of quartz grains to distinguish different quartz populations that developed during formation of the shearband boudin and, (v) Identification of fluid inclusion types, fluid volume density, fluid composition and density, probable isochoric path and consequent temperature and pressure of fluid entrapment, on core older quartz, intercrystalline domains and on the recrystallized quartz.

The Fabric Analyser instrument G50-RGB is an automated and very fast polarizing optical microscope that determines the orientation of *c*-axes of uniaxial crystals at each pixel in the field of view with 2.8 µm/pixel resolution (e.g. Wilson et al., 2007; Peternell et al., 2009; 2010). The output of the instrument is a set of data images and a pixel data file. *c*-axis trend and plunge, retardation (highest birefringence color), orientation, grain boundary and quality images are produced in addition to the conventional crossed polar images.

PolyLx is a Matlab toolbox for structural and microstructural analysis in rocks such as grain size and grain size distribution analysis, grain/grain boundary orientation, strain analysis and many more. The input file has to be a shapefile that contains the objects of interest (e.g. grains, clasts or voids).

By the use of the box-counting method area and perimeter of single crystals are determined on different scales and plotted in a log-log diagram. In case of crystals the data points show a clear linear correlation and the slope of the best fit determines the fractal area-perimeter dimension. A colour coded map of the whole boudin is presented regarding the variation of fractal area-perimeter dimensions.

Fluid inclusion studies. The study of the fluid inclusion population on the old core quartz, on the intercrystalline spaces and inside recrystallized quartz coupled with the metamorphic information of the region, will permit to envisage the PTVX characteristics of the boudin geological history.

Results and discussion - Quartz SPOs and CPOs inside the boudin can be grouped into several textural domains. Within the "internal" domains (Fig. 1) *c*-axis orientations are concentrated along a single girdle structure, whereas patterns from the "blunt tip" domains form symmetric and slightly asymmetric cross girdles. Unusually, the single girdle is asymmetric oriented in a low angle to strain X as well as the cross girdle open over strain X and not strain Z. This indicates that the domains exhibit a rotational increment during boudin formation in relation to the external simple shear regime of 90°. Quartz SPOs from these domains are approx. parallel to the related CPOs indicating that grain boundary and *c*-axis formation occurred in an early stage of boudin formation followed by domain rotation and minor grain boundary migration.

Structurally different domains are present at the boudin's sharp tips. The quartz is finer grained with SPO in a high angle to the CPO and the quartz pattern form a strongly asymmetric cross girdle with a strong maximum parallel strain X. The *c*-axis orientations again indicate a rotational component of the domain with different vorticity to the other domains.

The mapping of fractal area-perimeter dimensions indicates two quartz "populations" with coarser grained quartz in the "internal" and "blunt tip" domains. Along the grain boundaries and the internal "surfaces" (corresponding to c' types) and second quartz "population" formed that is also dominant at the "sharp tip" domains.

The results from the microstructural quantification indicate that the microstructures are different depending on their location inside the boudin but can be assigned to several domains. The results from the microstructural quantification indicate that the microstructures are different depending on their location

inside the boudin but can be assigned to several domains. Quartz microstructures of "internal" and "blunt tip" domains are once they are formed only show rotational component with minor grain boundary migration possibly related to slip on the internal "surfaces" and the "external" simple shear regime. Microstructural change, i.e. recrystallization, occurs along the internal "surfaces" and in the "sharp tip" domains possibly because of strain localization.

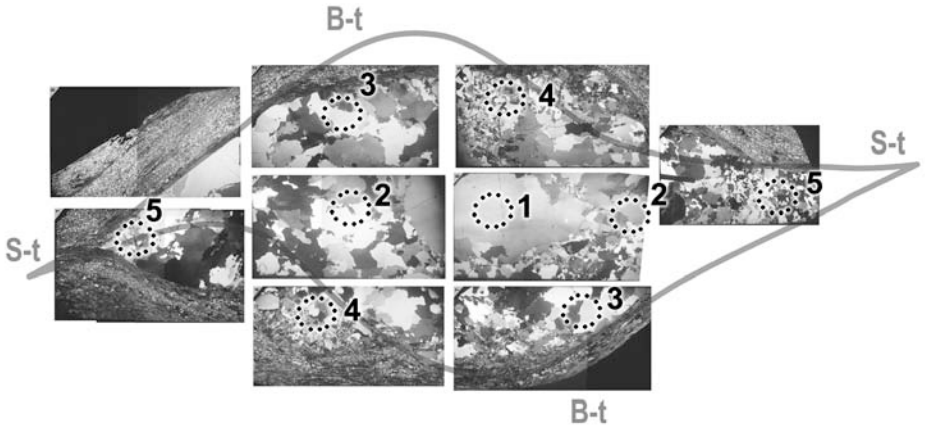

Figure 1 – Dominial analysis of internal structure of shearband boudin. 1- nucleus domain, 2- inner domains, 3- blunt-tip domain, 4- heterogeneous domain, 5- sharp-tip domain.

The textural domain corresponding to a possible original grain (nucleus domain) is defined by a large quartz crystal exhibiting a losangic pattern of sub-grain boundaries with dominance of a set sub-parallel to <c>. This direction materializes the internal c' type-I. The transition from this domain to the involving ones is made by a rational boundary "jigsaw type" and by muscovite alignments parallel to c' type-I.

B-t and S-t domains are opposite geometric tips on the boudin and also show contrasting textural features: S-t is characterized by a high frequency of regular boundaries with triple junctions delimiting small grains quartz without or slightly undulant extinction. Otherwise, B-t has coarser grains, with a certain amount of internal deformation registered on undulant extinction of quartz grains and a high boundary mobility with intergranular junctions fringed by neo and leftover grains.

The shearband boudin develops two heterogeneous domains were an additional paragenesis occurs formed by Qtz+And+Tur+Ms+Bt. The muscovite is typically hydrothermal (coarser flakes forming fans) and the andaluzite appears as coarse euhedrical grains with pleochroic zoning exhibiting a pink nucleus (Fe-rich) and colorless border.

The fluid inclusion observations, at this stage of the research, only permit to conclude general statements. The distribution of the fluid inclusions population on the older grains (nucleus domain) is heterogeneous; mm^2 scale areas of these grains are avoided of fluids with dimension that permit the observation under the optical microscope (up to 2000 x); also there are areas where it is easy to see groups of 5-20 micra biphasic fluid inclusions of possible primary origin. These are aqueous-rich inclusions with a degree of filling water around 80%. There are also transgranular trails of two fluid types: one with inclusions similar of the previous described (although smaller) and the other filled with small grey-coloured monophasic fluid inclusions possibly carbonic inclusions. Some of these inclusions have a small rim of water (around 10 % volume). Both types of inclusions have negative-shape morphologies which could be a re-equilibration feature instead of a primary characteristic.

Conclusions - The multi-approach studies of the internal structure of the shearband boudin identifies that the shearband boudins exhibit different domains (Bt domain, St domain, heterogeneous domain, internal domain and inner surfaces), with distincts mechanical and mineralogical evolutions. Each domain has characteristic that allows to support the deformational history of boudinage process.

The nucleus domain, as a heritage structure of the original tabular body, could be non-rotated during the boudinage process. The B-t domains are those were the mass transport phenomena is more intense and S-t domains those were the recrystallization phenomena is dominant. The heterogeneous domains represent regions were occurs dilatation during the boudinage allowing the migration, into the SiO2–rich inner boudin body, of alumina-rich fluids and volatiles, which crystallize the typical paragenesis of this domains.

The grain boundary and c-axis formation occurred in an early stage of boudin formation followed by domain rotation and minor grain boundary migration.

Drury M, Urai J (1990). Deformation-related recrystallization processes. Tectonophysics, 172: 235-253.

Lexa O (2003). Numerical approaches in structural and microstructural analysis. PhD thesis, Charles University, Prague, Czech Rep.

Moura A (2008). Metallogenesis at the Neves Corvo VHMS deposit (Portugal): a contribution from the study of fluid inclusions. Ore Geology, 34: 354-368.

Pamplona J, Rodrigues BC (2011a). Kinematic interpretation of shearband boudins: New parameters and ratios useful in HT simple shear zones. Journal of Structural Geology, 33: 38-50.

Pamplona J, Rodrigues BC (2011b). Fold boudins: what is that? Geophysical Research Abstracts, Vol. 13, EGU2011-7465.

Peternell M, Hasalová P, Wilson CJL, Piazolo S, Schulmann K (2010). Evaluating quartz crystallographic preferred orientations and the role of deformation partitioning using EBSD and Fabric Analyser techniques. Journal of Structural Geology, 32: 803-817.

Peternell M, Kohlmann F, Wilson CJL, Seiler C, Gleadow AJW (2009). A new approach to crystallographic orientation measurement for apatite fission track analysis: Effects of crystal morphology and implications for automation. Chemical Geology, 265: 527-539.

Van Den Kerkhof A, Hein U (2001). Fluid inclusion petrography. Lithos, 55: 27-47.

Wilson CJL, Russell-Head DS, Kunze K, Viola G (2007). The analysis of quartz c-axis fabrics using a modified optical microscope. Journal of Microscopy, 227: 30–41.

Stress-Induced Alteration of Sudoite

M.D. Ruiz Cruz[1], **M.D. Rodríguez Ruiz*[1]**, C. Sanz de Galdeano[2].

[1]Facultad de Ciencias. Campus de Teatinos. Universidad de Málaga. 29071-Málaga (Spain)
[2]Instituto Andaluz de Ciencias de la Tierra. CSIC-Universidad de Granada. 18071-Granada (Spain)
*mdrodriguez@uma.es

The aim of this study was to investigate the structural and chemical modifications associated to progressive deformation of phyllosilicates that occurred under natural conditions. We studied strongly deformed sudoite-bearing sinfolial quartz veins from Permo-Triassic, talc-bearing phyllites from the Beni Mezala unit (the deepest Federico unit of the Internal Zone of the Rif belt, Morocco). "Chlorite"-enriched areas of the veins were manually obtained, and studied by petrographic microscopy, X-ray diffraction (XRD), scanning (SEM), and transmission-analytical electron microscopy (TEM/AEM). Signals of sudoite deformation included kinks (Fig. 1A), chevron-like folds (Fig. 1C), and fractures (Fig. 1D). The samples also contain later, undeformed grains (Fig. 1B-C), which seal the fractures of grew with (001) perpendicular to the compressive stress.

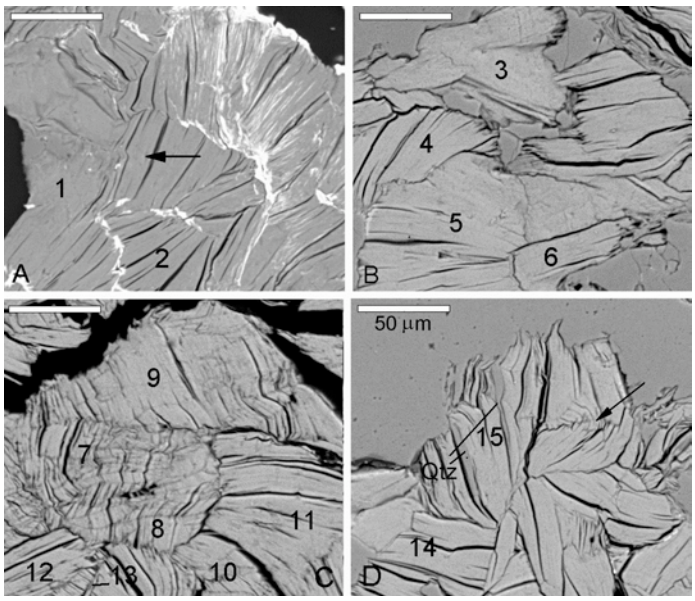

Figure 1. Back-scattered images of the several chlorite-like minerals. A: Arrows points to a kink in grains of sudoite. B: Slightly deformed grains. C: Area with chevron-like folds and undeformed grains (lower left corner). D: Fractured grains (arrow) and thin intergrowths "chlorite"-quartz. Scale-bar common to all the images.

Deformation-induced structural changes mainly consist of basal cleavages associated to ordered replacement of brucite sheets by hydrated sheets (Fig. 2 A), thus leading to irregular microdomians of chlorite-vermiculite mixed-layers and sudoite (Fig. 2 B). These structural modifications represent a mechanism for accommodating the compressive stress.

Structural changes were accompanied by minor chemical ones, which lead from di,tri-chlorite (sudoite) to phases with a more trioctahedral character (chlorite-vermiculite mixed-layer). The hydration reaction occurred throughout a topotactic replacement of the pre-existing sudoite grains. Later, undeformed grains consist of chlorite-vermiculite mixed-layers intergrown with retrogressive kaolinite and minor Fe-oxide, and are interpreted as formed through a dissolution-precipitation process, during deformation. Deformation and retrogression of sudoite probably occurred during the latest stage of exhumation, at low temperature conditions.

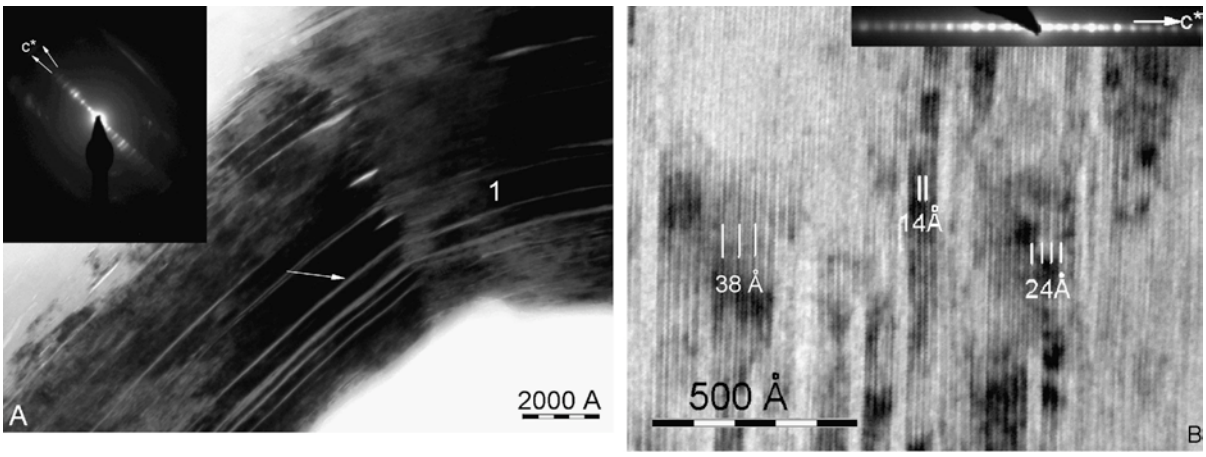

Figure 2. A: Low-magnification TEM image of a folded grain. This consists of sub-parallel packets with variable curvature radius. The deformation is revealed by the presence of numerous thin, parallel grey areas, which probably represent contribution of vermiculite-like layers contraction against the electron beam and micro-cleavages (white arrow)**. B:** HRTEM imaging of parallel intergrowths of chlorite (14 Å) and several types of chlorite-vermiculite mixed-layers, with dominant 24 and 38 Å periodicities.

Acknowledgements.
Thanks to M.M. Abad (CIC, Universidad de Granada) for help in obtaining TEM/AEM data. This study has received financial support from the Project CGL 2006-02481 (Ministerio de Educación y Ciencia) and from the Research Group RNM-199 (Junta de Andalucía).

Blueschists and Early Variscan HP/L-IT Units in the Spanish Ossa Morena - South Portuguese Boundary

F. J. Rubio Pascual[1], J. Matas[1] & **L. M. Martín Parra***[1]

[1]Instituto Geológico y Minero de España, Spain,
*lm.martin@igme.es

Two different units preserving HP/L-IT parageneses crop out in the Aracena Metamorphic Belt of the Ossa Morena Zone, and another one has been identified in the Spanish part of the South Portuguese Zone (Fig. 1).

The Cubito-Moura Schists is a pelitic unit that has been interpreted as an allochthonous nappe emplaced northwards on the Ossa Morena Zone. The schists have undergone a HP/L-IT metamorphic episode (M_1) and some of them present a mineral association of Phg + Chl + Ab + Rt + Qtz recording minimum pressures of 9 Kbar and 350-450 ºC (Fig. 2). Its basal detachment is a tectonic mélange incorporating eclogite blocks in Portugal and blueschists in Spain. Blueschists mineral association in metabasites is composed of Win/Crossite + Ab + Chl + Ttn + Ep(?). Semipelitic blueschists are formed by Phg + Gln/Rbk + Pg + Ab + Ttn + Qtz + Ep(?) formed at minimum P-T conditions of 12 Kbar and 300 ºC.

The Ossa Morena Zone sequence below Cubito-Moura is mainly formed by Neoproterozoic metasediments, Lower Paleozoic acid and basic metavolcanics and marbles, and the Beja-Acebuches Amphibolite. Most of the pile is affected by a HT/LP episode (M_2), but the Neoproterozoic metasediments of La Umbría Formation preserve an M_1 association of Grt + Phg + Bt + Ab + Rt + Qtz formed at 11 Kbar and 450 ºC.

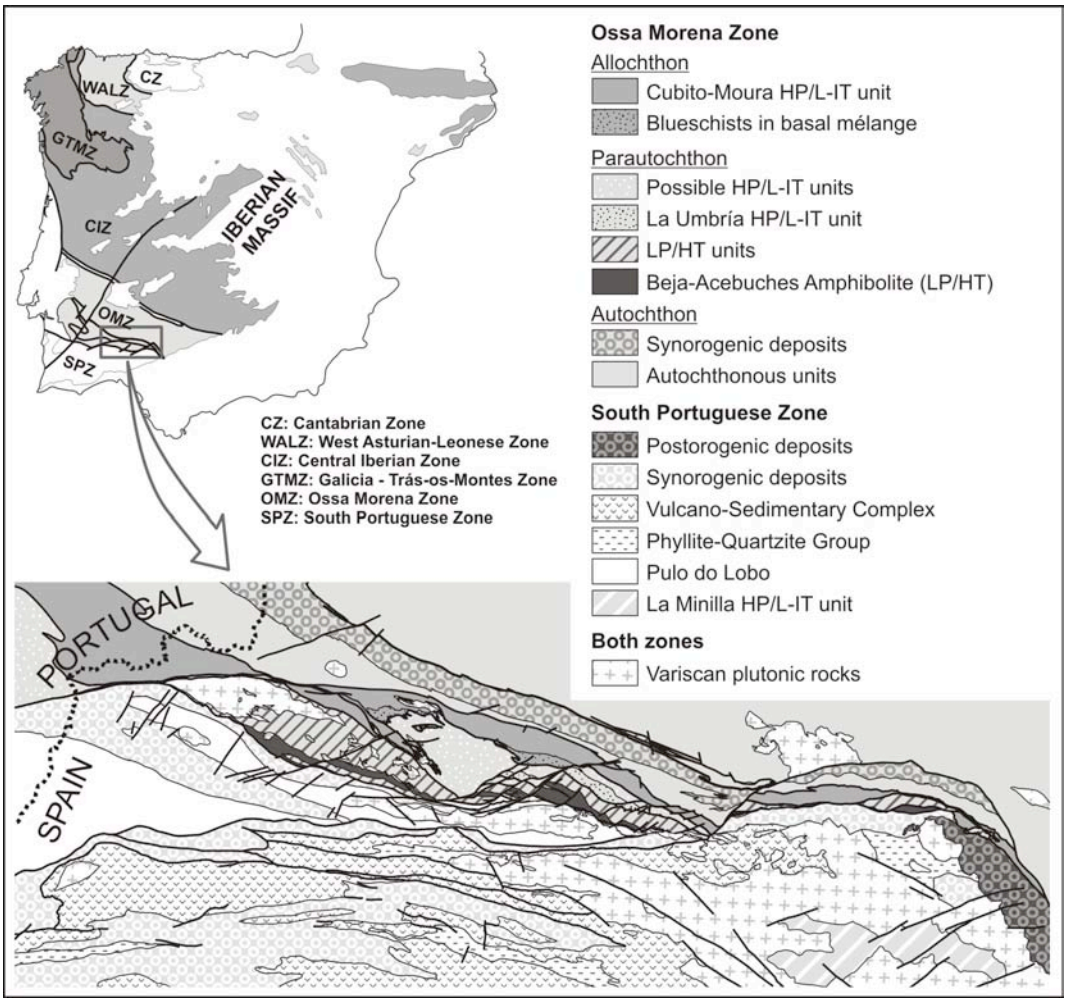

Fig. 1: Geological sketch of the Spanish part of the Ossa Morena – South Portuguese boundary showing the location of the HP/L-IT units.

The pelitic-psammitic La Minilla unit outcrops in the South Portuguese Zone surrounded by Variscan plutonic rocks. Poorly understood, this unit might represent a structural level below the low metamorphic grade metasediments of the Pulo do Lobo unit and its cover of Phyllite-Quartzite group and Vulcano-Sedimentary Complex. La Minilla unit locally contains mineral associations with Grt + Phg + Bt + Ab + Rt + Qtz, formed under M_1 conditions of 9 Kbar and 400 ºC. The presence of different units that have undergone a similar HP/L-IT metamorphic episode both in Ossa Morena and South Portuguese zones implies that they probably formed part of the same subduction complex and points to a southwards polarity of the Early Variscan subduction zone. The southernmost Ossa Morena units which have been implicated in the HP event represent a parautochthonous external margin of the zone, partially subducted southwards beneath the Pulo do Lobo accretionary wedge. The northwards underthrusting of the allochthon and parautochthon set beneath the Ossa Morena autochthon occurred during late collisional stages.

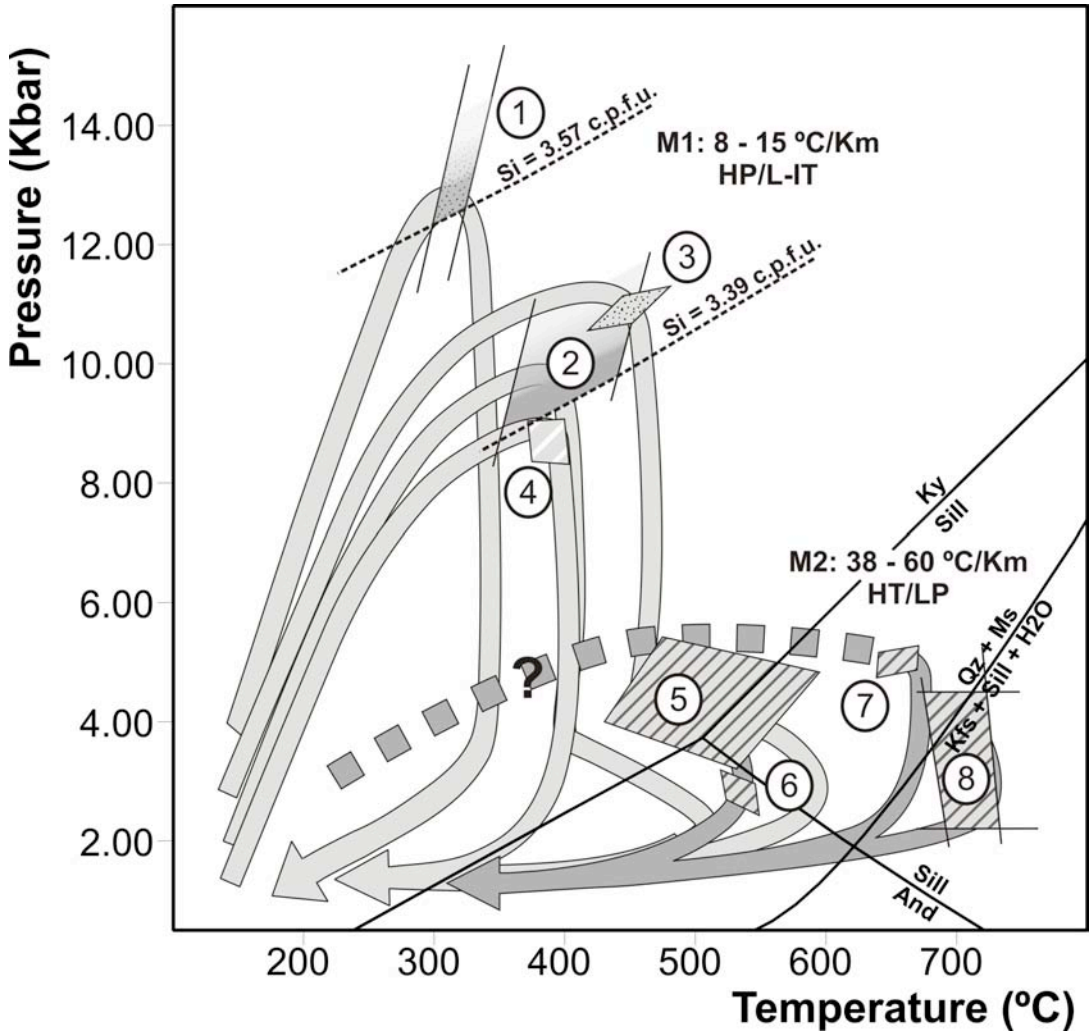

Fig. 2: Calculated P-T conditions of selected samples from different units: 1) Basal allochthon blueschists. 2) Allochthonous Cubito-Moura Schists. 3) La Umbría parautochthonous unit. 4) La Minilla unit. 5, 6, 7, 8) HT/LP parautochthon units. Thermobarometric calculations: 1, 2) Plagioclase-muscovite geothermometer (Green & Usdansky, 1986), Si-in-phengite geobarometer (Massonne & Schreyer, 1987). 3, 4, 5, 6, 7) TWQ v2.3 (Berman, 2007). 8) Hornblende-plagioclase geothermometer (Holland & Blundy, 1994), Al-in-amphibole geobarometer (Johnson & Rutherford, 1989).

Quartz Microstructures, the Key to Unravel an Orogenic History

Koen Van Noten[1], Hervé Van Baelen[1], Isaac Berwouts[1],
Philippe Muchez*[1], Manuel Sintubin[1]

[1] Geodynamics & Geofluids Research Group, Department of Earth and Environmental Sciences, K.U.Leuven, Celestijnenlaan 200E, 3001 Leuven, Belgium
*philippe.muchez@ees.kuleuven.be

Quartz veins in siliciclastic rocks contain useful information to decipher the orogenic history from burial to orogenic contraction and eventual orogenic collapse. Applying fluid inclusion and/or stable isotope studies on veins enable us to constrain the P-T conditions during orogenic history and also to estimate the origin of fluid flow assisting the deformation. At low greenschist metamorphic conditions (250°C - 350°C), development and deformation of such veins is liable to fracturing and recrystallisation, the latter because of the onset of quartz plasticity. In order to correctly assess the results of fluid inclusion and/or stable isotope studies, it is imperative that the timing of fracture opening, quartz infill and deformation is well-constrained. Macro- to microscopic fabric and microstructural studies on early, syn- to late orogenic veins, performed in different low-grade metamorphic slate belts, illustrate how detailed information on vein development during orogenic history provides crucial constraints on the interaction between fluids and geodynamics.

Vein infill of early orogenic bedding-normal quartz veins that are related to the latest burial stages of a Palaeozoic rift basin (High-Ardenne slate belt, Belgium, Germany), has been used to deduce the evolution of veins from a hairline fabric to a complex, composite vein fill. The majority of the veins are centimetre-thick with a fibrous to elongate-blocky fabric that has grown by ataxial and syntaxial mechanisms (Van Noten 2011 and references therein). The key parameter that controlled the formation of these early orogenic veins is that crystal growth exceeded the fracturing velocity. The alignment of pseudosecondary fluid inclusion planes within fibrous crystals and secondary inclusion planes cutting through the crystals are particularly useful to deduce the incremental steps of vein opening and later fracturing respectively, eventually serving as a proxy for the stress-state of the basin at the time of vein formation (Van Noten *et al*. 2011).

Synorogenic, foliation-parallel veins are recognised in a thick metapelite-quartzite Palaeozoic sequence (Central Armorica, Brittany, France) (Berwouts *et al*. 2008; Berwouts 2011 and references therein). The fracture opening occurred parallel to a bedding-parallel foliation in the metapelitic rocks. The quartz infill consists of elongate-blocky quartz crystals, which are folded and contain bulging recrystallisation. The quartz microstructures suggest that precipitation of quartz occurred faster than the development of the fracture. A microscopic study shows that fluid inclusions in these veins are always secondary, i.e. formed after the quartz infill.

Late-orogenic Palaeozoic veins (High-Ardenne slate belt, Belgium) range from thin, planar veins to thick, complex vein systems (Van Baelen 2010 and references therein). All veins initiated as steep extensional fractures (cf. thin veins). Shearing sub-parallel to the foliation became dominant during progressive non-coaxial deformation. This resulted in a very oblique opening of some of the fractures (cf. thick veins). These veins show a rim of saddle dolomite and an overgrowth of blocky quartz suggesting an opening velocity exceeding the crystal growth. The thin veins have a fibrous to elongate-blocky infill, suggesting a more or less equal opening and infill velocity. After infill of both vein types, deformation continued, as evidenced by the development of planar microstructures. One specific generation of rectangular fluid inclusions could be related to the development of these planar microstructures in quartz.

These case studies demonstrate that if the timing of emplacement of veins within the structural context is known, the internal microstructural fabric of quartz veins is a crucial key to unravel the geodynamic evolution of an orogenic system. Moreover, correlating the shape and orientation of fluid inclusions to vein formation, allows understanding the results of mineralogical and geochemical analysis properly. Eventually this enables to deduce P-T conditions during each specific veining event and hence during the whole orogenic history.

BERWOUTS, I. 2011. Reconstruction of fluid system evolution in a wrench tectonic setting. Implications for the geodynamic history of Central Armorica, Brittany, France. Aardkundige Mededelingen 26, 251p.

BERWOUTS, I., VAN NOORDEN, M., MUCHEZ, PH., BOYCE, A.J. & SINTUBIN, M. 2008. Inferring intermediate-scale fluid flow in a heterogeneous metasedimentary multilayer sequence during progressive deformation: evidence from the Monts d'Arrée slate belt (Brittany, France). Geofluids 8, 143-158.

VAN BAELEN, H. 2010. Dynamics of a progressive vein development during the late-orogenic mixed brittle-ductile destabilisation of a slate belt. Examples of the High-Ardenne slate belt (Herbeumont, Belgium). Aardkundige Mededelingen 24, 221p.

VAN NOTEN, K. 2011. Stress-state evolution of the brittle upper crust during early tectonic Variscan inversion as defined by successive quartz vein-types in the High-Ardenne slate belt, Germany. Aardkundige mededelingen 28.

VAN NOTEN, K., MUCHEZ, Ph. & SINTUBIN, M. 2011. Stress-state evolution of the brittle upper crust during compressional tectonic inversion as defined by successive quartz vein types (High-Ardenne slate belt, Germany). Journal of the Geological Society, London 168, 407-422.

Subduction-related alpine metamorphic evolution in low strain domains of the Lago della Vecchia Permian metagranite (Sesia-Lanzo Zone, Western Italian Alps)

Michele Zucali*[1], Gisella Rebay[2]

[1]Dipartimento di Scienze della Terra dell'Università degli Studi di Milano and CNR-IDPA,
Via Mangiagalli, 34 - 20133 Milano, Italy
[2] Dipartimento di Scienze della Terra e dell'ambiente, Università di Pavia, Via Ferrata, 1- 27100 Pavia, Italy.
*michele.zucali@unimi.it

The Lago della Vecchia Permian coronitic metagranite (Sesia-Lanzo Zone, Western Italian Alps, Valle del Cervo) preserves igneous textures and mineralogy despite the complete ecologitisation recorded by surrounding tectonitic to mylonitic metagranites and country rocks. Igneous biotite is preserved together with white mica and k-feldspar; the cores of igneous biotite preserve characteristic igneous compositions. No igneous plagioclase is preserved as the original microdomains are overgrown by aggregates of albite + phengitic mica + Fe-epidote. Metamorphic reactions, associated with subdukction, are also localized at the boundaries between biotite – plagioclase and between white mica – plagioclase. A continuous garnet corona with a characteristic partitioning of Ca^{2+}, Mg^{2+} and Fe^{2+} occurs between biotite and plagioclase.

The reactions involved in the transformation of the granite are described in terms of igneous microdomains:

Biotite microdomain:

$$Bt(I)\ (rims) + Ca^{2+} \rightarrow Bt(II) + Wm(II) + Grt$$

White mica-I microdomain:

$$Wm(I) + Ca^{2+} \rightarrow Wm(II) + Grt$$

Plagioclase microdomain:

$$Pl(I)\ (core) + K^{+} + Fe^{2+} + Mg^{2+} + Na^{+} + H_2O \rightarrow Pl(II)(Ab) + Wm(II)\ (fine\text{-}grained) + Ep \pm Grt;$$

White mica-II microdomain:

$$Pl(I)\ (rims) + Ca^{2+} + K^{+} + H_2O \rightarrow Wm(II)\ (coarse\text{-}grained) + Grt \pm Ep \pm Ab$$

The absence of deformation inhibits the complete development of the eclogite-facies parageneses occurring in the surrounding deformed rocks allowing to preserve the memory of the prograde subduction path in the metagranite during the Alpine subduction, generally hidden by the widespread development of HP-LT eclogite assemblages.

THE INTERRELATIONSHIP BETWEEN DEFORMATION AND METAMORPHISM

Granada, 23-26 May, 2011

AUTHOR INDEX

*presenting author printed bold

*presenting author printed bold

*presenting author printed bold